Vol. 9, No. 2
August, 1961

THE SOVIET JOURNAL OF

ATOMIC ENERGY

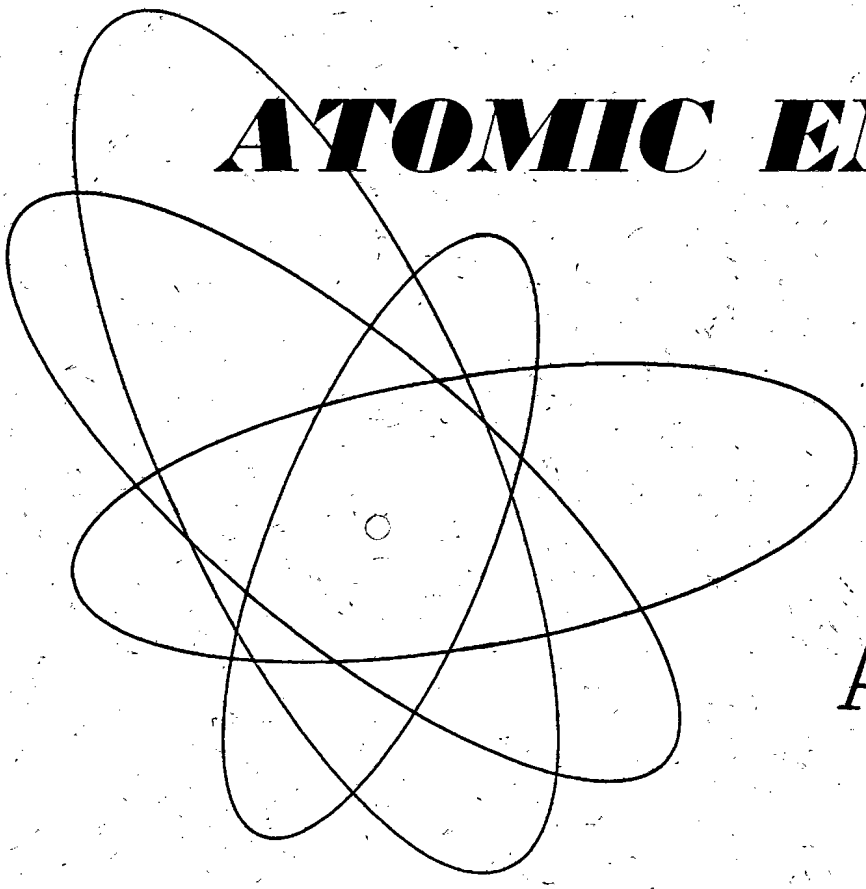

Атомная энергия

TRANSLATED FROM RUSSIAN

CONSULTANTS BUREAU

THE LATEST SOVIET RESEARCH — IN TRANSLATION

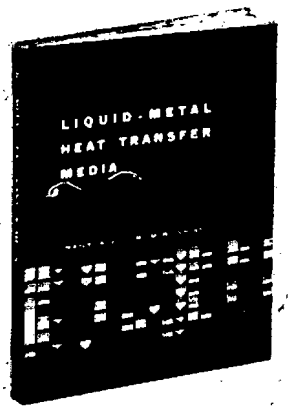

LIQUID-METAL HEAT TRANSFER MEDIA

by S. S. Kutateladze, V. M. Borishanskii, I. I. Novikov and O. S. Fedynskii

This informative volume is devoted to the problems of utilizing liquid-metal heat transfer media in nuclear power. Data on the study of heat removal by liquid metals, obtained during the past ten years in the USSR as well as abroad, in connection with problems of nuclear power are both systematized and generalized in this work. The book will be of considerable assistance to scientific workers and engineers in the field of reactor design and nuclear power and in other fields of technology where liquid-metal coolants can be utilized.

cloth 150 pp. illus. $22.50

CORROSION OF CHEMICAL APPARATUS

by G. L. Shvartz and M. M. Kristal

" . . . the book is concerned with stress corrosion cracking and intercrystalline corrosion, especially in connection with process equipment . . . a judicious mixture of facts, practice, and theory . . . It contains a good deal of Shvartz's own work, and, indeed, is useful for the many pertinent Soviet references . . . collects in one place much of the current Soviet thinking in this field . . . the chapter on methods of testing and the one on methods of retardation are particularly effective . . . Not only do they contain more detail than is usually found in such books, but they are clear and concise, and should prove useful to the practicing corrosion engineer . . . "

—Chemical & Engineering News

cloth 250 pp. $7.50

DENDRITIC CRYSTALLIZATION

by D. D. Saratovkin

"Translated from Russian, this 2nd edition has been revised to include fresh material derived from observations under the stereoscopic microscope. The bulk of this volume contains many original and unpublished ideas and observations, and is an example of the modern microscopic approach to the crystalline state by an experienced worker concerned with the infinite variety of real crystals. Line diagrams and sets of stereoscopic photographs are included."

—Journal of Metals

cloth 126 pp. illus. $6.00

CONSULTANTS BUREAU

227 West 17th Street, New York 11, N.Y.

THE SOVIET JOURNAL OF

ATOMIC ENERGY

A translation of ATOMNAYA ÉNERGIYA,
a publication of the Academy of Sciences of the USSR

(Russian original dated August, 1960)

Vol. 9, No. 2 August, 1961

CONTENTS

	PAGE	RUSS. PAGE
Theory of Heterogeneous Reactors with Cylindrical Lumps of a Finite Radius. A. D. Galanin.	591	89
A Study of the Transfer of Radioactive Materials by Steam and Water and the Chemical Stability of Deposits in the Steam-Water Loop of the First Atomic Power Station. P. N. Slyusarev, G. N. Ushakov, O. V. Starkov, L. A. Kochetkov, L. N. Nesterova, and V. Ya. Kozlov.	601	98
The Recrystallization of Cold Rolled Uranium. G. Ya. Sergeev, V. V. Titova, and L. I. Kolobneva	608	104
Separation of the Stable Isotopes of Boron. N. N. Sevryugova, O. V. Uvarov, and N. M. Zhavoronkov.	614	110
Determination of Energy Absorption in a Mixed Flux of Fast Neutrons and γ-Rays by an Ionization Method. Yu. I. Bregadze, B. M. Isaev, and V. A. Kvasov	630	126
LETTERS TO THE EDITOR		
"Irradiation Reactor". Yu. S. Ryabukhin and A. Kh. Breger	637	132
Approximate Determination of the Optimum Thermodynamic Cycle for a Nuclear Power Station. Yu. D. Arsen'ev and E. K. Averin	639	133
Approximate Calculation of the Mean Energy of Electrons Produced by γ-Rays in an Ionization Chamber. A. K. Wal'ter, M. L. Gol'din, and V. I. Slavin.	642	135
Investigation of the Behavior of Minerals Accompanying Uranium in the Acid Leaching of Ores. G. M. Nesmeyanova and N. K. Chernushevich	646	137
Attenuation of γ-Radiation from Volume Sources in Iron and Lead. G. V. Gorshkov and V. M. Kodyukov	649	139
Attenuation of γ-Radiation from Point Sources in Various Media. V. M. Kodyukov	651	140
Absorption Corrections in the Backing of the 4π-Counter. R. M. Polevoi	653	140
Particularities in the Variation of the Capacitance of Irradiated Air-Gap Capacitors. V. P. Sokolov	655	142
Application of Neutron Pulse Sources for Investigations in Oil Wells. B. G. Erozolimskii, A. S. Shkol'nikov, and A. I. Isakov	658	144
VIII Session of the Learned Council of the Joint Institute for Nuclear Research. V. Biryukov	661	146
Atomic Energy at the Czechoslovak Exhibit in Moscow. Yu. Koryakin and V. Parkhit'ko	664	148
[Japan's First Nuclear Power Station, see Nuclear Power, 5, No. 47 (1960)		
[USA Nuclear Power Development Plans for 1960-1970		
[USAEC Financial Report for 1959		

Annual subscription $ 75.00
Single issue 20.00
Single article 12.50

CONTENTS (continued)

	PAGE	RUSS. PAGE
A 680 Mev Synchrotron. V. A. Petukhov	665	154
A New Ore Dressing Plant in France	666	155
A Facility for Irradiating Personal Film Holders. B. M. Dolishnyuk	669	156
BRIEF COMMUNICATIONS	671	157
BIBLIOGRAPHY		
Reviews of Books and Symposia	672	159
Articles from Periodical Literature	674	161

NOTE

The Table of Contents lists all material that appears in Atomnaya Énergiya. Those items that originated in the English language are not included in the translation and are shown enclosed in brackets. Whenever possible, the English-language source containing the omitted reports will be given.

Consultants Bureau Enterprises, Inc.

THEORY OF HETEROGENEOUS REACTORS WITH CYLINDRICAL LUMPS OF A FINITE RADIUS

A. D. Galanin

Translated from Atomnaya Énergiya, Vol. 9, No. 8, pp. 89-97, August, 1960
Original article submitted December 21, 1959

This article presents a consistent theory of heterogeneous reactors with cylindrical lumps of a finite, but small, radius. The density of thermal neutrons inside a lump and in the moderator is described by taking into account the azimuthal dependence. The diffusion theory is applied to the entire reactor volume. Simple expressions for the diffusion length in the parallel and perpendicular directions with an accuracy to the first power of the lump surface to cell surface ratio are obtained. It is shown that the average scattering length for the perpendicular direction depends on the lump shape. A simple method for determining the diffusion tensor for the case of weak absorption and large spacing between the lumps is considered in section 4.

Introduction

The theory of heterogeneous reactors with point (more accurately, filament-shaped) lumps has been developed systematically and in sufficient detail [1 and 2]. The basic assumption of this theory consists in the fact that the neutron density in the lump and in the nearby moderator does not depend on the azimuthal angle. If we consider only an infinite lattice, the fact that the lumps are not point-like can be taken into account without violating this assumption [2]. For a regular lattice structure (for instance, for square cells), the resulting accuracy in determining the thermal efficiency is very high if the ratio of the lump cross-sectional area to the cell area is not close to unity. The author of paper [3] considered an infinite lattice renouncing the basic assumption, and he found the corresponding corrections for the magnitude of the lump-effect in the moderator.

In considering a lattice with finite dimensions, the azimuthal dependence of the neutron density around the lump arises not only due to the effect of the neighboring lumps on a certain given lump, as is the case in an infinite lattice, but also due to the over-all neutron field gradient. For this, the azimuthal dependence of the neutron field near the lump can be expressed by the following equation:

$$N(r, \vartheta) = A_0(r) + A_1(r)\cos\vartheta + A_2(r)\cos 2\vartheta + \ldots$$

The effect of neighboring lumps in a square lattice of infinite dimensions results in the dependence

$$N(r, \vartheta) = B_0(r) + B_1(r)\cos 4\vartheta + B_2(r)\cos 8\vartheta + \ldots,$$

i.e., the expansion in this case begins only with the fourth harmonic. The appearance of the first harmonic in $N(r, \vartheta)$ is caused by the lattice finiteness, and, therefore, this harmonic is connected with changes in neutron leakage and not with changes in the multiplication constant. Thus, if we form a theory according to which $A_1 \cos\vartheta$ terms will be taken into account, we shall obtain corrections for the diffusion length in the lattice.

We shall henceforth consider a square lattice consisting of a finite, but sufficiently large number of cylindrical lumps of finite length. Anisotropic diffusion, which has been considered in a number of papers [4-11], must arise in such a lattice. In this, many authors did not restrict their investigations to the diffusion approximation approach and, therefore, their results are more general with respect to this point. Nevertheless, it seems to us that

the method presented here deserves attention, since, in the first place, it represents a consistent development of the theory of heterogeneous reactors with point lumps, and, in the second place, the simple diffusion approximation equations can be useful as a physically fully justifiable limiting case in formulating more accurate theories. As far as the author knows, diffusion approximation equations for diffusion in the perpendicular direction in the case of cylindrical lumps have not been published before.

The following restrictions are used in the proposed theory:

1. All calculations are performed under the assumption of diffusion approximation, i.e., in the first place, it is required that the absorption in lumps be small, in the second place, the spacing of lumps must be large in comparison with the scattering length in the moderator, and, in the third place, either the lump dimensions must be large in comparison with the scattering length in the lump or the difference between the scattering lengths in the lump and the moderator must not be too large. It is possible that nondiffusion corrections, connected with intensive absorption in the lump, can be taken into account by introducing certain effective values.

2. Neutron absorption in moderation is not taken into account.

3. It is assumed that thermal neutron sources are not present in the lumps and that the distribution of sources outside the lumps is the same as in a homogeneous reactor of the same dimensions.

A simple method for determining the diffusion tensor for the case where the lump-effect is not taken into account and the lump volume is small in comparison with the cell volume is given in section 4. The obtained equations can be used for determining the moderation length anisotropy (if the diffusion approximation is applicable).

1. General Theory

Let the z axis be directed along the lump axis, and let the x and y axes be perpendicular to the z axis along the sides of the square cell. For the sake of simplicity, we shall assume that the reactor is finite only along the x and z axes. We shall also assume that there are no reflectors along the z axis. Then, the variables can be separated, and the neutron (thermal and moderated) density dependence on z is given by the over-all factor $\alpha_z z$, which will be thereafter omitted.

The neutron density k inside the lump will be expressed by the equation•

$$N_i^{(k)}(r, \vartheta_k) = \sum_{n=-\infty}^{+\infty} A_n^{(k)} I_n\left(\frac{r}{L_i'}\right) e^{-in\vartheta_k}, \tag{1}$$

where $L_i'^{-2} = L_i^{-2} + \alpha_z^2$. The over-all number of thermal neutrons absorbed by the lump per unit time per unit length is given by:

$$\int \frac{N_i^{(k)}(r, \vartheta_k)}{T_i}\, dv = \frac{2\pi\varrho D_i L_i'}{L_i^2} A_0^k I_1\left(\frac{\varrho}{L_i'}\right), \tag{2}$$

where ρ is the lump radius.

It is known that, in a lattice with point lumps, the density of thermal neutron sources depends on the coordinates only because of the reactor finiteness; there is no fine source field structure in the cell (we assume that the conditions necessary for this are fulfilled). There can hardly be any doubt that this condition will also hold for nonpoint lumps. Therefore, we shall calculate the density of sources as in the case of point lumps:••

$$S(r) = \frac{2\pi\varrho D_i L_i'}{L_i^2} I_1\left(\frac{\varrho}{L_i'}\right) \eta e^{-\alpha_z^2 \tau} \sum_k \frac{A_0^{(k)}}{4\pi\tau} e^{-\frac{(r_k - r)^2}{4\tau}} \tag{3}$$

• The quantities pertaining to the lump and the moderator will be denoted by the "i" and "e" indices, respectively. The designations of various geometric quantities are clear from the picture. All vectors are two-dimensional.

•• The age theory is used here. If we assume that it is not valid, the $e^{-\alpha^2 \tau}$ factor in Eq. (4) must be changed; it is only necessary that the neutron field fine structure not be present inside the cell. For the sake of simplicity, the diffusion anisotropy of moderated neutrons is not taken into account. In the diffusion approximation, it can be taken into account according to the method presented in section 4.

Assuming that $A_0^k = A_0^0 e^{i\alpha_x x_k}$, after summation,* we obtain:

$$S(r) = \frac{2\pi\varrho D_i L_i'}{a^2 L_i^2} A_0^{(0)} I_1\left(\frac{\varrho}{L_i'}\right) \eta e^{-\alpha^2\tau + i\alpha_x x}, \tag{4}$$

where $\alpha^2 = \alpha_x^2 + \alpha_z^2$; a is the lattice spacing. The $W(\tau) = (4\pi\tau)^{-1} \exp\left(-\frac{r^2}{4\tau}\right)$ function in Eq. (3) is normalized in such a manner that the integral over the entire volume is equal to unity. However, we assume that there are no sources inside the lump. Therefore, the regular $W(\tau)$ function, obtained by taking into account the lump finiteness, must be normalized in such a manner that the integral is equal to unity only over the moderator surface. Hence, it follows that, in the right-hand side of Eq. (4), the $(1-c)^{-1}$ factor must be introduced, where

$$c = \frac{\pi\varrho^2}{a^2}. \tag{5}$$

The neutron density in the moderator is

$$N_e(r) = N_{1e}(r) + N_{2e}(r), \tag{6}$$

where $N_{1e}(r)$ is the solution of the nonhomogeneous equation (4) for sources and $N_{2e}(r)$ is the homogeneous equation solution. By using Eq. (4), we readily obtain

$$N_{1e}(r_k, \vartheta_k) = \frac{\eta e^{-\alpha^2\tau}}{(1+\alpha^2 L_e^2) q_0 Q} A_0^{(k)} I_0 \times \left(\frac{\varrho}{L_i'}\right) e^{i\alpha_x r_k \cos\vartheta_k}, \tag{7}$$

where

$$q_0 = \frac{1-c}{c}\frac{l_{ai}}{l_{ae}}; \quad Q = \frac{I_0\left(\frac{\varrho}{L_i'}\right)}{\left(\frac{2L_i'}{\varrho}\right) I_1\left(\frac{\varrho}{L_i'}\right)}. \tag{8}$$

In Eq. (7), r_k is the distance of the given point from the lump center k (see figure). By expanding this equation in a Fourier series, we obtain:

$$N_{1e}(r_k, \vartheta_k) = \frac{\eta e^{-\alpha^2\tau}}{(1+\alpha^2 L_e^2) q_0 Q} A_0^{(k)} I_0 \times \left(\frac{\varrho}{L_i'}\right) \sum_{n=-\infty}^{+\infty} i^n J_n(\alpha_x r_k) e^{-in\vartheta_k}. \tag{9}$$

The solution of the homogeneous equation can be written thus:

$$N_{2e}(r_k, \vartheta_k) = \sum_{n=-\infty}^{+\infty} \sum_{k'} B_n^{(k')} K_n\left(\frac{R_{kk'}}{L_e'}\right) e^{-in\vartheta_{k'}}, \tag{10}$$

where $L_e'^{-2} = L_e^{-2} + \alpha_z^2$; $\sum_{k'}$ denotes summation for all lattice lumps including the k'th lump; in this case, $R_{kk'}$ is equal to r_k.

By using the addition theorem [12]

$$e^{in\psi} K_n\left(\frac{R_{kk'}}{L_e'}\right) = \sum_{m=-\infty}^{+\infty} I_m\left(\frac{r_k}{L_e'}\right) \times K_{n+m}\left(\frac{r_{kk'}}{L_e'}\right) e^{im\varphi} \tag{11}$$

and the relationships between angles $\varphi = \vartheta_k - \chi_{kk'}$; $\vartheta_{k'} = \pi - \psi + \chi_{kk'}$, we obtain

$$N_{2e}(r, \vartheta) = \sum_{n=-\infty}^{+\infty} e^{-in\vartheta} U_n(r), \tag{12}$$

*It is assumed that the number of lumps in the reactor is sufficiently large; paper [2] describes how this summation is performed.

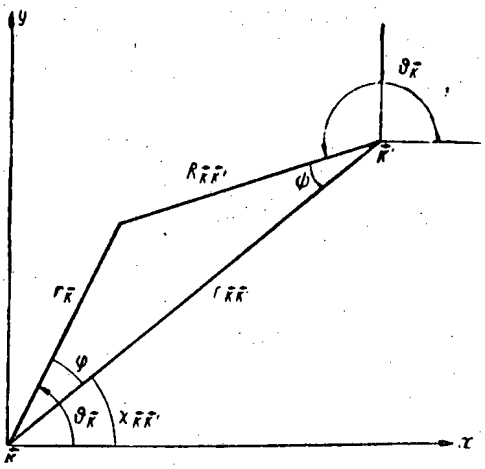

Diagram explaining the mutual position of the k and k' lumps.

where

$$U_n(r) = B_n^0 K_n\left(\frac{r}{L_e'}\right) + I_n\left(\frac{r}{L_e'}\right)\sum{}' \sum_{m=-\infty}^{+\infty} (-1)^m B_n^{k'} K_{n-m} \times \left(\frac{r_{k'}}{L_e'}\right) e^{i(n-m)\chi_{k'}}, \tag{13}$$

where the **k**th lump is conventionally taken as the 0th lump $r \equiv r_0$, $r_{k'} \equiv r_{0k'}$, $\chi_{k'} \equiv \chi_{0k'}$ and Σ' denotes summation with respect to **k'** under the condition that $\mathbf{k'} \neq 0$.

The limiting conditions

$$N_i(\varrho, \vartheta) = N_e(\varrho, \vartheta); \quad D_i \frac{\partial N_i(r, \vartheta)}{\partial r}\Big|_{r=\varrho} = D_e \frac{\partial N_e(r, \vartheta)}{\partial r}\Big|_{r=\varrho} \tag{14}$$

are valid for each harmonic separately, i.e.,

$$A_n I_n\left(\frac{\varrho}{L_i'}\right) = i^n \frac{\eta e^{-\alpha^2\tau}}{(1+\alpha^2 L_e^2) q_0 Q} \times A_0 I_0\left(\frac{\varrho}{L_i'}\right) J_n(\alpha_x \varrho) + U_n(\varrho);$$
$$\frac{D_i}{L_i'} A_n I_n'\left(\frac{\varrho}{L_i'}\right) = i^n \frac{D_e \alpha_x \eta e^{-\alpha^2\tau}}{(1+\alpha^2 L_e^2) q_0 Q} \times A_0 I_0\left(\frac{\varrho}{L_i'}\right) J_n'(\alpha_x \varrho) + \frac{D_e}{L_e'} U_n'(\varrho), \tag{15}$$

where the prime denotes the derivatives with respect to the argument of the corresponding Bessel function. The system of equations (15) makes it possible to determine the $A_n^{(k)}$ and $B_n^{(k)}$ constants.

2. Small Lump Theory

Hereafter, we shall consider only the first correction to the theory of point lumps, and we shall assume that $A_n^{(k)} = B_n^{(k)} = 0$ for $|n| \geq 2$. The solution of the system of Eqs.(15) will be given by an expression of the following form (it is assumed here that the lattice is sufficiently large):

$$B_n^{(k)} = B_n^0 e^{i\alpha_x x_k}, \quad B_0^0 = 1. \tag{16}$$

By assuming that n = 0 and eliminating A_0 from the system of Eqs.(15), we obtain the characteristic lattice equation [hereafter, $J_n(\alpha_x \rho)$ is replaced by the first expansion term for $\alpha_x \rho \ll 1$]:

$$\frac{\eta e^{-\alpha^2\tau}}{1+\alpha^2 L_e^2}\left(1 - \alpha_x^2 L_e^2 \frac{c\xi}{1-c} \frac{L_i'^2}{L_i^2}\right) = q_0 Q + \xi, \tag{17}$$

where

$$\xi = -\frac{\alpha^2(1-c)}{2\pi L_e^2} \frac{L_i^2}{L_i'^2} \frac{U_0(\varrho)}{\frac{\varrho}{L_e'} U_0'(\varrho)}. \tag{18}$$

Here, $U_0(\rho)$ also contains the unknown $B_{\pm 1}^0$ coefficients. For their determination, we must consider the system of equations (15) for n = ± 1. Let us introduce the following notation:

$$U_{+1} + U_{-1} = 2W_1; \quad U_{+1} - U_{-1} = 2W_2 \tag{19}$$

and

$$B_1^0 = \gamma + i\gamma_1; \quad B_{-1}^0 = \gamma - i\gamma_1. \tag{20}$$

Equations (15) yield:

$$\frac{D_e}{D_i}\frac{\varrho}{L'_e}\frac{1}{2Q-1}W'_1(\varrho)-W_1(\varrho)=i\alpha_x L'_e U'_0 C;\quad \frac{D_e}{D_i}\frac{\varrho}{L'_e}\frac{1}{2Q-1}W'_2(\varrho)-W_2(\varrho)=0, \tag{21}$$

where

$$C=\left(1-\frac{D_e}{D_i}\frac{1}{2Q-1}\right)\frac{\dfrac{ne^{-\alpha^2\tau}}{1+\alpha^2L_e^2}\dfrac{L_i'^2L_e^2}{L_i^2L_e'^2}\dfrac{c}{1-c}}{1+\dfrac{\eta e^{-\alpha^2\tau}}{1+\alpha^2L_e^2}\dfrac{c\alpha_x^2L_e^2}{1-c}\dfrac{L_i'^2}{L_i^2}} \tag{22}$$

By using Eqs. (13) and (16), we obtain

$$\left.\begin{aligned} W_1&=\gamma K_1\left(\frac{\varrho}{L'_e}\right)+I_1\left(\frac{\varrho}{L'_e}\right)\times[i\Sigma_1-\gamma(\Sigma_0+\Sigma_2)-\gamma_1\tilde{\Sigma}_2];\\ W_2&=i\gamma_1K_1\left(\frac{\varrho}{L'_e}\right)+iI_1\left(\frac{\varrho}{L'_e}\right)\times[\tilde{\Sigma}_1-\gamma_1(\Sigma_0+\Sigma_2)-\gamma\tilde{\Sigma}_2];\end{aligned}\right\} \tag{23}$$

where

$$\left.\begin{aligned} U_0&=K_0\left(\frac{\varrho}{L'_e}\right)+I_0\left(\frac{\varrho}{L'_e}\right)\times[\Sigma_0-2i\gamma\Sigma_1-2\gamma_1\tilde{\Sigma}_1],\\ \Sigma_0&=\sum{}'e^{i\alpha x_k}K_0\left(\frac{r_k}{L'_e}\right);\ \Sigma_1=\frac{1}{i}\sum{}'e^{i\alpha x_k}\cos\chi_kK_1\left(\frac{r_k}{L'_e}\right);\ \tilde{\Sigma}_1=\sum{}'e^{i\alpha x_k}\sin\chi_kK_1\left(\frac{r_k}{L'_e}\right);\\ \Sigma_2&=\sum{}'e^{i\alpha x_k}\cos2\chi_kK_2\left(\frac{r_k}{L'_e}\right);\ \tilde{\Sigma}_2=\sum{}'e^{i\alpha x_k}\sin2\chi_kK_2\left(\frac{r_k}{L'_e}\right).\end{aligned}\right\} \tag{24}$$

For reasons of symmetry, it is readily found that

$$\tilde{\Sigma}_1=\tilde{\Sigma}_2=0. \tag{25}$$

Then, the second of the Eqs. (21) yields $\gamma_1 = 0$, and the first makes it possible to determine γ in the following manner:

$$i\gamma=\frac{\left[\frac{s\varrho}{L'_e}I'_1\left(\frac{\varrho}{L'_e}\right)-I_1\left(\frac{\varrho}{L'_c}\right)\right]\Sigma_1+\left[K_1\left(\frac{\varrho}{L'_e}\right)-\Sigma_0I_1\left(\frac{\varrho}{L'_e}\right)\right]\alpha_xL'_eC}{\frac{s\varrho}{L'_e}\left[K'_1\left(\frac{\varrho}{L'_e}\right)-I'_1\left(\frac{\varrho}{L'_e}\right)\left(\Sigma_0+\Sigma_2\right)\right]-\left[K_1\left(\frac{\varrho}{L'_e}\right)-I_1\left(\frac{\varrho}{L'_e}\right)\left(\Sigma_0+\Sigma_2\right)\right]-2\alpha_xL'_eI_1\left(\frac{\varrho}{L'_e}\right)C\Sigma_1} \tag{26}$$

where

$$s=\frac{D_e}{D_i}(2Q-1)^{-1}. \tag{27}$$

For $\rho / L'_e \ll 1$, the Bessel functions in Eq. (26) can be expanded in the series

$$-i\gamma=\frac{\alpha_xL'_eC\left(1-\frac{\varrho^2}{2L_e'^2}\Sigma_0\right)+(s-1)\frac{\varrho^2}{2L_e'^2}\Sigma_1}{1+s+\frac{\varrho^2}{2L_e'^2}(s-1)\left(\Sigma_0+\Sigma_2\right)+\alpha_xL'_e\frac{\varrho^2}{L_e'^2}C\Sigma_1} \tag{28}$$

Let us now calculate the sums (24). The sum Σ_0 can be calculated according to the method described in [2]. As a result, we obtain:*

$$\Sigma_0=\frac{2\pi L_e'^2}{a^2(1+\alpha_x^2L_e'^2)}-\ln\frac{4\pi L'_e}{1{,}78a}+\frac{\pi}{6}+\ldots. \tag{29}$$

* It is assumed that $\frac{2\pi L_e^2}{a^2}\gg1$, $\frac{a\alpha_x}{2\pi}\ll1$.

The Σ_1 and Σ_2 sums can be written as

$$\sum_1 = \sum_{k_1,\,k_2}{}' \frac{k_1 \sin \alpha_x a k_1}{\sqrt{k_1^2+k_2^2}} K_1\left(\frac{a}{L_e'}\sqrt{k_1^2+k_2^2}\right); \tag{30}$$

$$\sum_2 = \sum_{k_1,\,k_2}{}' \frac{(k_1^2-k_2^2)\cos \alpha_x a k_1}{k_1^2+k_2^2} K_2\left(\frac{a}{L_e'}\sqrt{k_1^2+k_2^2}\right). \tag{31}$$

In calculating these sums in the first approximation, the summation can be replaced by integration from $-\infty$ to $+\infty$ with respect to k_1 and k_2 (including the $k_1 = k_2 = 0$ point), as a result of which we obtain:

$$\sum_1^{(0)} = \frac{2\pi L_e'^2}{a^2} \frac{\alpha_x L_e'}{1+\alpha_x^2 L_e'^2}; \tag{32}$$

$$\sum_2^{(0)} = -\frac{2\pi L_e'^2}{a^2} \frac{\alpha_x^2 L_e'^2}{1+\alpha_x^2 L_e'^2}. \tag{33}$$

A more accurate value will be required only for Σ_1. Consider the difference $\Sigma_1 - \Sigma_2^{(0)}$, for the calculation of which small values of k_1 are important. Therefore, for $\alpha_x a \ll 1$, we can expand $\sin \alpha_x a k_1$ in series and take only the first term. After symmetrization with respect to k_1 and k_2, we find:

$$\sum_1 - \sum_1^{(0)} \cong -\frac{\alpha_x a}{2} \frac{\partial}{\partial\left(\frac{a}{L_e'}\right)}\left[\sum{}' K_0\left(\frac{a}{L_e'}\sqrt{k_1^2+k_2^2}\right) - \int K_0\left(\frac{a}{L_e'}\sqrt{k_1^2+k_2^2}\right) dk_1\, dk_2\right]$$

or, by using expression (29), we obtain the following expression for Σ_1 instead of expression (32):

$$\sum_1 = \frac{2\pi L_e'^2}{a^2} \alpha_x L_e' \left(\frac{1}{1+\alpha_x^2 L_e'^2} - \frac{a^2}{4\pi L_e'^2}\right). \tag{34}$$

The given problem is now solved completely. Let us analyze the obtained results. It should be first noted that, since we used only the first harmonic, we cannot keep the higher powers of the small quantity c; only its linear value can be retained. Neglecting c^2 and assuming that $L_i^2/L_i^2 = (1 + \alpha_z^2 L_i^2)^{-1} \cong 1$, we obtain from Eq. (28) the following simple expression for γ:

$$i\gamma = c\alpha_x L_e' \frac{s-1}{s+1}(1+\alpha_z^2 L_e^2)\left[\frac{\eta e^{-\alpha^2\tau}-1}{1+\alpha^2 L_e^2} + \frac{a^2}{4\pi L_e^2}\right]. \tag{35}$$

Consider now the basic Eq. (17). In its left-hand side, ξ can be replaced by the ξ value for $c \to 0$, i.e. [2],

$$\xi\Big|_{c\to 0} = \frac{a^2}{2\pi L_e^2} \frac{K_0\left(\frac{\varrho}{L_e'}\right) + I_0\left(\frac{\varrho}{L_e'}\right)\sum_0}{\frac{\varrho}{L_e'}\left[K_1\left(\frac{\varrho}{L_e'}\right) - I_1\left(\frac{\varrho}{L_e'}\right)\sum_0\right]} = \frac{1}{1+\alpha^2 L_e^2} + q_1, \tag{36}$$

where [2]

$$q_1 = \frac{a^2}{4\pi L_e^2}\left(\ln\frac{a^2}{\pi\varrho^2} - \frac{3}{2}\right) \tag{37}$$

represents the external lump-effect.

Let us now consider Eq. (17) for $\gamma = 0$:

$$\frac{\eta e^{-\alpha^2\tau}}{1+\alpha^2 L_e^2}\left[1 - \alpha_x^2 L_e^2 c\left(\frac{1}{1+\alpha^2 L_e^2} + q_1\right)\right] = q_0 Q + \frac{a^2}{2\pi L_e^2}\frac{L_i^2}{L_i'^2} \frac{(1-c)\left[K_0\left(\frac{\varrho}{L_e'}\right) + I_0\left(\frac{\varrho}{L_e'}\right)\sum_0\right]}{\frac{\varrho}{L_e'}\left[K_1\left(\frac{\varrho}{L_e'}\right) - I_1\left(\frac{\varrho}{L_e'}\right)\sum_0\right]} \tag{38}$$

By the series expansion of the Bessel functions and by using expression (29), we find for the right-hand side of Eq. (38):

$$q_0 Q + \frac{L_i^2}{L_i'^2} \frac{(1-c)\left(\frac{1}{1+\alpha^2 L_e^2} + q_1\right)}{1 - \frac{c}{1+\alpha_x^2 L_e'^2}}.$$

After elementary transformations, we obtain with an accuracy to the first power of c the following characteristic equation:

$$ke^{-\alpha^2\tau} = 1 + \alpha_x^2 L_\perp^2 + \alpha_z^2 L_\parallel^2, \tag{40}$$

where*

$$k = \frac{\eta}{1+q_0\zeta}; \tag{41}$$

$$L_\perp^2 = L_0^2[1 + c(1-\zeta^{-1})]; \tag{42}$$

$$L_\parallel^2 = L_0^2\left[1 + c\zeta^{-1}\left(\frac{l_{si}}{l_{se}} - 1\right)\right]; \tag{43}$$

$$L_0^2 = \frac{q_0\zeta L_e^2}{1+q_0\zeta}(1 + c\zeta^{-1}). \tag{44}$$

Here,

$$\zeta = Q + \frac{q_1}{q_0} \tag{45}$$

expresses the total lump-effect, i.e., the ratio of the average densities in the moderator and the lump. According to definition, the $L_\perp$ and $L_\parallel$ quantities in Eq. (40) will be called the diffusion lengths in the perpendicular and parallel directions, respectively.

We shall now take into account γ. If we take only the linear terms with respect to c, we can readily see that the following expressions should be added to (39):

$$\frac{2(1-s)}{1+s} c\alpha_x^2 L_e^2\left(\frac{\eta e^{-\alpha^2\tau} - 1}{1+\alpha^2 L_e^2} + \frac{a^2}{4\pi L_e^2}\right)\frac{1}{1+\alpha^2 L_e^2}. \tag{46}$$

Considering that, approximately, $\frac{\eta e^{-\alpha^2\tau} - 1}{1+\alpha^2 L_e^2} = q_0\zeta$, instead of expression (46), we have:

$$\frac{2(1-s)}{1+s} c\alpha_x^2 L_e^2 \quad q_0\zeta + \frac{a^2}{4\pi L_e^2} \quad \frac{1}{1+\alpha^2 L_e^2}.$$

Hence, it follows that Eq. (43) does not change and that (42) assumes the form:

$$L_\perp^2 = L_0^2\left[1 + \frac{2(1-s)}{1+s} c(1+\delta) + c(1-\zeta^{-1})\right], \tag{47}$$

where

$$\delta = \frac{3\varrho^2}{4l_{ai}l_{se}\zeta} = \frac{a^2}{4\pi^2 L_e^2 q_0\zeta}, \tag{48}$$

and s is determined by Eq. (27).

3. Analysis of the Results

Let us analyze the obtained equations. We shall first write the $L_\parallel^2$ and $L_\perp^2$ expressions for the case where the lump-effect is absent, i.e., where the absorption is rather weak in the moderator as well as in the lump. We shall compare the obtained results with the well-known equations for laminar lumps:

$$L_i^2 = L_0^2\left(1 + c\frac{1-s}{f}\right), \tag{49}$$

where the f coefficient is equal to s for plates or cylinders in the parallel direction; for plates in the perpendicular direction, this coefficient is equal to 1, and, for cylinders in the perpendicular direction, it is equal to $1 + s/2$.

* The last factor in Eq. (44) was introduced in order to make it possible to write the average absorption length in the form given by (51). In this, the quadratic terms with respect to c were not calculated, and, thus, Eqs. (42) and (43) are accurate only to the order of c.

The difference between the f coefficients for plates and cylinders in the case of a perpendicular direction is connected with the fact that the direction of the neutron field gradient coincides with the normal to the interface in the first case, and, that in the second case, they are at an angle which changes from 0 to $\pi/2$ at different points on the cylinder surface (see also section 4).

In the case of laminar lumps (and cylindrical lumps for $L_{\parallel}^2$), we can introduce the average absorption and scattering lengths, which are obtained by averaging either the microscopic cross sections ($\bar{l}_{\alpha}$ and $\bar{l}_{s\perp}$), or the scattering lengths ($\bar{l}_{s\parallel}$):

$$L_{\parallel}^2 = \frac{1}{3}\bar{l}_a\bar{l}_{s\parallel}; \quad L_{\perp}^2 = \frac{1}{3}\bar{l}_a\bar{l}_{s\perp}. \tag{50}$$

In taking into account the lump-effect, the average lengths $\bar{l}_{\alpha}$ and $\bar{l}_{s\parallel}$ are expressed by the following equations:

$$\bar{l}_a^{-1} = \frac{l_{a1}^{-1}V_1\bar{N}_1 + l_{a2}^{-1}V_2\bar{N}_2}{V_1\bar{N}_1 + V_2\bar{N}_2}; \tag{51}$$

$$\bar{l}_{s\parallel} = \frac{l_{s1}V_1\bar{N}_1 + l_{s2}V_2\bar{N}_2}{V_1\bar{N}_1 + V_2\bar{N}_2}, \tag{52}$$

where $\bar{N}_1$ and $\bar{N}_2$ are the average neutron density values in the V_1 and V_2 volumes, respectively. For $\bar{l}_{s\perp}$ in the case of cylindrical lumps, such a simple equation cannot be derived.

For weak absorption, we have the following ratio:

$$\frac{L_{\parallel}^2}{L_{\perp}^2} = 1 + c\frac{(1-s)^2}{s(1+s)}, \tag{53}$$

i.e., $L_{\parallel}^2 \geqslant L_{\perp}^2$.

It should be noted that Q and q_1 can be replaced by their values, which are obtained by taking into account nondiffusion corrections only in the expression for L_0^2 in Eq. (44). As regards the deviation of $L_{\parallel}^2$ and $L_{\perp}^2$ from L_0^2, in this case, generally speaking, Q and q_1 cannot be replaced by values obtained in nondiffusion calculations which are performed without taking into account the azimuthal dependence of the neutron density in the lump and in the nearby moderator. It should be noted that the diffusion approximation error can be corrected to a considerable extent if the following quantity is taken as the diffusion coefficient:

$$D = \frac{1}{3}vl,$$

where l is the total length, i.e., $l^{-1} = l_s^{-1} + l_a^{-1}$ (strictly speaking, if l differs from l_s, the diffusion approximation ceases to be valid; therefore, the substitution of l for l_s can be considered only as a certain remedy, justified by a comparison with a more rigorous approach). Therefore, l_s can be considered as l in all equations; more accurate results are thereby obtained.

A comparison between the obtained equations with the results obtained by other authors [6 and 9] indicates that, in the case of parallel diffusion, a correction proportional to $(1-s)^2\frac{l_{si}}{d}$, where d is the lump dimension, should be introduced in Eq. (49), i.e., for $l_{si} \simeq d$, our equations are valid only in the first order with respect to $1 - s = \frac{l_{si} - l_{se}}{l_{si}}$. In the case of perpendicular diffusion, it is more difficult to make a comparison (for cylindrical lumps), since the development of the nondiffusion theory has not been completed [9]. On the basis of general considerations, one can expect to obtain a similar correction, but with a smaller coefficient. The diffusion theory is valid only for the limiting case of small lumps for perpendicular diffusion and laminated lumps [6 and 7]. In this, the neutron distribution function depends only on a single coordinate (perpendicular to the plate) and on a single angle (between the velocity direction and the normal to the plate). In this case, it can be demonstrated [2] that the smallness of the neutron density gradient is the only condition for the diffusion equation applicability.

Let us now consider the character of the neutron density distribution inside the lump:

$$N_i^{(k)}(r,\ \vartheta) = Re\left\{\left[A_0 I_0\left(\frac{r}{L_i'}\right)\ (A_1 e^{i\vartheta} + A_{-1}e^{-i\vartheta})\, I_1\left(\frac{r}{L_i'}\right)\right] e^{i\alpha_x x_k}\right\}. \tag{54}$$

On the basis of the above equations, we find that A_0 is real, that $A_{\pm 1}$ is imaginary, and that $A_{-1} = A_{+1}$. Then,

$$N_i^{(k)}(r,\ \vartheta) = A_0 I_0\left(\frac{r}{L_i'}\right)\cos\alpha_x x_k \quad - 2\,Im\,(A_1)\, I_1\left(\frac{r}{L_i'}\right)\sin(\alpha_x x_k)\cos\vartheta. \tag{55}$$

By using the obtained results, we can obtain the following expression for $N_i^{(k)}$ in the first approximation with respect to c (in this, it is necessary to change the normalization in Eq. (16) ($B_0^0 = -1$); this change of sign will not affect the previous results):

$$N_i^{(k)}(r,\ \vartheta) = \frac{I_0\left(\frac{r}{L_i'}\right)}{I_0\left(\frac{\varrho}{L_i'}\right)}\cos\alpha_x x_k - \frac{2s}{1+s}\zeta(1+\delta)\frac{I_1\left(\frac{r}{L_i'}\right)}{I_1\left(\frac{\varrho}{L_i'}\right)}\varrho\alpha_x\sin(\alpha_x x_k)\cos\vartheta. \tag{56}$$

Let us consider a point on the lump surface and introduce the quantity $x_{k,\vartheta} = x_k + \varrho\cos\vartheta$. From Eq. (56), for $\rho\alpha_x \ll 1$, we obtain:

$$N_i^{(k)}(\varrho,\ \vartheta) = \cos(x_{k,\vartheta}\alpha_x) + b\varrho\alpha_x\sin(\alpha_x x_k)\cos\vartheta, \tag{57}$$

where

$$b = 1 - \frac{2s}{1+s}\zeta(1+\delta). \tag{58}$$

The first term in expression (57) gives the same density value which would be found for a homogeneous reactor of the same dimensions. If the lump-effect is small, we have

$$b = \frac{1-s}{1+s}. \tag{59}$$

4. The Case of Weak Absorption and Small Lump Concentration

Equation (49) can be obtained in a very simple manner. If absorption is neglected, the neutron density satisfies the same equation which is satisfied by the electrical potential in a dielectric. In this case, the dielectric permeability plays the role of the diffusion coefficient. Therefore, the determination of the diffusion anisotropy in a nonhomogeneous medium is equivalent to the determination of the dielectric permeability tensor in a medium with the same geometry and with dielectric permeabilities proportional to the corresponding diffusion coefficients.

Consider a dielectric containing sparse impurities of another dielectric. If the volume of each region filled with the impurity is sufficiently small and the distances between the impurities are large, it can be considered that the impurities do not interact and that each is located in a uniform external field. We shall assume that the dielectric permeability of the external medium is equal to unity.

Let the impurities have the shape of plates or cylinders, which are positioned parallel to the external field. In this case, $\mathbf{E}_i = \mathbf{E}_e$, and a dipole moment arises in each impurity:

$$\boldsymbol{p} = v_0 = \frac{\varepsilon_i - 1}{4\pi}\boldsymbol{E}_e, \tag{60}$$

where v_0 is the impurity volume. The average polarization of unit volume is

$$\boldsymbol{P} = \varkappa\boldsymbol{E}_e; \quad \varkappa = c\,\frac{\varepsilon_i - 1}{4\pi}, \tag{61}$$

where c is the impurity volumetric concentration. Hence, it follows that the average dielectric permeability is

$$\varepsilon = 1 + 4\pi\varkappa = 1 + c(\varepsilon_i - 1). \tag{62}$$

In passing to neutron diffusion, $\frac{1}{s}=\frac{l_{si}}{l_{se}}$. should be substituted for ε_i. Thus, we obtain the following expression for the parallel diffusion coefficient:

$$D_{\parallel}=D_e\left(1+c\frac{1-s}{s}\right). \tag{63}$$

If the impurities have the shape of plates and are positioned perpendicularly to the external field, $\varepsilon_i\mathbf{E}_i = \mathbf{E}_e$, and the average polarization of the medium is $\boldsymbol{P}=c\frac{\varepsilon_i-1}{4\pi}\varepsilon_i\boldsymbol{E}_e$, whence $\varepsilon = 1 + c\varepsilon_i(\varepsilon_i-1)$. In this case, the perpendicular diffusion coefficient is

$$D_{\perp}=D_e[1+c(1-s)]. \tag{64}$$

In the case where the impurities have a cylindrical shape and are positioned perpendicularly to the external field, a uniform field is created inside the cylinder [13]:

$$\boldsymbol{E}_i=\frac{2}{1+\varepsilon_i}\boldsymbol{E}_e. \tag{65}$$

Hence, the average polarization is $\boldsymbol{P}=c\frac{\varepsilon_i-1}{4\pi}\times\frac{2}{1+\varepsilon_i}\boldsymbol{E}_e$ and the perpendicular diffusion coefficient is

$$D_{\perp}=D_e\left[1+c\frac{2(1-s)}{1+s}\right]. \tag{66}$$

Equations (63), (64), and (66) coincide with Eq. (49). In the same manner, it can be shown that, in the case of spherical lumps, the diffusion coefficient is

$$D=D_e\left[1+c\frac{3(1-s)}{2+s}\right]. \tag{67}$$

The obtained equations are valid in the first order with respect to c. For this approximation, the diffusion coefficient depends only on concentration c. If the concentration increases, the field "acting" on each lump differs from the "average" field in the lattice, and, generally speaking, the average diffusion coefficient depends on the lattice structure.

The author is indebted to B. I. Il'ichev, N. I. Laletin, and Ya. V. Shevelev for the discussion of this paper.

LITERATURE CITED

1. S. M. Fainberg, Transactions of the International Conference on the Peaceful Uses of Atomic Energy, Geneva, 1955 [in Russian] (Izd. AN SSSR, Moscow, 1957) Vol. 5, p. 578.
2. A. D. Galanin, Theory of Thermal Neutron Nuclear Reactors [in Russian] (Atomizdat, Moscow, 1959).
3. Ya. V. Shevelev, Atomnaya Energ. 2, 3, 217 (1957).*
4. D. Behrens, Proc. Phys. Soc. A 62, 607 (1949).
5. B. Spinrad, J. Appl. Phys. 26, 548 (1955).
6. Ya. V. Shevelev, Atomnaya Energ. 2, 3, 224 (1957). *
7. L. Trlifai, Atomnaya Energ. 2, 3, 231 (1957).*
8. V. V. Smelov, Atomnaya Energ. 6, 5, 546 (1959).*
9. N. I. Laletin, Transactions of the Second International Conference on the Peaceful Uses of Atomic Energy, Geneva, 1958. Reports by Soviet Scientists: Nuclear Reactors and Nuclear Power Engineering [in Russian] (Atomizdat, Moscow, 1959) Vol. 2, p. 634.
10. P. Benoist, Rapport S. P. M., No. 522, Saclay (1958).
11. B. Davison, J. Nucl. Energy. 7, 51 (1958).
12. I. M. Ryzhik and I. S. Gradshtein, Tables of Integrals, Sums, Series, and Products [in Russian] (Gostekhteorizdat, Moscow, 1951) Equation 6.540.2.
13. L D. Landau and E. M. Lifshits, Electrodynamics of Continuous Media [in Russian] (Gostekhteorizdat, Moscow, 1957) p. 63.

*Original Russian pagination. See C. B. translation.

A STUDY OF THE TRANSFER OF RADIOACTIVE MATERIALS BY STEAM AND WATER, AND THE CHEMICAL STABILITY OF DEPOSITS IN THE STEAM-WATER LOOP OF THE FIRST ATOMIC POWER STATION

P. N. Slyusarev, G. N. Ushakov, O. V. Starkov, L. A. Kochetkov, L. N. Nesterova, and V. Ya. Kozlov

Translated from Atomnaya Énergiya, Vol. 9, No. 8, pp. 98-103, August, 1960
Original article submitted November 23, 1959

An important problem in the design of boiling reactors or reactors with boiling and superheating of the steam in channels is the study of the level of contamination of steam by radioactive materials, generated and directed into the turbine, the physicochemical properties of the radioactive deposits and the possibility of deactivation of the internal surfaces of the pipes and turbine.

At the first atomic power station, studies were made on the transfer of radioactive materials by steam and water in the loop built into the first circuit of the power station. A determination was made of the coefficient of deposition of the materials on the internal surface of the pipes, and the chemical stability of the deposits was studied. Studies were made on problems of deactivation of some parts of the steam power equipment of the station.

Introduction

It is well known [1-3] that the radioactivity of steam in boiling reactors with nuclear superheating, due to the entrainment of radioactive materials in the boiling zone, can be about 0.01% of the level of radioactivity in the boiling water. However, this value depends to a considerable extent on the type of reactor operation and the design of evaporators and separators. The radioactivity of steam caused by activation of impurities in the steam when it passes through the active zone (τ = 0.02 sec) is very small in practice. It is difficult to calculate the radioactivity of steam caused by washing out active corrosion products and deposits from the internal surface of the circuit, especially for certain systems and unstable operation of the installation. The oxygen radioactivity of the steam was not taken into account.

Description of the Installation

The steam-water loop [4] consisted of two circuits of 1Kh18N9T stainless steel (Table 1), insulated from one another and mounted in the reactor of the first atomic power station (Fig. 1). The coolant was regular distilled water. The heat source was provided by heat-evolving elements of the reactor channels of the atomic power station.

The working channels B I of the circuit were cooled by water which passed through the heat exchanger 1 and was further cooled in the cooler 2, and the working channels A II of the circuit were cooled by steam superheated to the given temperature. The coolant was circulated by the circulation pumps 3 and 4. The steam obtained in the vaporizer 1 was directed to the steam superheating channels (SSD) and then through a heat exchanger 6 and cooler 5 they were returned to the vaporizer.

TABLE 1

Characteristics of Circuits I and II of the Steam-Water Loop

Parameters	Circuit I	Circuit II
Pressure, atm	95-100	40-60
Flow of coolant, ton/hr	10	1
Volume, m^3	0.33	0.61
Pressure drop along route, atm	11	11
Number of channels	10	3

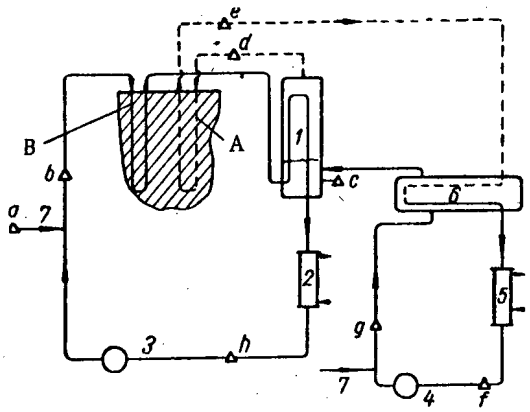

Fig. 1. Arrangement of steam-water loop. Samples were taken from the following points: a) from feed tank; b) from the head of pump I of the circuit; c) from the vaporizer of circuit II; d) from the inlet to the steam superheating channel of circuit II; e) from the outlet of the steam superheating channel of circuit II; f) from the suction side of the pump of circuit II; g) from the head of the pump of circuit II; h) from the suction part of the pump of circuit I.

The first and second circuits of the loop were fed with distilled water 7. Two systems were investigated: with superheating of the steam (working channels) and without superheating of the steam (blank channels). The water temperature at the inlet to the SSD was 265°C, at the outlet it was 310°C (with steam content of 25%) and in the case of superheating of the steam—at the inlet 275°C, at the outlet—340-365°C.

Points for the removal of coolant samples were placed along the routes of circuits I and II of the loop. The samples were taken with a steady system. The places where samples were taken along the circuits of the loop are designated by Latin letters (see Table 2).

In each sample of the coolant, measurements were made of the β and γ activity, the amount of dry residue, pH of the medium, studies were made of the radioisotope, anion and cation compositions of the impurities.

Transfer of Radioactive Materials by Steam and Water

The transfer of radioactive materials by steam and water was studied from the change in level of the radioactivity of the dry residue along the route of the loop. Samples of the coolant were taken regularly over a long period of time. Table 2 gives the results of measurements on the level of radioactivity of the coolant along the route of circuit II of the loop during various periods of operation. The periods are due to the fact that the operation of the loop was interrupted or was changed to a different system. In the first and second periods the steam passed through channels without superheating the steam; in the third and fourth periods it passed through the channels with superheating of the steam. The days were counted from the day when a stable system was established. The system was changed over to steam by gradually replacing water in the SSD by steam [5].

In the initial period when the loop operated on steam the radioactivity of the dry residue of the coolant at the outlet from the SSD was much greater than at the input. This difference is gradually reduced since the deposits or corrosion products are washed out. Deposition takes place during this period at the section of outlet from the SSD—the suction part of the pump of circuit II; the radioactivity of the dry deposit at the suction part of the pump is less than at the outlet from the SSD. This difference is also gradually reduced. These phenomena are caused by the change in rate of elution and precipitation of deposits in the loop, and also by the change in quality of the coolant. Before exit into the steam system in the working channels, water was circulated with a

TABLE 2

Radioactivity of Dry Residue of the Coolant in Circuit II of the Loop, 10^{-8} C/kg

Points of sample removal	Periods													
	first	second				third				fourth				
	days													
	5	2	3	4	5	2	3	4	5	5	6	7	10	11
d	2,6	7,0	3,8	3,6	2,8	19	2,9	1,0	1,4	2,1	1,0	0,5	2,5	6,0
e	3,2	19	5,3	4.5	3,0	41,0	9,2	3,2	3,6	2,8	1,7	0,8	1,7	2,1
f	2,8	7,1	3,3	samples were not taken		14	4,6	2,5	3,3	—	2,4	1,8	4,1	8 8
d, *e*	+0,6	+12	+1,5	+0,9	+0,2	+22,0	+6,3	+2,2	+2,2	+0,7	+0,7	+0,3	−0,8	−3.9
e, *f*	−0,4	−12	−2,0	samples were not taken		−27,0	−4,6	−0,7	−0,3	—	+0,7	+1,0	+2,5	+6.7

Note. The accuracy of measurements was ± 0.1 · 10^{-8} C/kg.

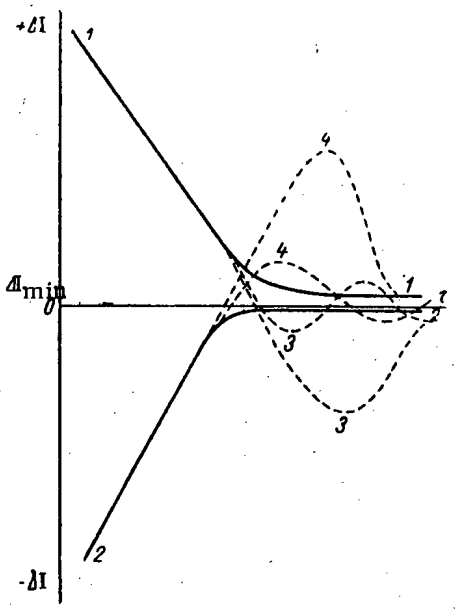

Fig. 2. Relative changes in radioactivity ΔI of a dry residue of steam and water in relation to the time of operation of the loop: 1) difference in radioactivity of the dry residue of steam and water at the points d and e; 2) the difference in radioactivity of the dry residue of steam and water at the points e and f; 3, 4) the curves for difference in radioactivity with fluctuations in the quality of the steam.

higher content of salts, which were deposited on the walls of the channels. Since the steam has a lower content of salts, in the steam system the prevailing process is the elution of the previously settled deposits. The contaminated steam, passing the section of outlet from the SSD—the suction part of the pump of circuit II, loses a part of the previously washed radioactive deposits, as a result of which the radioactivity at the sampling point f is reduced. With the passage of time, these selective processes are retarded and dynamic equilibrium should be established between the content of impurities in the coolant and deposits at the inside surfaces of the loop. Figure 2 shows the experimental curves representing the change in difference of radioactivities of the dry residue of the superheated steam and water in relation to the time of operation of the loop. The symbol ΔI_{min} represents the increase in radioactivity due to activation of the impurities or due to elution of the corrosion products from the channels of the active zone. With changes in the quality of steam, the curves can assume the form of curves 3, 4 of Fig. 2.

The Physicochemical Factors of the Coolant in Circuits I and II

These factors are given in Table 3. The radioisotope composition of impurities in the coolant of the loop circuit and the first circuit of the atomic power station are the same.

The radioactivity of water in the evaporator during blowing is reduced from 5 · 10^{-8} C/kg. The radioactivity of the steam is ~ 10% of the radioactivity in the evaporator (the entrainment factor is 1 · 10^{-1}).

The entrainment factor obtained in our experiments is 100-1000 times greater than the factors given in [6]. This is due to the features of design of the evaporators and separator and to the fact that in our experiments the concentration of active impurities of the water in the evaporator differs considerably from the activity of solutions described in [6].

TABLE 3

Physicochemical Factors of Feed Water and Water of Circuits I and II of the Loop

Point of sample removal	Dry residue, mg/liter	Total β and γ activity, 10^{-8} C/kg	pH	Concentration of ions, mg/kg			Concentration of chromium		
				CO_2	NO_3'	Cl'	total, mg/kg	CrO_4'', %	Cr^{+3}, %
Feed water	0,9—1,3	0	6,2	0,6	<0,4	<0,02	0	0	0
Water of circuit I	2,5	220—2200	5,4	0,9	1,2	<0,02	0,27	~90	~10
	4,2	500—5000	5,2	Not determined					
Water of circuit II	1,3—2,1	5—50	5,2—5,8	0,9	1,2	<0,02	0,048—0,24	~80	~20
	0,6—1,1	1—7	5,4	0,9	<0,4	<0,02	0,008—0,024	~20	~80
	0,6—1,1	0,5—19	5,4	0,9	<0,4	<0,02	0,016—0,032	~20	~80
	0,6—1,1	3—7	5,2	0,9	<0,4	<0,02	0,032—0,040	~50	~50
	0,6—1,1	3—5	5,5	0,9	<0,4	<0,02	0,024—0,032	~50	~50

Note: Radioisotope composition of impurities: Co^{60}, Fe^{59}, Cr^{51}, Ca^{45} (4-10% of the total β and γ activity); Na^{24}, Cu^{64}, Ni^{65}, Si^{31}, Mn^{56} (90-96% of the total β and γ activity). Radioactive components with $T_{1/2}$ < 1 hr were not considered.

In the evaporator the dry residue with long-lived radioisotopes becomes concentrated, and also the ions NO_3' and CrO_4''. The total quantity of chromium, a corrosion product, changes along the loop. The relationship of the valence states of chromium at the sample collection points is different. From the evaporator there is selective entrainment of the unoxidized chromium, including Cr^{3+}.

In the coolant at the suction part of the pump, there is an increase in the chromium content (in the form of CrO_4''). This can be explained either by the elution of the chromates from the surface of the loop at the section of outlet of the SSD to the suction part of the pump, or by a temporary factor during the establishing of equilibrium under the action of products of radiolysis or radiation;

$$Cr_{red}\ (Cr^{+3}) \rightleftharpoons Cr_{ox}\ (CrO_4'').$$

On the header side of the pump from circuit II the total content of chromium decreases due to dilution of the circuit water by distilled feed water. Despite the absolute fluctuations, the relationship of the pH values of the coolant along the loop remains constant with a stable operating system. When the stability of the system is disturbed the relationship of the pH of the coolant is disturbed at the points where samples are taken. In all cases the pH of the coolant is less than that of the feed water, which can be explained by the formation of carbonic, nitric and chromic acids.

Deposits on the Walls of the Tubes and Their Chemical Stability

To evaluate the level of radioactivity and the chemical stability of deposits on the internal surface of the pipes of the loop, studies were made of deposits forming on a special apparatus. The apparatus consisted of two identical tubes of ÉI-695 steel (d = 9.4 × 0.6 mm and L = 1200 mm) with an electrical heater.

One tube, operating in a boiling water system, was in the blow line from the first circuit of the reactor. The water temperature at the inlet to the tube was 235°C, at the outlet it was 290°C; the steam content was 5%. The other tube was placed at the blow line of the superheated steam from circuit II of the loop. Here the temperature of the steam at the inlet to the tube was 247°C, steam content 94%, steam temperature at the outlet 345°C and steam content 100%. The flow of water and steam was 200 kg/hr, the time of operation in the boiling system was 900 hr, in the superheated steam system it was 600 hr, water pressure 95-110 atm, steam pressure 40-60 atm.

TABLE 4

Characteristics of Deposits Forming in Tubes

Characteristics of deposits	Superheated steam			Boiling system		
	Specimens					
	1	2	3	4	5	6
External appearance	Brown-black, dense, mat.			Black, small crystalline with lustre		
Thickness, μ	30	14	21	19	24	17
Radioactivity (on third day), C/cm^2	$1.5 \cdot 10^{-9}$	$0.7 \cdot 10^{-9}$	$1.1 \cdot 10^{-9}$	$1.6 \cdot 10^{-6}$	$1.8 \cdot 10^{-6}$	$1.7 \cdot 10^{-6}$
Temperature of walls of tubes, °C	300	400	600	235	350	400

After the end of the experiment, specimens were cut from the tubes—rings of height 3 mm, which were then cut up into two half cylinders; specimens were cut from three sections of each tube. The deposits on the inner surface were studied to measure the thickness of deposits, the level of β and γ activity, the energy of the γ radiation, the half-life period of the long-lived radioisotopes and the chemical stability of the deposits. The characteristics of the deposits are given in Table 4. An investigation of deposits on all specimens showed that the quantity of radioisotopes with $T_{1/2} \geq 27$ days (Co^{60}, Fe^{59}, Cr^{51}, Ca^{45}) is 70%, with $T_{1/2} \leq 13$ hr (Na^{24}, Cu^{64}, Mn^{56}, Ni^{65}, Si^{31})—30%.

As regards the half-life period and the energy of γ radiation, the composition of the radioactive components is constant in all specimens. The chemical stability of deposits on the specimens was determined from the reduction in their radioactive after the action of various chemical reagents on them. The data of chemical stability of deposits of specimens are given in Table 5.

The chemical stability of deposits forming in the superheated steam system increases noticeably with increase in temperature of heating. On the basis of the obtained data it was possible to calculate the deposition factor for long-lived radioisotopes (Co^{60}, Fe^{59}, Cr^{51} and Ca^{45}) for both systems. The deposition factor for the boiling system $K_b = 1.4 \cdot 10^{-1}$, for the superheated steam system $K_s = 1.1 \cdot 10^{-2}$.

A characteristic of the boiling system is the high content of salts in the coolant, increased pressure and lower linear speed of movement of the coolant. The thickness of the radioactive layer obtained on the basis of experimental data is 3 μ for the boiling system, the total thickness of deposits is about 25 μ. The deposits should apparently be considered as the products of reaction between the material of the structure and the medium. From this standpoint we propose the presence of three layers in the deposits: a layer of radioactive deposits, an intermediate layer and a nonradioactive corrosion layer.

Deactivation of Equipment in an Atomic Power Station

Experience in the operation of the first atomic power station shows that during operation the inner surface of the first circuit (1Kh18N9T steel) has a layer of β and γ active deposits. The main sources of radiation are Co^{60}, Fe^{59}, Ca^{45}, and Cr^{51}. Deactivation was carried out on sections of the incoming and outgoing pipes of the operating channels, isolating the devices, T-joints, flow-measuring discs and components of the heat exchanges.

For the deactivating media we used various aggressive solutions both with inhibitors and without them. The inhibited solutions are solutions of 6% HCl with urotropine and a mixture of 5% HNO_3 and 2.0% HCl with a solution of $K_2Cr_2O_7$ (concentration of the latter ~ 0.05 g/liter); the uninhibited solutions were a mixture of 5% HNO_3 and 5-7% HCl. The experiments were carried out under static conditions at a temperature of 20°C and treatment time of 24-48 hr at a temperature of 40-60°C and time of treatment 2-4 hr. The coefficient of deactivation K_d was calculated from the ratio of the initial activity of the specimen to the final activity, and the coefficient of rate of corrosion K_c was determined by the usual method and expressed in $g/m^2 \cdot hr$. It was found that the use of inhibited solutions of 6% HCl with urotropine and a mixture of HNO_3 and HCl with potassium bichromate was

TABLE 5

Chemical Stability of Deposits, %

Deactivating medium time and temp. of treatment	Specimens					
	1	2	3	4	5	6
H_2O, $\tau = 1$ hr, $t = 100$°C	100	100	100	100	100	100
HNO_3 (5%), $\tau = 1$ hr, $t = 100$°C	100	100	100	100	100	100
HNO_3 (30%), $\tau = 2$ hr, $t = 20$°C	99	99	98	98	98	98
HNO_3 (30%), HCl (5%), $\tau = 0{,}5$hr, $t = 20$°C	0	50	98	0	0	0
	10* / 90	11 / 89	4 / 96	26 / 74	10 / 90	4 / 96

*The numerator shows the percentage of dissolved radioactive materials, the denominator shows the percentage of radioactive material in the suspended state.

ineffective for the deactivation of the first circuit, since for K_c equal to 0.5 g/m^2 · hr for the first solution and 0.003 g/m^2 · hr for the second, $K_d < 3$. Disturbing the inhibiting process increases not only the rate of corrosion of the steel, but also K_d. After deactivation, the specimens were washed to the lower limit of sensitivity of the measuring instrument.

The corrosion takes place intensively at the metal-deposit boundary, therefore the destroyed layer (in the form of brown flakes) is removed. This layer containing 60-800% of the initial activity of the specimen and is a chemically stable compound. The deposits are only completely dissolved in a mixture of 25% HCl and 30% HNO_3 at a temperature of 30°C over a period of 50 min. For uninhibited solutions of a mixture of 5% HNO_3 and 0.6-0.7% HCl, the dependence of the coefficients of deactivation $K_d = f(\tau)$ was obtained for certain concentrations of HCl, and also values of K_d and K_c for a mixture of 12% HCl and 5% HNO_3. Under our conditions the optimum conditions of deactivation were a mixture of 5% HNO_3 and 2.1% HCl, $K_d \rightarrow \infty$ (to the lower limit of sensitivity of the instrument), K_c equal to 2-3 mg/m^2 · hr, temperature 20°C, time of treatment 18-20 hr.

During the experiments a number of practical problems were solved concerned with the deactivation of individual components of the structures and parts of circuit I of the atomic power station loop. The initial radioactivity reached 16 microrutherfords. The medium was a mixture of 5% HNO_3 and 7% HCl, having a temperature of 60°C, in 20 min this medium completely deactivated the isolating device, the T-joint, the flow-measuring discs and the heat-exchanger components. The deactivation was carried out under static conditions, after which the components were washed with water and kerosene by Petrov contact. After treatment, the components were put back into operation.

A mixture of 5% HNO_3 and 5% HCl was used to deactivate the circuit I of the dismantled loop of the Atomic Power Station. The time of deactivation was 130 min, temperature 50-60°C, amount of removed radioactivity $1 \cdot 10^{-2}$ C with volume of solution about 1.5 m^3. Spectrum analysis of the solution after deactivation showed that the content of iron, silicon, nickel, chromium and calcium had increased considerably. There was no selective elution of the radioisotopes during deactivation. The radioactivity of the solution after deactivation was mainly due to radioactive suspensions. Their fraction of radioactivity increased with the temperature at which the deposits were formed.

The radioactive deposits are more chemically stable to the action of aggressive deactivating media than construction material of 1Kh18N9T steel.

In conclusion we take pleasure in thanking A. K. Krasin for his interest in this work.

LITERATURE CITED

1. N. A. Dollezhal', Atomnaya Énerg. 3, 11, 391 (1957).•
2. T. H. Handley and S. Untermeyer, Collection: Corrosion in High-Purity Water [Russian translation](Moscow, 1958) article 25, p. 25.
3. A. Shor, et al., Nuclear Sci. and Eng. 2, 2, 126 (1957).
4. N. A. Dollezhal', et al., Proceedings of the Second International Conference on the Peaceful Uses of Atomic Energy, Geneva, 1958. Report of Soviet Scientists. Nuclear Reactors and Nuclear Power [in Russian] (Atomizdat, Moscow, 1959) p. 30.
5. N. A. Dollezhal', Atomnaya Énerg. 5, 3, 223 (1958). •
6. W. Zienn, Nuclear Sci. and Eng. 1, 5, 420 (1957).

•Original Russian pagination. See C. B. translation.

THE RECRYSTALLIZATION OF COLD-ROLLED URANIUM

G. Ya. Sergeev, V. V. Titova, and L. I. Kolobneva

Translated from Atomnaya Énergiya, Vol. 9, No. 8, pp. 104-109, August, 1960
Original article submitted February 3, 1960

This paper gives the results of investigations into the effect of rolling and annealing in the α region on the structure and mechanical properties of uranium. The initial material was uranium which had been cast, rolled in the γ region and quench-hardened from the β region. Small-grain recrystallized uranium has much higher strength than the initial coarse-grained uranium. Approximate recrystallization diagrams are plotted for 5-40% degrees of reduction and annealing at temperatures of 350-650°C with soaking for 10 hr. The recrystallization is almost independent of the investigated initial states of the material. Data are given on the kinetics of the recrystallization processes. The addition of 0.1 wt.% of molybdenum slows down considerably the recrystallization of uranium and increases the strength of the small-grained uranium by ~ 20%.

Plastic deformation with subsequent annealing at fixed temperatures in the α region is one of the most widely used methods for making components from uranium and, in particular, the cores of heat-evolving elements in the form of bars, tubes, discs, etc. In this connection it is necessary to know the changes in structure and physical and mechanical properties of uranium as a result of deformation and annealing, i.e., to know the recrystallization processes. In a number of cases the recrystallization of deformed uranium is observed when components are irradiated [1] or subjected to cyclic heat treatment [2, 3].

Some information on the recrystallization of uranium which has been deformed in the α region is given in [4-9], however, data on the recrystallization diagram and the change in mechanical properties of uranium during recrystallization have not been published in these papers. The recrystallization diagrams were first given in [10].

Material and Method of Investigation

The investigated material had the following chemical composition (wt. %): 99.7 U; $(5-8)\cdot 10^{-3}$ Fe; $(2-4)\cdot 10^{-3}$ Si; $(1-2)\cdot 10^{-4}$ Ni; 0.02 C; $(4-5)\cdot 10^{-3}$ N. Before cold rolling the cast uranium was rolled in the γ region (at temperatures of 950-900°C, degree of deformation ~ 80%, with slow cooling) and quench hardening from the β region (at temperatures of 720-730°C, soaking for 30 min, cooling in water).

The deformation was carried out at room temperature by rolling to sheet with 5-40% reductions. The deformed uranium was annealed at temperatures of 350-650°C in vacuum furnaces; the vacuum was 10^{-4} mm Hg. The structure of the uranium was revealed by electrolytic polishing and etching. The sections were investigated in ordinary illumination and in polarized light; they were photographed in a bright field. The mechanical properties were determined with small specimens of length 17 mm and diameter of the working part 3 mm.

Results of Investigation

Change in the microstructure and mechanical properties of uranium during cold rolling. Figure 1(a,b,c) gives typical structures of uranium in three initial states. Uranium which has been cast and rolled in the γ region is very coarse grained. The grains measure up to 1.5-2.5 mm and have very different orientation; they consist of

a

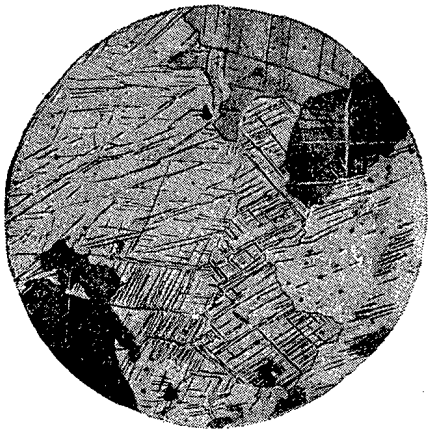

b

c

Fig. 1. Microstructure of initial uranium: a) cast (× 70); b) rolled in the γ region (× 70); c) quench-hardened from the β region (× 134).

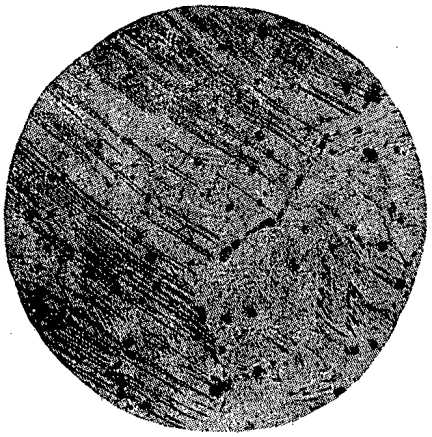

Fig. 2. Microstructure of uranium cold rolled with 15% reduction (× 34).

sub-grains of size 200-500 μ with close crystallographic orientation. Quench-hardening from the β region reduces the grain size of uranium to 100-200 μ.*

Rolling with small reductions (5-15%) does not give uniform deformation. The greatest deformation takes place in grains which are favorably orientated with respect to the acting force. The numerous fine twins have a preferred direction within the limits of one grain, which changes somewhat at the boundaries of the sub-grains (Fig. 2). With increase in the reduction the deformation is gradually extended to the whole volume of the specimen, and with reductions exceeding 40% the uranium acquires a typical fibrous structure.

Figures 3 and 4 a illustrate the changes in the mechanical properties of rolled uranium as a function of the degree of deformation. With increase in deformation to 40-50%, the hardness H_V increases by about 35% (from 230-240 to 320-330 kg per mm^2), the tensile strength σ_b increases by 75% (from 40 to 70 kg/mm^2) and the relative elongation δ remains almost constant.

The effect of annealing in the α region on the structure and mechanical properties of cold-rolled uranium. Rolled specimens with 5-40% deg of deformation were annealed for 10 hr at temperatures of 350, 400, 450, 500, 550, 600, 625, and 650°C. Figure 5 illustrates the structural changes in uranium as a function of the degree of deformation and the system of annealing in the α region.

Annealing at 400°C leads to the appearance of separate new grains only in specimens deformed by 20-40%. As a rule, the new grains are very small (less than 10 μ); they are at places of maximum deformation on the twins and have a drawn-out shape. After annealing at 450°C, individual sections with

*During the investigation it was found that the initial state of the material does not have very much effect on its structural changes during cold deformation and subsequent recrystallization annealing. These data are therefore mainly given for uranium which has first been rolled in the γ region.

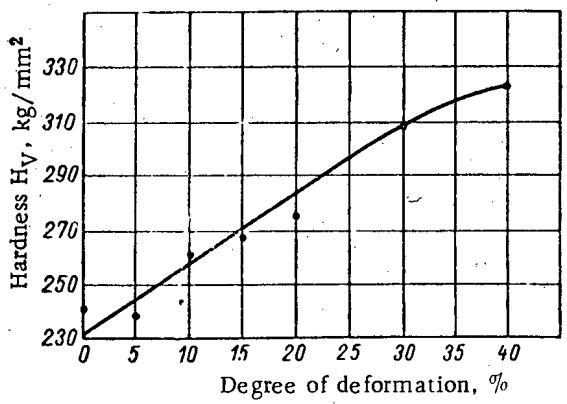

Fig. 3. Change in the hardness of uranium as a function of the degree of deformation during cold rolling.

recrystallized grains also appear in specimens deformed by 5-15%. The volume of metal subjected to recrystallization increases with the degree of deformation; with 40% deformation almost the whole of the specimen is recrystallized. The length of the recrystallized grain at all stages of deformation is equal to ~ 10 μ.

With increase in the annealing temperature (500, 550, 600°C) the recrystallization processes also develop at low degrees of deformation. In all cases the length of the recrystallized grain increases. The temperature of 600°C is the temperature of total recrystallization for all investigated degrees of deformation. The structure of weakly deformed specimens differs in the unevenness in dimensions and the variety of grain shapes. At high degrees of deformation (20-40%) the

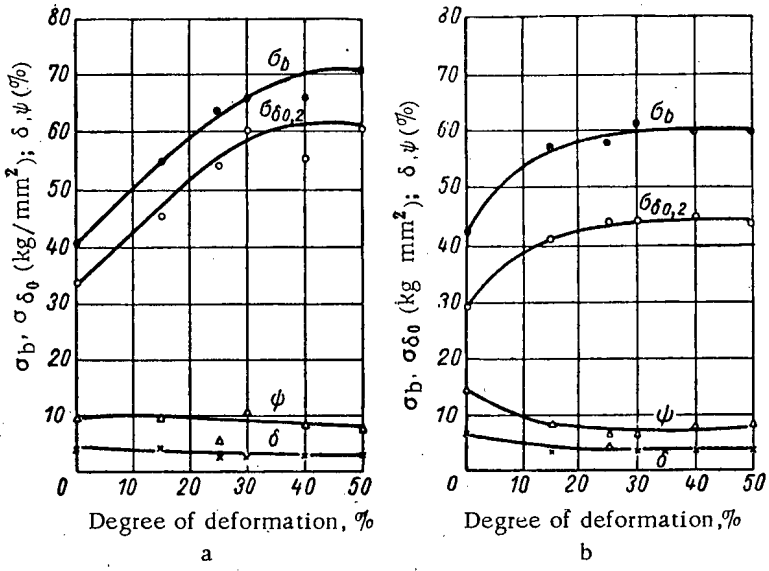

Fig. 4. Mechanical properties of deformed (a) and recrystallized (b) uranium.

grains take on clear shapes and become polygonal. Annealing at 650°C leads to selective recrystallization and, at small degrees of deformation, to the formation of a coarse-grained heterogeneous structure. Thus, with a 5% reduction the average size of the grain is equal to 150-220 μ with maximum and minimum values of 350 and 40 μ.

On the basis of data obtained in metallographic investigations, approximate recrystallization diagrams were plotted for uranium which had been rolled in the γ region (Fig. 6a) and quench-hardened from the β region (Fig. 6b). The features of the diagrams are of the same type. The x-ray analysis method* was used to determine the temperature threshold of the start of recrystallization (the dotted line on the diagrams of Fig. 6a,c), which corresponds to 380-420°C, depending on the degree of deformation. The critical degree of deformation appears sufficiently clearly at temperatures exceeding 600°C, and with increase in the annealing temperature it is displaced towards smaller values with ~ 10% at 600°C to < 5% at 650°C. (According to the data of [4, 9] the critical degree of deformation for uranium corresponds to 2.5%.)

The kinetics of the recrystallization processes were studied on uranium which had been cast and treated in the γ region, cold rolled with reductions of 10 and 40% (Fig. 7a, b). Annealing was carried out at 550, 600

*The x-ray studies were carried out by P. P. Egorov.

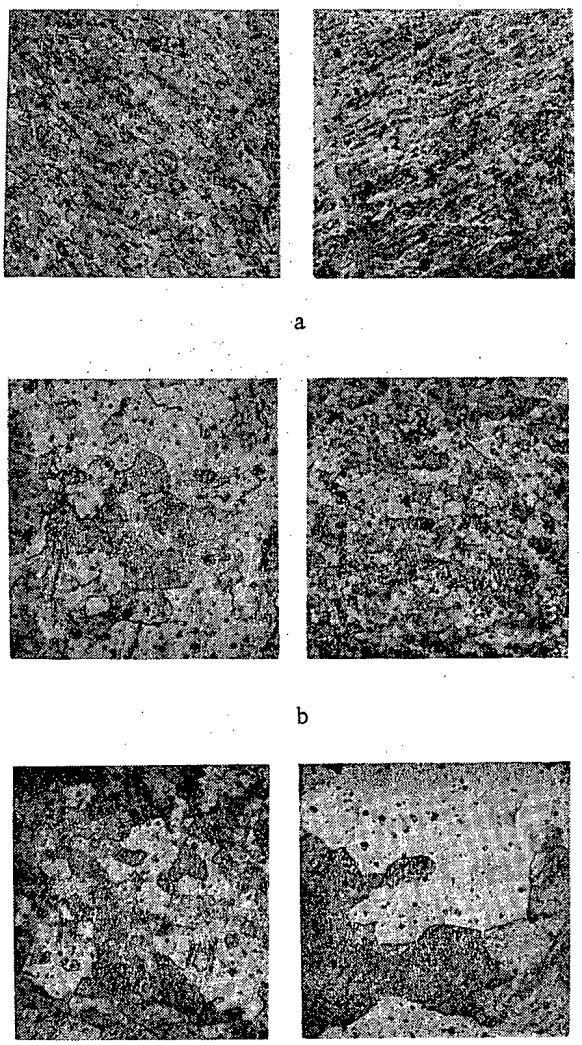

Fig. 5. The microstructure of deformed uranium after 10 hr of recrystallization annealing at: a) 450°C; b) 600°C; c) 650°C (× 134). Reduction: left—40%, right—5%.

and 625°C. The time of annealing varied from 5 min to 48 hr. The data obtained for uranium which had been cast and that which had been treated in the γ region, are of the same type (see Fig. 7a). Increasing the time of annealing at 550°C has almost no effect on the grain size for both small (10%) and for large (40%) degrees of deformation. With increase in the time of annealing at 600°C in specimens deformed by 10%, at first there is total recrystallization and then selective recrystallization commences (the grain size increases from 15 μ after annealing for 5 min, to 110-120 μ after annealing for 48 hr). Specimens deformed by 40% are completely recrystallized; however, the grain growth is insignificant. At 625°C intensive selective recrystallization is also observed in specimens deformed by 40% (Fig. 8a).

Results for the hardness of deformed and annealed specimens of uranium showed that noticeable disordering of the cold-rolled uranium only occurs at annealing temperatures above 400°C (Fig. 9), which is in good agreement with the temperature threshold of recrystallization, determined metallographically. The most complete disordering occurs at 600-650°C, when after 2 hr annealing the hardness for all degrees of deformation is 195-210 kg/mm^2.

Recrystallization annealing reduces the strength characteristics of deformed uranium, however for all degrees of deformation they remain higher than the corresponding characteristics of the initial material (see Fig. 4 a,b).

The effect of an addition of 0.1 wt. % of molybdenum on the recrystallization of uranium. As is well known, impurities in metals hinder the recrystallization processes. There are only a few, incomplete accounts of the effect of impurities on the recrystallization of uranium [4]. We studied recrystallization processes in uranium alloys with 0.1 wt.% of molybdenum.

The structure of the cast alloy is almost the same as that of cast uranium. The changes in the structure of the cast alloy during cold rolling are similar to those which were observed when studying cast uranium. In this case, as in the case of uranium, the hardness at a reduction of 40% increases by about 35%.

Figure 6c shows the recrystallization diagram for cold-rolled alloy of uranium with 0.1 wt.% molybdenum. A comparison of this diagram with those for the recrystallization of unalloyed uranium (see Fig. 6a,b) shows that the addition of molybdenum in the amount shown considerably retards the recrystallization. Thus, the start of recrystallization for this alloy is observed microscopically at higher temperatures (50-100°C higher, depending on the degree of deformation). A considerable reduction is observed in the value of the recrystallized grain when annealing at 650°C, especially for low degrees of deformation. The critical degree of deformation of the alloy, as for pure uranium, is displaced towards lower degrees of deformation with increase in temperature.

Figure 7b gives the critical curves for change in the size of the recrystallized grain of a uranium alloy with 0.1 wt.% of molybdenum, deformed by 40%. Whereas selective recrystallization of unalloyed uranium, deformed by 40%, was observed at 625°C (see Figs. 7a and 8a), the annealing of the alloy even at 650°C only leads to a very small increase in the grain (see Figs. 7b and 8b). It has been calculated that the rate of selective

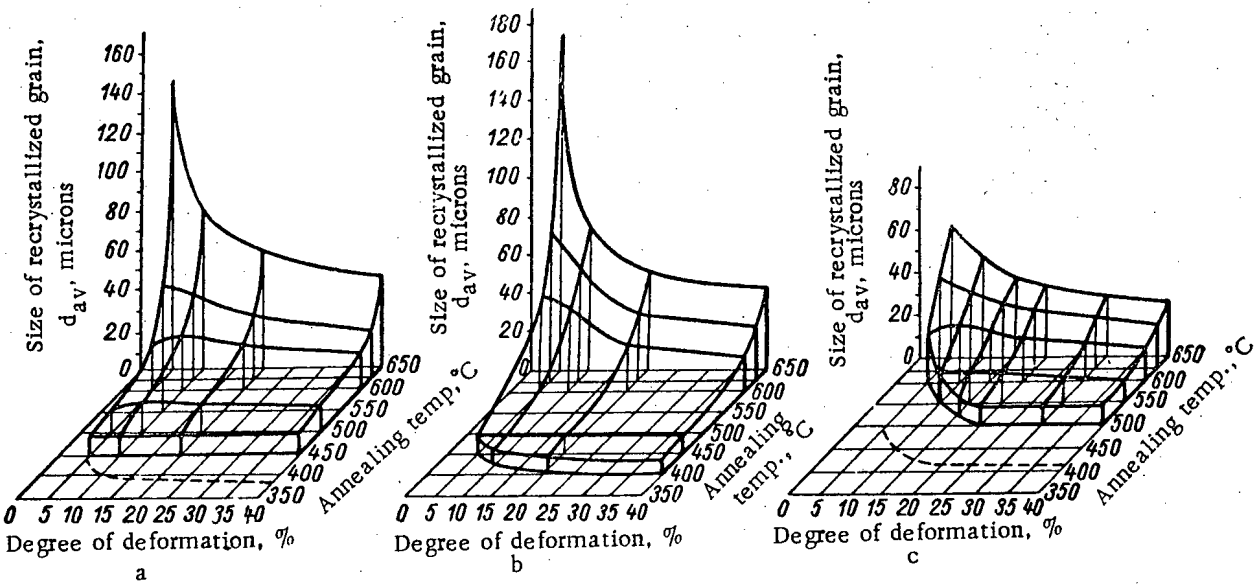

Fig. 6. Approximate diagrams for the recrystallization of uranium (time of annealing 10 hr). Initial material: a) uranium rolled in the γ region; b) uranium quench-hardened from the β region; c) cast alloy of uranium with 0.1 wt. % molybdenum.

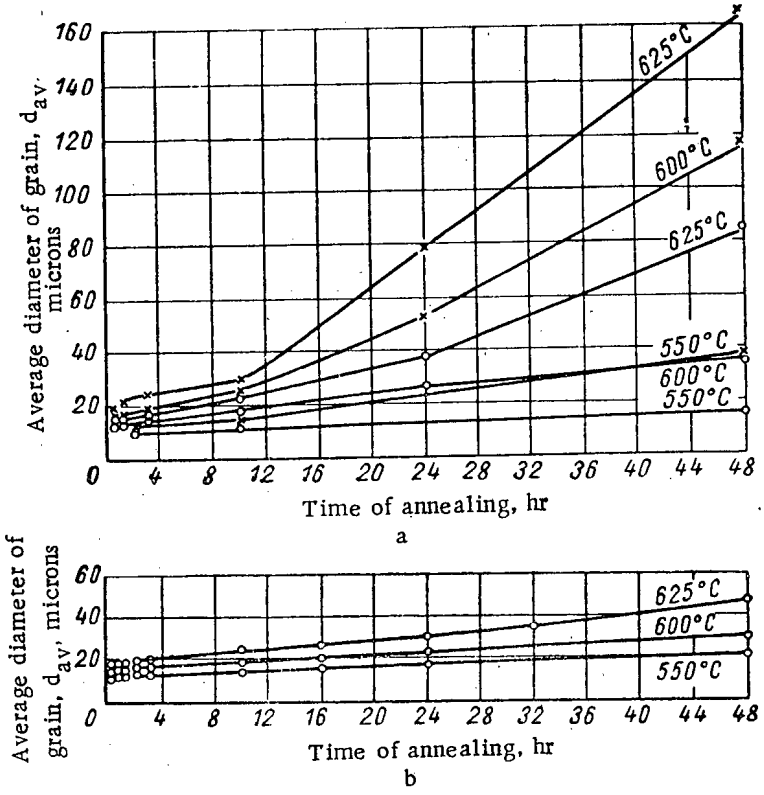

Fig. 7. Kinetic curves for the change in grain size of uranium (a) and its alloy with 0.1 wt.% molybdenum (b) depending on the degree of reduction and the type of recrystallization annealing. Degree of reduction: x – 10%; O – 40%.

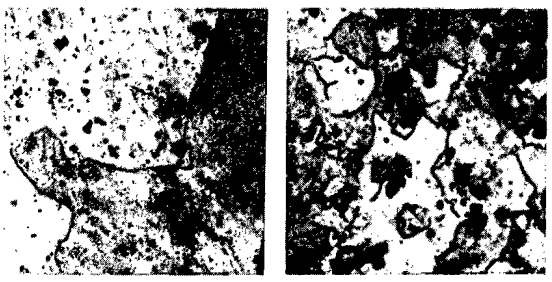

a b

Fig. 8. Change in the microstructure of uranium and its alloy with 0.1 wt.% molybdenum, deformed by 40%, depending on the type of annealing (x 189): a) uranium annealed at 625°C for 48 hr; b) alloy of uranium with 0.1 wt. % molybdenum, annealing at 650°C for 48 hr.

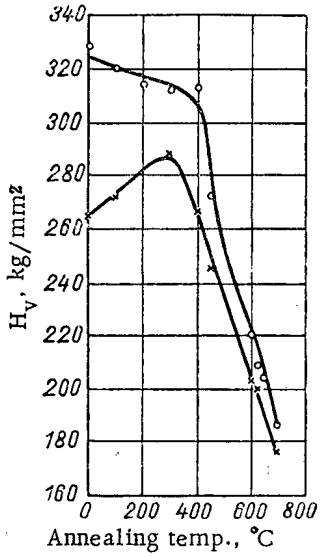

Fig. 9. Change in the hardness of cold-rolled uranium vs annealing temperature. Duration of annealing, 2 hr. Degree of reduction: x – 10%; O – 40%.

recrystallization of the alloy at 650°C is almost a third of the rate of selective recrystallization of uranium at 625°C (0.66 and 1.9 μ/hr, respectively).

Measurements of the hardness of annealed specimens of the alloy showed that the temperatures for the start of disordering and total disordering, as in the case of uranium, are displaced towards higher values (500 and 625°C instead of 400 and 600°C compared with uranium). The addition of 0.1 wt.% of molybdenum considerably hardens the fine-grained recrystallization uranium. Thus, for the same grain size the strength of the alloy is about 20% greater than that of uranium.

LITERATURE CITED

1. J. Bloch, Acta Met. 6, 2, 126 (1958).
2. B. Mott and H. Haines, J. Inst. Metals 80, 621 (1952).
3. A. A. Bochvar, G. I. Tomson, and N G. Chebotarev, Atomnaya Énerg. 4, 6, 555 (1958).*
4. Foot, Proceedings of the International Conference on the Peaceful Uses of Atomic Energy, Geneva, 1955 [in Russian] (Leningrad, State Chemistry Press, 1958) Vol. 9, p. 51.
5. G. Cabane and J. Petit, Rev. métallurgie 51, No. 9, 609 (1954).
6. M. Englander, Rev. métallurgie 51, No. 11, 758 (1954).
7. C. Harrington and A. Ruenle, Uranium Production Technology (New York, 1959).
8. G. Hanks, J. Taub, and D. Doll, Nucl. metallurgie, A Symposium on U and UO_2, A. J. M. M. P. E. A. J. M. E. (1957) Vol. 4, pp. 73-86.
9. G. Hanks, J. Taub, and D. Doll, Nucl. metallurgie. A Symposium on U and UO_2, A.J. M. M. P. E. A. J. M. E. (1957) Vol. 4, pp. 95-106.
10. G. Ya. Sergeev, et al., Proceedings of the Second International Conference on the Peaceful Uses of Atomic Energy, Geneva, 1958. Report of Soviet Scientists, Nuclear Fuel and Reactor Metals [in Russian] (Atomizdat, Moscow, 1959) Vol. 3, p. 333.

*Original Russian pagination. See C. B. translation.

SEPARATION OF THE STABLE ISOTOPES OF BORON

N. N. Sevryugova, O. V. Uvarov, and N. M. Zhavoronkov

Translated from Atomnaya Énergiya, Vol. 9, No. 8, pp. 110-125, August, 1960
Original article submitted April 4, 1960

This article describes methods for separating the stable isotopes of boron. Three of them can be used to prepare concentrates of B^{10} isotope in industrial quantities. The method of chemical exchange has a comparatively high coefficient of separation ($\alpha = 1.03$); however, the production rate of the apparatus is small due to the high molecular weight of the complex. The preparation of B^{10} by fractionating BF_3 offers possibilities ($\alpha = 1.0075$); however this process must be carried out at a temperature of $-100°C$, and requires the use of large quantities of liquid air. The method of separation by fractionation of BCl_3 has a low value of $\alpha(1.003)$, but can be carried out at atmospheric pressure and room temperature.

It is a well-known fact that boron has two stable isotopes with masses 10 and 11, discovered in 1920 by Aston [1] when studying BF_3 with the mass spectrometer. He found that natural boron contains 19.8 mole % B^{10} and 80.2 mole % B^{11}. Later, various investigators using other methods also carried out isotopic analysis of some compounds of boron (Table 1).

As can be seen from Table 1, the results for the determination of the isotopic composition of boron are different for various authors. In the mass-spectrometric investigations of specimens of some boron-containing minerals of different origin, the values of the isotopic ratios were between 4.27 and 4.42. Paper [7] explains the difference in the data of the separation of isotopes during chemical transformations and also shows that with a 100% yield of BF_3 from the initial products, the isotopic composition of boron does not change.

For the reaction of B^{10} with neutrons

$$B^{10}_5 + n^1 = He^4_2 + Li^7_3$$

there is a characteristic large section of capture of thermal neutrons, equal to 400 barns [16], whereas the isotope B^{11}, on the other hand, effects very little capture of neutrons (6 ± 0.005 barns). This large difference in the properties of the boron isotopes is of interest for solving certain problems in nuclear engineering. For example, B^{10} is used to measure the intensity of a stream of neutrons both with counting tubes, filled with gaseous BF_3, and with photographic plates, whose emulsion contains a boron salt. Furthermore, B^{10} is also used in reactor construction for protection against neutrons and to control the operation of the reactors. In small quantities, B^{10} is used in the treatment of cancerous tumors since it selectively concentrates in the cancerous tissues and localizes the neutron stream during treatment by radiation. B^{11} can be used in the production of heat-resistant materials, which do not absorb neutrons.

For the separation of the boron isotopes a number of methods are proposed, including the electromagnetic method, thermal diffusion, the method of diffusion in a current of inert vapor, chemical isotope exchange, and fractionation of the boron halides.

TABLE 1

Results of Determinations of the Isotopic Composition of Natural Boron

Compound	Content mole, % B^{10}	Content mole, % B^{11}	Method of determination	Literature
BF_3	19,8	80,2	Mass spectrometric	[1]
BF_3	18,83	81,17	The same	[2]
BF_3	18,7	81,3	»	[3]
BF_3	19,5	80,5	»	[4]
BF_3	20,5	79,5	»	[5]
BF_3	19,1	80,9	»	[6]
BF_3	18,85	81,15	»	[7]
BF_3	18,38	81,62	»	[8]
BF_3	18,19	81,81	»	[9]
BF_3	19,3	80,7	»	[10]
BF_3	18,8	81,2	By absorption of neutrons	[11]
BF_3	17,1	82,9	Band spectrum	[12]
BF_3	21,6	78,4	The same	[13]
BF_3	18,4	81,6	Line spectrum	[14]
BCl_3	19,58	80,42	Mass-spectrometric	[7]
BCl_3	19,5	80,5	The same	[9]
B_2O_3	19,36	80,64	»	[15]

Electromagnetic Method

The enrichment of isotopes is characterized by the separation factor

$$\alpha = \frac{N(1-n)}{n(1-N)}, \qquad (1)$$

where n is the content of the rare isotope in the initial product; N is its content after the separation. For most of the methods for separating isotopes the value of α is small and differs very little from unity. In the electromagnetic method α reaches exceptionally high values (several hundreds and even thousands). Almost pure isotopes can be obtained in practically one operation of separation. In [17] a product was obtained containing more than 99 mole % B^{10}. Since in magnetic fields in a high vacuum the material is transported in the form of ions, the rate of production of the equipment is very small. It is normally only possible to obtain a gram or even milligrams of material after many hours of work. The separation of boron in highly efficient equipment has been described in a number of papers [17-21]. For the preparation of B^{10} on an industrial scale, the electromagnetic method is of no practical interest due to the high production cost.

Thermal Diffusion Method

It is a well-known fact that the thermal diffusion method can be used to separate both gaseous and liquid mixtures in relatively short columns with high efficiency. However, the repeated attempts of a number of authors [5, 6, 22-24] to separate boron isotopes by thermal diffusion of BF_3 have not given the expected results. They usually used separation columns of the Dikkelya* type. Thus with the BF_3 pressure equal to atmospheric and at a filament temperature of 600°K on columns of total length 10 m after three days the enrichment of B^{10} was only 1.34 times [5]. Reducing the pressure did not improve the separation to any great extent. A 1.14-fold enrichment was obtained on a 3 m column, at a BF_3 pressure of 55 mm Hg [6]. A somewhat better enrichment (1.9-fold) was obtained on an apparatus from thermal diffusion columns of total length 12 m at a filament temperature 400°C [22].

Unfortunately, as yet the thermal diffusion method has not been able to achieve high enrichments of boron isotopes. This may be due to the small value of α (1.0024) [25] and to some extent to the losses of BF_3 when it reacts with the incandescent filament and with the glass.

Method of Diffusion in a Current of Inert Vapor

At the start of the 1920's, Hertz [26] suggested the use of a stream of inert vapor as a medium for separating gaseous mixtures of components with different diffusion coefficients. In the pump developed by Hertz in 1934 [27], it was possible to combine in one device a separation element and a circulation pump; it was therefore possible to establish a cascade process without additional circulation pumps.

Figure 1 shows the operation of this diffusion pump. In this apparatus the diaphragm only serves to create hydrodynamic currents and is a partition with pores whose diameters are much greater than the free path of the molecules. The working materials for the diffusion pumps should be materials with a high molecular weight, having thermal stability, low solubility in their gases and low vapor pressure at room temperature (mercury, heptane, xylene, etc). When using the monatomic vapors of mercury the diffusion coefficients of the boron isotopes are greater than those in the presence of monatomic vapors of the same molecular weight.

*Transliteration of the Russian original

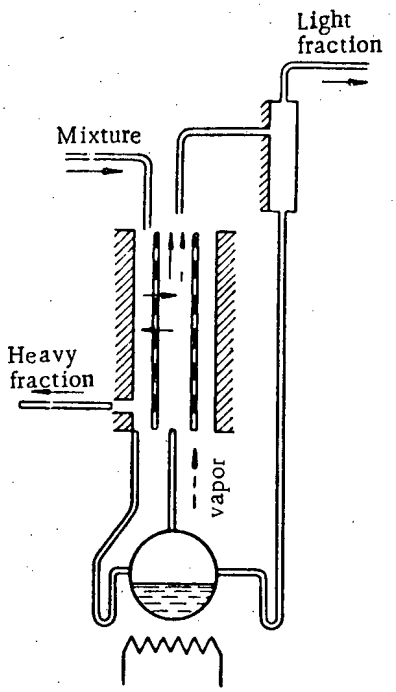

Fig. 1. Operation of separation pump.

Considerable advances in the development of the method of diffusion in a stream of inert vapor have been achieved in the Soviet Union [28] and East Germany, where apparatus has been built with high separation capacity. In this apparatus using a cascade with 70-80 metal and glass pumps, it has been possible to obtain almost pure $B^{10}F_3$ and $B^{11}F_3$. For the system $B^{10}F_3-B^{11}F_3$ α of the pump was 1.016. Owing to the high consumption of energy to evaporate the inert material, the method of diffusion in a stream of vapor can only be recommended for the preparation of a highly enriched product on a laboratory scale. Equipment of this type should be fed with products which have first been enriched by other methods which require the expenditure of less energy; this will considerably improve the output of the diffusion apparatus.

Chemical Isotope Exchange

At the present time the method of chemical isotope exchange is used successfully for separating stable isotopes of nitrogen, carbon and sulfur. Urey [29] in 1935 calculated the equilibrium constants of many isotope exchange reactions of light elements, including boron isotopes. However, most of the isotope exchange reactions of boron could not be realized due to the difficulties in changing the phases. Only later were liquid complex compounds of BF_3 found with organic substances [30].

In halogen compounds in the external electron shell of the boron atom there are six electrons, due to which the molecule of the boron halide has a sharply defined tendency to combine with atoms having an unshared pair of electrons. As a result, a stable grouping is formed, the coordination bond of which is comparable in energy with the covalent bond.

In all complex compounds of boron halides with organic substances the donors are oxygen atoms, nitrogen or sulfur. In most cases these complexes are liquids, readily forming at room temperature or in the cold and dissociating on heating. The phases can therefore be changed by simple heating or cooling, as is the case in fractionation.

Panchenkov, Moiseev and Makarov [31] were among the first to suggest for the separation of boron isotopes, the method of chemical exchange between the boron halides and their complex compounds with organic substances.

In its general form the exchange proceeds according to the reaction

$$RB^{11}F_{3(l)} + B^{10}F_{3(g)} \rightleftarrows RB^{10}F_{3(l)} + B^{11}F_{3(g)}, \qquad (2)$$

where R is an organic substance, and B^{10} is concentrated in the liquid phase. The phases are changed according to the reaction

$$R_{(l)} + BF_{3(g)} \underset{\text{Heating}}{\overset{\text{Cooling}}{\rightleftharpoons}} RBF_{3(l)} \qquad (3)$$

The experimental values of α for a number of systems $RBX_{3(l)}-BX_{3(g)}$ were determined by various methods by different investigators. The value of α was usually determined by measuring with a mass spectrometer the isotopic composition of the liquid and gaseous phases after isotopic equilibrium had been established between them

$$\alpha = \frac{\frac{B^{10}}{B^{11}_{(l)}}}{\frac{B^{10}}{B^{11}_{(g)}}}. \qquad (4)$$

TABLE 2

Relationship Between the Value of α for Boron Isotopes and the Temperature for the System $(C_6H_5)(CH_3)OBF_{3(l)}-BF_{3(g)}$

Temp., °C	Value of $\alpha_{exp.}$	Value of $\alpha_{av.}$
0	1,041±0,002 1,037±0,002	1,039
15	1,033±0,002	1,033
20	1,030±0,002 1,029±0,002	1,030
22	1,035+0,004	1,035
25	1,035±0,003	1,035
26	1,030+0,001	1,030
28	1,025+0,005 1,031+0,001	1,028
30	1,028+0,002	1,028

TABLE 3

Relationship Between α and the Temperature for the System $(C_4H_9)_2SBF_{3(l)}-BF_{3(g)}$

Temp., °C	Value of $\alpha_{exp.}$	Value of $\alpha_{av.}$
24,5	1,0330 1,0400 1,0292 1,0300	1,033
12	1,0290 0,0343	1,032
−2,5	1,0399 1,0370 1,0470	1,041
−4	1,0460 1,0490	1,048
−20	1,0520 1,040 1,0590 1,0563	1,054

The system studied in greatest detail by this method was $(C_6H_5)(CH_3)OBF_{3(l)}-BF_{3(g)}$. Data on the determination of the dependence of α on the temperature in the range 0-30°C are given in Table 2 [32]. As can be seen from the table, the value of α decreases very little with increase in temperature. In [33-35] this method was used to determine α at 20°C for a number of systems, including the complexes of BF_3 with diethyl and dibutyl ethers, tetrahydrofuran, water and other substances. In all these complexes the bond with BF_3 was through an oxygen atom.

Studies were made of the exchange between BF_3 and complex compounds in which the bond was through the sulfur atom. Detailed studies were made of the relationship between the value of α and the temperature for the system $(C_4H_9)_2SBF_{3(l)}-BF_{3(g)}$. The results of the measurements are given in Table 3 [36]. It can be seen from the table that the value of α, as in the complex with anisole, decreases with increase in temperature.

The experimental determination of α for boron isotopes by the method of chemical isotopic exchange by various authors is given in Table 4. The method of single establishment of isotopic equilibrium between liquid and vapor (single-stage method) gives only a very small change in the isotopic ratio, which on the mass spectrometer cannot always be measured with sufficient accuracy. Therefore, for some systems the establishment of equilibrium was repeated several times (the multistage method).

The value of α for the systems $(C_6H_5)(CH_3)OBF_3$ and $(C_4H_9)_2SBF_3$ was determined by 5-fold establishment of equilibrium [38]. In [37] the value of α was determined for a complex of BF_3 with anisole by a 9-stage method. In the calculations the value of α was obtained equal to 1.013 ± 0.005. Later, this value was obtained from the data of fractionation in a column. As can be seen from Table 4, this result differs from those of [32], where α = 1.035. The method used in [37] differed somewhat from that of other authors. In [37] the equilibrium was established by slowly passing BF_3 gas through the complex. It is possible that equilibrium was not established, thus leading to a reduction in the value of α. The value of α in the system $(C_2H_5)_2OBF_{3(l)}-BF_{3(g)}$ was determined for two temperatures [33, 40] by the method of relay distillation [41].

As can be seen from Table 4, in all systems the values of α determined by various methods are close to one another and vary on the average from 1.025 to 1.035. Only the data of [37] differ from these data to any great extent.

TABLE 4

The Value of α for Boron Isotopes in Reactions of Chemical Isotope Exchange

System	Temp. of exchange °C	Value of α	Method of determination	Literature
$(C_6H_5)(CH_3)OBF_{3(l)}$—$BF_{3(g)}$	20	1,013	Equilibrium (9 stages)	[37]
	25	1,032	" (5 stages	[38, 39]
	25	1,035	" (1 stage)	[32]
$(C_2H_5)_2OBF_{3(l)}$—$BF_{3(g)}$	127	1,023	Relay distillation	[40]
	70	1,028	Fractionation in a column	
	20	1,034	Relay distillation	[41]
	75	1,026		
	20	1,031	Equilibrium (1 stage)	[33, 34]
$(CH_3)_2OBF_{3(l)}$—$BF_{3(g)}$	100	1,025 1,016	Fractionation in a column	[42]
	103	1,027 1,016	The same	[43]
$(C_4H_9)_2SBF_{3(l)}$—$BF_{3(g)}$	25	1,033	Equilibrium (5 stages and 1 stage)	[36, 37]
$(C_6H_6)OBF_{3(l)}$—$BF_{3(g)}$	25	1,027	Equilibrium (1 stage)	[37]
$(C_4H_9)_2OBF_{3(l)}$—$BF_{3(g)}$	20	1,0288	The same	[33, 34]
$(CH_3)(C_2H_5)OBF_{3(l)}$—$BF_{3(g)}$	20	1,029	» »	[33, 34]
$H_2OBF_{3(l)}$—$BF_{3(g)}$	20	1,0256	» »	[33, 34]
$C_4H_8Cl_2OBF_{3(l)}$—$BF_{3(g)}$	20	1,015	Chemical exchange in a column	[44]
$C_6H_5NBF_{3(l)}$—$BF_{3(g)}$	25	1,023	Equilibrium (1 stage)	[35]
$C_4H_4O_5BF_{3(l)}$—$BF_{3(g)}$	25	1,036	The same	[35]
$(C_6H_5)_2OBF_3$— Complex does not form	25	1,000	Chemical exchange in a column	[35]
$(C_2H_5)_2SBF_{3(l)}$—$BF_{3(g)}$	25	1,040	Equilibrium (1 stage)	[36]
$(CH_3)_2SBF_{3(l)}$—$BF_{3(g)}$	25	1,036	The same	[36]
$CH_3COClBCl_{3(l)}$—$BCl_{3(g)}$	25	0,996	» »	[38]
$(C_6H_5)_2OBCl_{3(l)}$—$BCl_{3(g)}$	20	1,002	» »	[38]

It is interesting that for the system $(CH_3)_2OBF_{3(l)}$ —$BF_{3(g)}$ there are two values of α: 1.025 and 1.016 [42]. The second value was determined from the data of work on a large-scale cascade apparatus. The opinion was held [42, 43] that the decrease in the value of α during fractionation of the complex occurs due to the incomplete (by 60%) dissociation of the vapors. However, this conclusion can hardly be correct since the determinations of α

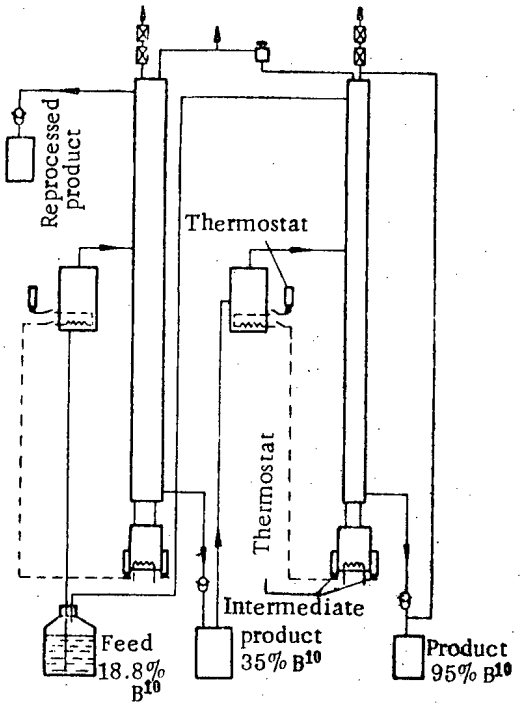

Fig. 2. Arrangement of a 2-stage cascade with output of 2 kg/yr of elementary boron, enriched to 95% B^{10}—flow of product;---electrical leads.

both by the relay distillation method and by the method of multistage exchange gave the same results: $\alpha = 1.025$.

Table 4 also gives values of α for exchange reactions between gaseous BCl_3 and complexes formed by BCl_3 and organic substances. These values are small compared with the values of α obtained for systems in which BF_3 was used.

It should be remembered that BF_3 does not form a complex with diphenyl ether whereas BCl_3 forms a comparatively stable compound with it. This indicated that the strength of the electron acceptor in boron halogen compounds decreases in the order $BI_3 > BBr_3 > BCl_3 > > BF_3$ [38].

All the investigated complexes with BF_3 can be divided into two groups: complexes which at the normal boiling point dissociate almost completely into an organic compound and BF_3, and complexes which at the normal boiling point decompose partially (up to 50%). The first group includes complexes of BF_3 and dimethyl, ethyl and butyl sulfides and also with anisole. In a detailed investigation of the latter complex [32] it was found that the time for the half exchange is 3 sec; this was quite satisfactory for carrying out a counter-current process. These investigations also showed that the most of the BF_3 is readily extracted from the complex on heating to 155-160°C; the undecomposed material is only 5-6 moles per 10^5 moles of anisole; the degree of extraction is perfectly satisfactory for obtaining a product with a high content of B^{10}.

In a laboratory column of height 2 m and diameter 21 mm filled with 2.5 mm diameter Fenske glass rings, investigations were carried out on the exchange of boron isotopes between gaseous BF_3 and the anisole complex at room temperature [45-46]. On this apparatus a product was obtained which was 1.33-fold enriched with B^{10}. Further work [44] on a column packed with nichrome wire helices at a temperature of 60°C gave a 1.6-fold enrichment. These authors studied the complex between BF_3 and dichloroethyl ether and obtained similar results. The complex was also completely dissociated at a temperature of 160°C and at atmospheric pressure. On the basis of this work the authors suggested a triple-section cascade which should produce BF_3 enriched with up to 96% B^{10}.

Later, studies were carried out on the separation of boron isotopes by the exchange of BF_3 with the anisole complex in laboratory columns of height 0.8 m, diameters 25, 38 and 50 mm and with various packings: plate-like, bubble-cap, Helipak packings (dimensions 12.5 × 2.5 × 2.5 mm) and Cannon packings (semi-cyclinders of dimensions 4 × 4 and 6 × 6 mm of netting) [47]. The last two types of packing were the most effective. The heights equivalent to theoretical stages were: for columns of diameter 25 mm—from 3 to 8 cm, depending on the flow rates, for columns of diameter 50 mm—from 5 to 8 cm.

All the investigations therefore showed that the complex of BF_3 with anisole can be recommended for producing concentrates of B^{10} by exchange with gaseous BF_3, since with a relatively large value of α, BF_3 has a sufficient rate of exchange and also simple conversion of the phases.

The papers [33, 48] studied the possible use for the separation of boron isotopes of the compound between BF_3 and water. In laboratory columns of height 0.25 and 0.6 m, diameter 13 mm, filled with Dixon packing (cylinders with a partition of netting of dimension 1.6 × 1.6 mm), the chemical exchange reaction was carried out

$$4BF_3 + 3H_2O \rightarrow 3HBF_4 + H_3BO_3; \quad (5)$$

$$3HBF_4 + H_3BO_3 + 3SO_3 \rightarrow 4BF_3 + H_2SO_4. \quad (6)$$

TABLE 5

The Characteristics of Columns Used to Separate B^{10} Isotopes by Methods of Exchange Fractionation and Chemical

Parameters of apparatus	Literature									
	[40]	[41]	[54]		[55]	[42]			[43]	
Stages	—	—	First stage	Second stage	—	First stage	Second stage	Third stage	First stage	Second stage
Complex	$(C_2H_5)_2OBF_3$					$(CH_3)_2OBF_3$				
Number of columns	1	1	1	1	1	3	3	3	5	1
Packing	Dixon (1.6×1.6 mm)		Cylinders of wire (4.7 mm diam.)	Cannon (6 × × 6 mm)	Dixon	Stedman		Cylinders of monel alloy (6 × 6 mm)		
Height of one column, m	5	5	9,7	9,8	13	9,1	9,1	9,1	15,2	6,1
Diameter of column, mm	—	25, 38	100	50	300	450	300	150	500	150
Charge in grams of elementary boron per 1 cm^2 of column cross-section per 1 hr receiver	—	2	10	6	—	—	—	—	40	40
Temperature in receiver of column, °C	75	70	70	70	70	100	100	100	105	101
Temperature in receiver of column, °C	—	—	—	—	—	91	91	91	91	91
Pressure at bottom of column, mm Hg	70	50	53	53	50	450	450	450	450	430
Pressure at top of column, mm Hg	20	20	20	20	20	150	150	150	150	150
Number of theoretical stages	220	315	55	200	300—350	180**	180**	220***	220***	40***
Height of column, equivalent to a theoretical stage, cm	2,3	1,6	105	3,7	4,5	110	110	110	160	150
Concentration of B^{10} in receiver of column	55	98	—	95	95	—	—	95	—	92
Output of elementary boron, kg/year	—	0,28	—	2	10	—	—	300	—	500

*Height equivalent to a theoretical stage and number of stages from [44-47] are given for the same densities, $\alpha = 1.03$.

**Temperature in exchange columns.

***Number of stages in apparatuses in which the complex $(CH_3)_2OBF_3$ was fractionated, was calculated for $\alpha = 1.016$.

[44—46]*			[44]*			[47]*			[33]
First stage									
$(C_6H_5)(CH_3)OBF_3$			$(C_2H_4Cl)_2OBF_3$			$(C_6H_5)(CH_3)OBF_3$			H_2OBF_3
1	1	1	1	1	1	1	1	1	1
Glass helices (2.5 mm diam.)		Nichrome wire helices				Helipak (1.25 × × 0.25 × × 0.25 mm)	Cannon 4 × 4 mm)	Cannon (6 × 6 mm)	Dixon (2 × × 3 mm)
2	2	2	2	2	2	0,8	0,8	0,8	0,6
20	20	20	20	20	20	25	38	50	13
10	10	10	10	10	5	10	10	10	2—2,5
150—160	150—160	150—160	150—160	150—160	150—160	150—160	150—160	150—160	200
20**	50**	60**	20**	40**	60**	25**	26**	25**	25**
Atmospheric									
Atmospheric									
7	10	16	7	8	16	24	9	12	17
30	20	12,5	30	25	12,5	3,8	10	7,5	3,5
23	20,5	28	23,3	23,7	28	29	24,5	26	26
—	—	—	—	—	—	—	—	—	—

The height obtained was equivalent to a theoretical stage and was equal to 3.5 cm. Despite the good results, this method can hardly find practical application due to the very aggressive nature of the products and the high consumption of pure sulfur trioxide.

Extensive practical use has been made of the complexes $(C_2H_5)_2OBF_3$ and $(CH_3)_2OBF_3$. At the normal boiling point they are partially irreversibly decomposed according to the reactions

$$(C_2H_5)_2OBF_3 \longrightarrow C_2H_5F + C_2H_5OBF_2; \quad (7)$$

$$(CH_3)_2OBF_3 \longrightarrow CH_3F + CH_3OBF_2. \quad (8)$$

During 24 hr in the apparatus $\sim$ 50% of the complex is decomposed. However, the decomposition can be reduced to 2-3% per day if the system is boiled at lower temperatures. In [40, 49-52] for the separation of boron isotopes fractionation is suggested of complexes at reduced pressure; this process is called "exchange fractionation", since the exchange of components in this case is established by mass exchange between the vapor and liquid phases, and also due to the chemical reaction. In these processes B^{10} is concentrated in the liquid phase. Using the complex $(C_2H_5)_2OBF_3$, the author of [40, 49-52] in a column of height 5 m, filled with Dixon packing of dimensions 1.6 x 1.6 mm, at a temperature in the jacket of the column of 75°C and a pressure of 50-70 mm Hg, obtained a 5-fold enrichment with respect to B^{10}. In a column of height 5 m and diameter 38 mm by fractionation of the same complex at a pressure of 50 mm Hg [41, 42], a very high degree of enrichment was obtained (up to 98% B^{10}) with a very small output—0.28 kg/yr of elementary boron.

In a 2-stage cascade (Fig. 2) consisting of columns of diameters 100 and 50 mm and total length of packed section 20 m, only 2 kg/yr elementary boron was obtained [53, 54], enriched with up to 95% B^{10}. This process was established on a large scale in [55], where in a column of height 13 m and diameter 300 mm, filled with Dixon packing, an output of 10 kg/yr of boron was obtained, enriched with up to 95% B^{10}. As can be seen, the output of even the large equipment is very small, since the use of low pressure (50-70 mm Hg) increases the hydraulic resistance of the packing and limits the column height.

The complex between BF_3 and dimethyl ether at a higher pressure (150 mm Hg) boils at 100°C. The first separation of boron isotopes by fractionation of this complex was achieved in the USA during the Second World War.

In 1944 they started to operate a large industrial apparatus [42], consisting of three stages (with three columns in each). The total height of the packed section of the cascade was over 80 m. At first, work was carried out on the selection of the packing, determining the height, equivalent theoretical stage and the conditions for carrying out the process. The output of the apparatus was 300 kg/yr of elementary boron, enriched up to 95% in B^{10}. The apparatus worked for 11 months and was then dismantled. However, the increasing demand for materials which could absorb neutrons led to the building of a second large plant in the USA [43, 56], producing 500 kg/yr of elementary boron. At this plant the isotopes were also separated by the fractionation of a $(CH_3)_2OBF_3$ complex. The apparatus was a 2-section cascade of more than 80 m total height of the packed section. It began operation in 1954 and worked for $2\frac{1}{2}$ yr [57]. At the present time in the USA they sell compounds containing B^{10} for 3000-8600 dollars per 1 kg of elementary boron, depending on the concentration of B^{10} [58-60].

Exchange fractionation is not the best method despite the fact that it has been used as the basis for large plants. The more serious drawbacks to the method are the following: 1) the process must be carried out at low pressure, which reduces the output and requires perfect sealing of the apparatus, since the moisture of any air leaking into the apparatus would hydrolyze the complex and some of the product would be lost; 2) the partial irreversible decomposition of the complex to the extent of 2-3% per day, due to which the products of the reaction choke the apparatus and increase the "parasitic separation"; 3) the complex must be broken down, since for the most complete separation of BF_3 with subsequent conversion to elementary boron under ordinary conditions from the complex only 60-80% BF_3 can be separated; the following reactions are used [58]:

$$(CH_3)_2OBF_3 + CaF_2 \longrightarrow (CH_3)_2O + CaF_2BF_3; \quad (9)$$

$$CaF_2BF_3 \xrightarrow{\text{Heating to } 200^\circ C} CaF_2 + BF_3. \quad (10)$$

Table 5 gives the characteristics of columns used to separate boron isotopes by methods of exchange fractionation and chemical exchange. It can be seen from the table that these methods, based on the use of complex

TABLE 6

Temperature Dependence for Separation of Boron Isotopes by Fractionation of BF_3

Temperature °C	Temperature °K	Pressure, mm, Hg	$\alpha = \frac{P_{B^{11}F_3}}{P_{B^{10}F_3}}$
−101,7	171,4	760	1,0076
−104,6	168,5	600	1,0072±0,0003
−106,5	166,6	500	1,0068
−109,6	163,5	400	1,0064±0,0010
−115,9	157,2	200	1,0046±0,0006
−123	150,1	100	1,0027

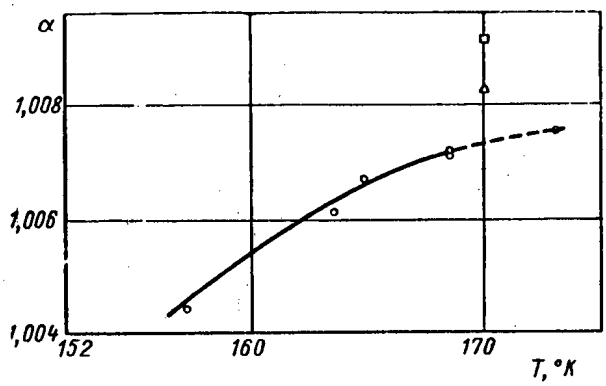

Fig. 3. Temperature dependence of α for the system $B^{10}F_3$–$B^{11}F_3$. Data of papers: □–[61-63] (differential method); Δ–same authors (from operation of column); ●–[64]; ○–[65].

compounds of BF_3 with organic substances, offer good possibilities, since they have a comparatively large value of α and permit ready phase conversion. The most suitable for chemical exchange is the complex of BF_3 with anisole. This complex readily and practically completely dissociates on heating and is also readily formed in the cold. Using this complex, boron isotopes can be separated at atmospheric pressure.

Fractionation of Boron Halides

Fractionation is one of the simplest and most productive methods for separating boron isotopes. For the separation of mixtures it is essential to select those conditions (temperature and pressure) at which the material would exist in two phases: in the vapor and in the liquid states. The boron halides are the more suitable compounds for fractionation. It is probable that other boron compounds could also be used, for example boranes (compounds with hydrogen), however they are very unstable. In 1943 an attempt was made [55] to separate boron isotopes by fractionation of $BO_3(CH_3)_2$. However, the value of α was very small (1.001). In halogen compounds of boron the value of α decreases from fluorine to iodine. Furthermore, bromine and iodine compounds are relatively expensive, therefore only BF_3 and BCl_3 have found practical application.

Fractionation of BF_3. The value of α for boron isotopes in the equilibrium evaporation of BF_3 was determined in [61-63] both in investigations in a column and by the differential method. The authors of these papers showed that the heavy molecule $B^{11}F_3$ is highly volatile. The coefficient of separation determined by the differential method at −103°C was equal to 1.0091 ± 0.0003. When working with a column with this temperature, the value obtained was $\alpha = 1.0082$ [62], and at a temperature of −100°C it was $\alpha = 1.0075$ [64]. In the evaporation of BF_3 we determined the value of α [65], by the method of relay distillation in the temperature range from 168.5°K (−104.6°C) to 157.2°K (−115.9°C). The experimental data for the relationship between α and the temperature is described by the equation

$$\alpha = 1.0488e^{-6.17/T}. \qquad (11)$$

as given in Table 6 and in Fig. 3. As can be seen from Table 6, the value of α increases with temperature, therefore the fractionation process is best carried out at atmospheric or at higher pressures.

The first efficient separation of boron isotopes with the preparation of fairly large quantities of B^{10} was accomplished in the Soviet Union by fractionating BF_3 [61, 62]. This separation was accomplished by using original methods. Although these methods somewhat complicated the device of the column and the whole apparatus, they provided high stability in the system.

The design of one of the first columns is shown in Fig. 4. The column was made from a german silver tube of length 12 m, with an internal diameter of 12 mm. The packing was 1.2 mm diameter rings of constantan wire of diameter 0.25 mm. The height equivalent to one theoretical stage was ~ 2.0 cm and depended very little on the diameter of the column (7, 12 mm) and on the reflux density (8-25 $cm^3/cm^2 \cdot sec$). The vapors were condensed by liquid air. To ensure constant temperature conditions the column was surrounded by a jacket with evaporating ethylene at a temperature of −103°C and a reflecting screen. The column, the ethylene jacket,

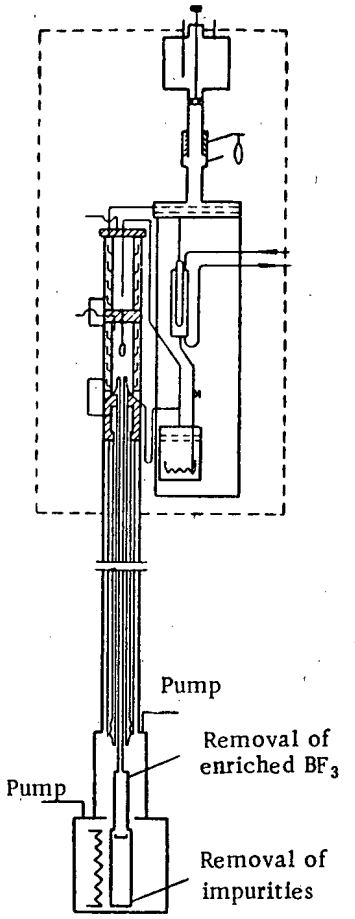

Fig. 4. Design of a low temperature fractionating column.

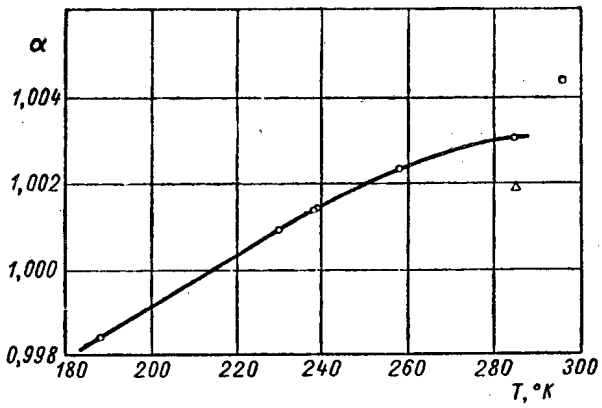

Fig. 5. Temperature dependence of α for the system $B^{10}Cl_3$–$B^{11}Cl_3$. Data of papers: □–[67]; Δ–[68]; ○–[9].

the screen and condenser, consisting of two chambers, were placed in a vacuum container, the pressure in which was kept at about 10^{-4} mm Hg. The following results were obtained with the apparatus: the number of theoretical stages was 600, after 20 days in the column the stationary state was reached and the concentration in the receiver was 95-96% $B^{10}F_3$. On removing the enriched product the concentration in the receiver was reduced, depending on the removal, and with a productivity in the apparatus of 4 liters of gas per day, the concentration was ~ 82%. The content of B^{10} at the top of the column was then reduced to 15-16%.

The authors of [64] designed an apparatus to prepare large quantities of B^{10} by fractionation of BF_3. The data for the design work were taken from work with a glass column of diameter 54 mm and height of the packed section 95 cm. The column was filled with Dixon packing measuring 1.6 × × 1.6 mm. In this small column a determination was made of the value α, equal to 1.065 at −100°C and the height equivalent to a theoretical stage was 2.5 cm. This confirmed the results previously obtained with a column of diameter 20 mm [66].

The production apparatus is a cascade of two columns of height 17.4 m each. The height of the columns was greater than the calculated value (due to the danger that the height equivalent to the theoretical stage increases with the height of the columns). To ensure an adiabatic process the column was placed in two vacuum vessels, one inside the other. This prevented disruption of the system in the event of the vacuum dropping in one of the vessels. The first column of diameter 56 mm put into the receiver a product enriched by up to 50% with B^{10}, and at the top in the condenser, the content of B^{10} in the product was reduced to 9%. In the second column of diameter 44 mm, the content of B^{10} in the vessel was 95%. The vapors were cooled by liquid nitrogen through a heat-exchange resistance. The pressure in the upper part of the first column was kept automatically at 850 mm Hg with a reflux rate of 14.5 kg/hr. The apparatus produced 26 kg/yr of elementary boron enriched with up to 95% of B^{10}. The authors of [64] concluded that the value of α is not equal to 1.0065, as was obtained on the laboratory column, but 1.0075.

It can therefore be seen that the separation of boron isotopes can be successfully achieved by the fractionation of BF_3; however a serious drawback to this method is the necessity for conducting the process at low temperature and a large amount of liquid oxygen has to be used as a cooling agent.

Fractionation of BCl_3. In 1935 Urey [29] suggested the fractionation of BCl_3 for the separation of the boron isotopes. He calculated that at 25°C the value $\alpha = \frac{P_{B^{10}Cl_3}}{P_{B^{11}Cl_3}}$ is equal to 1.013. However, in [10, 67, 68] it was

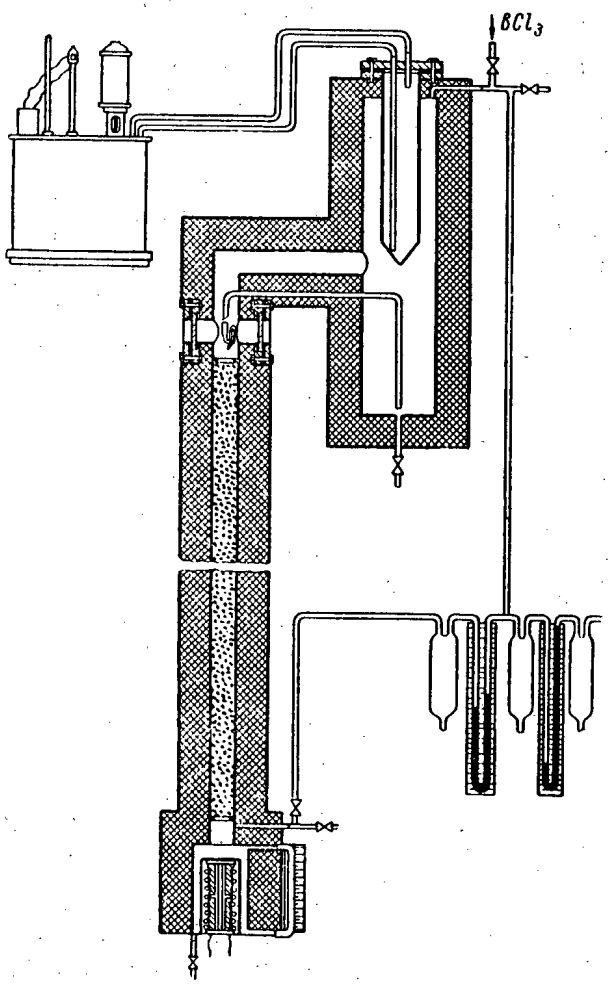

Fig. 6. Design of fractionation column.

shown experimentally that the readily volatile material is not $B^{10}Cl_3$, but $B^{11}Cl_3$. In separation in a column, carried out with a certain removal and without removal [67] according to the relationship

$$\Phi = \frac{\theta - (1-p)}{\theta - (1-p)\,\Phi_0^{\theta(\alpha-1)}} \qquad (12)$$

a value of $\alpha = 1.0018$ was determined at +12.7°C. In formula (12) Φ and Φ_0 are the enrichments obtained when working on a column with removal and without removal; p is the removal; $\theta = p/1-\alpha$. From the results of operation of a fractionating column, other authors [68] determined a value $\alpha = 1.0043$ at 25°C.

In [9] we found the relationship between α and the temperature by the method of relay distillation in the temperature range from +12.7 to −85°C. We found that α decreases with temperature; at −61.7°C the vapor pressures of the two isotopic forms of BCl_3 are equal, and with further reduction in temperature $B^{10}Cl_3$ is the more volatile. This dependence is represented in Fig. 5; it can be expressed by the equation

$$\alpha = 1.0112e^{-2.33/T} \qquad (13)$$

The fractionation of BCl_3 is apparently best carried out either at atmospheric or at increased pressure.

Boron isotopes were first separated by fractionation of BCl_3 in [67] in a glass laboratory column of height 160 cm and diameter 20 mm filled with Dixon packing measuring 1.6 × 1.6 mm. The separating capacity of the column was equivalent to 192 theoretical stages. In this column the enrichment with respect to B^{10} was 1.35-fold.

TABLE 7

Comparative Data on Various Methods for Separating Boron Isotopes

Method of separation	Packing	Density of liquid in grams/1 cm^2 cross-section of the column in 1 hr	Density in grams of boron per 1 cm^2 cross-section of the column in 1 hr	Value of α	Literature
Chemical isotopic exchange of BF_3 and its complex with anisole	Nichrome wire helices	120-360	3-9	1.032	[44]
Exchange fractionation of the complex $(C_2H_5)_2OBF_3$	Dixon packing (1.6 × 1.6 mm)	130-150	2-3	1.026	[41]
Fractionation of BF_3	Rings of constantan wire (1.2 mm diameter)	252	41	1.0075	[62]
Fractionation of BCl_3	Stainless steel wire helices (1.5 × 2 mm)	340	44	1.0032	[70]

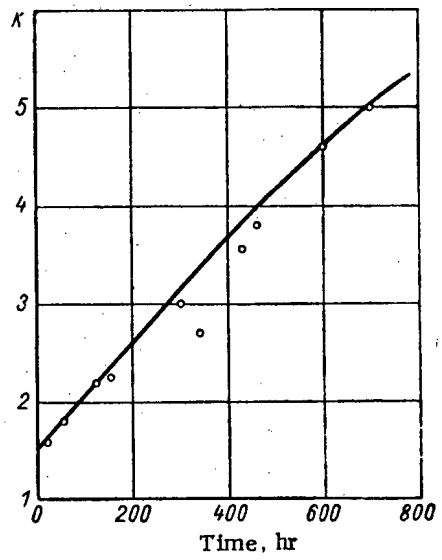

Fig. 7. Increase in enrichment of B^{10} in the column receiver vs. time (from the start of the apparatus). K—ratio of concentration of B^{10} in the column receiver to the concentration at the top of the column.

In [68] on a two-meter column made of stainless steel and filled with packing in the form of nickel mesh rings, the enrichment with respect to B^{10} was 1.4-fold. The fractionation was carried out at increased pressure and a temperature of 23°C.

In order to develop a pilot-plant method for preparing B^{10} we studied the fractionation of BCl_3. Two designs of columns were tested [69, 70], differing in the methods of insulation. Each of them was a tube of stainless steel of diameters 21 and 25 mm and height of the packing layer 12 m. As suggested in [71] the packing was in the form of helices measuring 1.5 × 2 mm and made from 0.2 mm diameter wire.

One of the columns was placed in a vacuum vessel in which the pressure was kept at 10^{-4} mm Hg. The vapors were condensed by a mixture of acetone and dry ice. The process was carried out at atmospheric pressure and a temperature of 12.7°C. The work resulted in a 5.5-fold enrichment of the product with respect to B^{10}. The second column (Fig. 6) differed from the first in that instead of a vacuum jacket the thermal insulation was provided by a 100 mm layer of foamed plastic (mipor). The vapors of BCl_3 were condensed by cooling with tap water, the temperature of which was 20 ± 0.2°C. The reflux density was 340 $cm^3/cm^2 \cdot$ · hr. The fractionation process was carried out at a pressure of 500 mm Hg above atmospheric and at a temperature of 23-25°C. After 700 hr a 5-fold enrichment with respect to B^{10} was obtained; as can be seen from Fig. 7, the stationary state was not reached. A calculation showed that the maximum separation capacity of this column is equivalent to 800 theoretical stages and a cascade of two columns can give an enrichment with respect to B^{10} of up to 85-95%.

It follows that, despite the small value of α, this method can be used to separate boron isotopes on an industrial scale, since this process of fractionation can be carried out at room temperature, which simplifies both the design of the columns and their operation, and also makes it possible to use tap water as the cooling agent..

SUMMARY

On an industrial scale, boron isotopes can be separated by exchange fractionation or chemical exchange and fractionation of BF_3 or BCl_3. Table 7 presents data on the values of α and the reflux densities with regard to elementary boron for various methods. A calculation of the data of Table 7 was carried out for efficient packings having approximately the same properties: Dixon packing and a packing in the form of helices of nichrome and stainless steel wires.

As can be seen from Table 7 the methods of chemical isotopic exchange and exchange fractionation using complex compounds have a comparatively high value of α. The greater α, the smaller the volume of the apparatus. However, for the method of exchange the reflux density is small with regard to elementary boron, since the complex has a high molecular weight. The reflux density with regard to the isotope determines the productivity of the apparatus.

Boron isotopes have been successfully separated by fractionation of BF_3(α = 1.0075). However, the fractionation must be carried out at a low temperature (−100°C), which complicates both the design of the columns and operation with them, and also requires large amounts of liquid air. The method of separating boron isotopes by fractionation of BCl_3 has a small value of α (1.003); however, despite this serious fault, it has a number of advantages: simplicity of design of the columns and maintenance on the apparatus, the easy availability of the raw material, the fact that liquid is not needed and, finally, the readiness with which the product is converted into elementary boron.

LITERATURE CITED

1. F. B. Aston, Mass Spectra and Isotopes [Russian translation] (Moscow, IL, 1948) p. 138.
2. M. Inghram, Phys. Rev. 70, 652 (1946).
3. H. Thode, et al., J. Am. Chem. Soc. 70, 9, 3008 (1948).
4. I. Osberghaus, Z. Phys. 8, 366 (1950).
5. W. Watson, I. Buchanan, and F. Elder, Phys. Rev. 71, 887 (1947).
6. B. Cooke, J. Hawes, and H. Mackenzie, J. S. Afric. Chem. Inst. 7, 1, 11 (1954).
7. V. Shyuttse, Zhur. Éksp. i Teoret. Fiz. 29, 4, 486 (1955).
8. G. M. Panchenkov, and V. D. Moiseev, Zhur. Fiz. Khim. 30, 6, 1118 (1956).
9. N. N. Sevryugova, O. V. Uvarov, and N. M. Zhavoronkov, Atomnaya Énerg. 4, 113 (1956).*
10. P. Bentley and A. Hamer, Nature 182, 1156 (1958).
11. M. Legal, Rev. Tech. CFTH, 25, 47 (1957).
12. F. Paton and G. Almy, Phys. Rev. 37, 1710 (1931).
13. A. Elliot, Nature 126, 845 (1930).
14. L. Ornstein and J. Vreeswijk, Z. Phys. 80, 57 (1933).
15. G. A. Semenov and Yu. A. Zonov, Zhur. Anal. Khim. 14, 1, 137 (1959).*
16. D. Hughes and J. Horvey, Neutron Cross-Sections (New York, McGraw-Hill Book Co., 1956) p. 3.
17. V. S. Zolotarev, All-Union Conference on the Use of Isotopes and Nuclear Radiations [in Russian] (Izd. AN SSSR, Moscow, 1958) p. 60.
18. E. Vates, Proc. Roy. Soc. A. 168, 148 (1938).
19. J Koch and B. Bendt-Nielsen, Matematiks–Fysike, Meddelser 21, 8, 28 (1944).
20. H. Lu, Nuclear Sci. Abs. 4, 6, 1745 (1950).
21. C.Keim, J. Appl. Phys. 24, 10, 1255 (1953).
22. D. MacMillan, Material of the International Conference on the Peaceful Uses of Atomic Energy Geneva, 1955, (Metallurgizdat, Moscow, 1958) Vol. 8, p. 714.
23. G. M. Panchenkov, V. D. Moiseev, and Yu. A. Lebedev, Zhur. Fiz. Khim. 10, 2348 (1956).
24. W. Denton, Nuclear Sci. Abs. 8, 6 A, abs. 1625 (1954).
25. L. Gerardin, Rev. Tech. CFTH 25, 21 (1957).
26. G. Hertz, Z. Phys. 23, 433 (1922).
27. G. Hertz, Z. Phys. 91, 810 (1934).
28. I. G. Gverdtsiteli and V. K. Tskhakaya, All-Union Conference on the Uses of Isotopes and Nuclear Radiations [in Russian] (Izd. AN SSSR Moscow, 1958) p. 113.

*Original Russian pagination. See C. B. translation.

29. H. Urey, J. Chem. Soc. 4, 562 (1947).
30. G. Booth and D. Martin, The Chemistry of Boron Trifluoride and its Derivatives [Russian translation] (IL, Moscow, 1955) p. 41.
31. G. M. Panchenkov, V. D. Moiseev, and A. V. Makarov, Author's Certificate No. 14754 from June, 16, 1954.
32. A. Palko, R. Healy, and L. Landay, J. Chem. Phys. 28, 2, 214 (1958).
33. S. Ribnikar, Proceedings of the International Symposium on Isotope Separation (Amsterdam, North-Holland Publ. Co., 1958) p. 204.
34. S. Ribnikar, Bull. Inst. Nuclear Sci., "Boris Kidrich" 8, 147, 31 (1958).
35. S. Ribnikar, Bull. Inst. Nuclear Sci., "Boris Kidrich" 9, 177, 91 (1959).
36. A. Palko, Bull. J. Chem. Phys. 30, 5, 1187 (1959).
37. G. M. Panchenkov, V. D. Moiseev, and A. V. Makarov, Zhur. Fiz. Khim. 31, 8, 1851 (1957).
38. R. Healy and A. Palko, J. Chem. Phys. 28, 211 (1958).
39. R. Healy, et al., Proceedings of the International Symposium on Isotope Separation (Amsterdam, North-Holland Publ. Co., 1958) p. 199.
40. K. Holmberg, et al., Proceedings of the International Symposium on Isotope Separation (Amsterdam, North Holland Publ. Co., 1958) p. 201.
41. R. McLlroy and F. Pummery, Proceedings of the International Symposium on Isotope Separation (Amsterdam, North-Holland Publ. Co., 1958) p. 178.
42. A. Conn and J. Wolf, Industr. and Eng. Chem. 50, 9, Part 1, 1231 (1958).
43. G. Miller, et al., Presented by the USA to the Second International Conference on the Peaceful Uses of Atomic Energy (Geneva, 1958) Report No. 1836.
44. G. M. Panchenkov and A. V. Makarov, Report to the Eighth Mendeleev Meeting. Section on Radiochemistry and the Chemistry of Isotopes [in Russian] (Moscow, March, 1959).
45. G. M. Panchenkov, V. D. Moiseev, and A. V. Makarov, Doklady Akad. Nauk SSSR 112, 4, 659 (1957).
46. G. M. Panchenkov, I. A. Semiokhin, and P. A. Akishin, Vestnik Moskov, Univ. 6, 201 (1957).
47. A. Palko, Industr. and Eng. Chem. 2, 121 (1959).
48. S. Ribnikar and Z. Knezevic, Bull. Inst. Nuclear Sci. "Boris Kidrich" 9, 180 (1959).
49. K. Holmberg, Kosmos Phys. Uppsatser 33, 167 (1955).
50. K. Holmberg, Swed. Pat. 149, 918, May 10 (1955).
51. K. Holmberg, Brit. Pat. 736, 459 (September 7, 1955).
52. Angew. Chemie 7, 564 (September, 1957).
53. Atomics Eng. and Tech. 7, 12, 429 (1956).
54. A. Edmunds and F. Loveless, Proceedings of the Second International Conference on the Peaceful Uses of Atomic Energy, Geneva, 1958. Selected Reports of Foreign Scientists. The Preparation and Use of Isotopes [Russian translation] (Atomizdat, Moscow, 1959) Vol. 10, p. 150.
55. H. Durand, L'age nucl. 11, 194 (1958)
56. Chem. Eng. 64, 5, 148a, 176 (1957).
57. Nuclear Power 3, 6, 147 (1958).
58. The Atomic Energy Guide letter, 109, 25 (1957).
59. Nuclear Eng. 2, 13, 167 (1957).
60. Nuclear Sci. Abs. 12, 2, 205 (1958).
61. First International Conference on the Peaceful Uses of Atomic Energy, Geneva, 1955. Scientific and Technical Exhibition of the USSR, pp. 30-34.
62. J. Muhlenpfordt, et al., All-Union Conference on the Use of Isotopes and Nuclear Radiations [Russian translation] (Izd. AN SSSR, Moscow, 1958) p. 120.
63. J. Muhlenpfordt, et al., Proceedings of the International Symposium on Isotope Separation (Amsterdam, North Holland Publ. Co., 1958) p. 408.
64. P. Netley, D. Cartwright, and H. Kronberger, Proceedings of the International Symposium on Isotope Separation (Amsterdam, North-Holland Publ. Co., 1958) p. 385.
65. N. N. Sevryugova, O. V. Uvarov, and N. M. Zhavoronkov, Zhur. Fiz. Khim. 34, 1010 (1960).
66. O. Dixon, J. Soc. Chem. Industr. 68, 88 (1949).
67. M. Green and G. Martin, Trans. Faraday Soc. 48, 5, 416 (1952).
68. M. Ya. Kats, G. M. Kukavadze, and R. L. Serdyuk, Zhur. Tekh. Fiz. 26, 12, 2744 (1956).

*Original Russian pagination. See C. B. translation.

69. N. N. Sevryugova, O. V. Uvarov, and N. M. Zhavoronkov, Proceedings of the Conference on the Chemistry of Boron and its Compounds [in Russian] (Goskhimizdat, Moscow, 1958) p. 30.
70. N. N. Sevryugova, O. V. Uvarov, and N. M. Zhavoronkov, Doklady Akad. Nauk SSSR 129, 5, 1044 (1959).
71. A. I. Levin, Neftyanoe Khoz. 10, 40 (1949).

DETERMINATION OF ENERGY ABSORPTION IN A MIXED FLUX OF FAST NEUTRONS AND γ-RAYS BY AN IONIZATION METHOD

Yu. I. Bregadze, B. M. Isaev, and V. A. Kvasov

Translated from Atomnaya Énergiya, Vol. 9, No. 8, pp. 126-131, August, 1960
Original article submitted April 11, 1960

The possibility of separate determinations of the energy absorption of fast neutrons and γ-rays in the mixed radiation flux from a reactor has been studied with ionization chambers Three chambers with different hydrogenous fillers were used: polyethylene with an ethylene filler; graphite with a CO_2 filler and a chamber made from aerion, a conducting plastic, which was filled with a mixture of ethylene and CO_2. Calculations have been carried out to ascertain the sensitivity of these chambers to neutrons with energies ranging from 0.2-8 Mev. Variation of the neutron spectrum over wide limits has no effect on the accuracy in the determination of the absorbed dose in the hydrogenous substrates. A calculation shows that the error in the determination of the absorbed energy for fast neutrons is approximately 15% and is a weak function of the relative doses of neutrons and γ-rays.

One of the basic problems of present-day ionizing-radiation dosimetry is the determination of the energy transferred by the radiation to a unit mass of matter. There is available a great deal of data concerning γ-radiation; these data allow us to determine accurately the absorbed dose (in rads) for various energies of the γ-radiation and various source-object configurations.

The determination of the absorbed dose for a neutron flux has not been as nearly widely studied [1]. The great bulk of the work on fast and intermediate neutron fluxes is of theoretical nature and has been carried out for monoenergetic neutron fluxes [2-4]. The use of these data requires a knowledge of the neutron spectrum; hence, the accuracy in the determination of the absorbed dose is very low under most conditions. If the neutron flux is accompanied by γ-radiation, the determination of the absorbed dose becomes still more difficult. For a small γ-background and absorbed dose D_γ (10-15% of the absorbed fast-neutrons dose D_n), the quantity D_γ can be determined by a photographic-emulsion technique. This method has been used by a number of authors [7, 8], in conjunction with the uniform thimble chamber [5, 6] (the composition of the walls and the gas is the same).

When the background due to γ-radiation is significant and D_γ is comparable with D_n, the use of the photographic technique in conjunction with an ionization technique can lead to large errors in the determination of the neutron absorption dose because of the low accuracy of the first technique.

Separation of the γ and neutron components by means of chemical methods has not been used widely because these methods are characterized by low accuracy. The use of threshold detectors in neutron dosimetry is also very limited, because of the difficulty involved in the measurements. These considerations apply especially in measurements in dummys, in which case one must determine the absorbed dose at various points of an object. Furthermore, the threshold-detector method requires additional measurements of the accompanying γ-radiation, in which connection differential measurements with ionization chambers become important; these chambers are made from materials with different hydrogenous content.

TABLE 1

Chemical Composition of Muscle Tissue and Bone Tissue, Polyethylene and Aerion (per cent weight)

Element	Muscle tissue	Bone tissue	Poly-ethylene	Aerion
H	10,2	6,4	14,4	4,75
C	12,3	27,8	85,6	72,5
N	3,5	2,7	—	—
O	72,9	41,0	—	22,75
Na	0,08	—	—	—
Mg	0,02	0,2	—	—
P	0,2	7,0	—	—
S	0,5	0,2	—	—
K	0,3	—	—	—
Ca	0,07	14,7	—	—

Neutron reactors are being more widely used as sources in radiobiological than in neutron experiments. The experiments can be carried out with both thermal and fast neutrons. In this case, the background γ-radiation can become very large, so that the absorbed dose of γ-radiation may become comparable with the absorbed dose of thermal or fast neutrons [9].

In the present work we present the results of an experimental determination of the absorbed dose in biological objects which was carried out by means of uniform thimble chambers in mixed neutron-gamma fluxes.

In principle, having two chambers with different hydrogenous contents in the walls, we should be able to separate the neutron component from the γ-component [10, 11]. In order to carry out these experiments, it is important that the chambers be truly uniform, that is to say the chemical composition of the walls must be identical with the chemical composition of the gas used in the chamber. Under these conditions the true absorption coefficient and bulk stopping power of the walls are the same as those of the gas.

The radiation energy transferred to one gram of chamber wall material per unit time consists of two components in the case of a mixed neutron and γ-flux. 1) The energy D_γ^i absorbed by the chamber walls by virtue of the interaction with the γ-ray flux and 2) the energy D_n^i absorbed by the chamber walls by virtue of the interaction with the neutron flux. For two chambers we have

$$\left.\begin{aligned} D_\gamma^1 + D_n^1 = D^1; \\ D_\gamma^2 + D_n^2 = D^2, \end{aligned}\right\} \tag{1}$$

where D^1 and D^2 represent the total energy transferred to one gram of wall material per unit time in the first and second chambers, respectively.

We use the symbols D_γ and D_n to denote the energy transferred by the γ-radiation and the neutron flux, respectively, to one gram of biological tissue. Then

$$\left.\begin{aligned} D_\gamma^1 = a_1 D_\gamma; \\ D_\gamma^2 = a_2 D_\gamma. \end{aligned}\right\} \tag{2}$$

The coefficients a_1 and a_2 are equal to the ratio of the true bulk absorption coefficients for γ-rays in the wall material in the first and second chambers to the true bulk absorption coefficient for tissue. Similar equations hold for the neutrons:

$$\left.\begin{aligned} D_n^1 = b_1 D_n; \\ D_n^2 = b_2 D_n, \end{aligned}\right\} \tag{3}$$

where b_1 and b_2 are equal to the ratio of the energy absorbed by one gram of wall material in the first and second chambers to the energy absorbed by one gram of tissue.

TABLE 2

True Bulk Absorption Coefficients for γ-Rays, μ/ρ, and Values of the Coefficients α_i

Energy of γ-rays, Mev	μ/ρ					a_i^M			a_i^B		
	muscle tissue	bone tissue	polyethylene	aerion	graphite	polyethylene	aerion	graphite	polyethylene	aerion	graphite
0,15	0,0276	0,0304	0,0280	0,0250	0,0246	1,03	0,92	0,905	0,92	0,82	0,81
0,5	0,0323	0,0316	0,0339	0,03110	0,0297	1,04	0,96	0,92	1,07	0,98	0,94
1	0,0308	0,0297	0,0319	0,0292	0,0279	1,04	0,95	0,915	1,07	0,98	0,94
2	0,0257	0,0249	0,0267	0,0246	0,0234	1,04	0,96	0,915	1,07	0,98	0,94
3	0,0223	0,0219	0,0231	0,0214	0,0204	,04	0,96	0,915	1,06	0,98	0,94

Substituting the values of Eqs. (2) and (3) in Eq. (1), we have

$$\left.\begin{aligned} a_1 D_\gamma + b_1 D_n &= D^1; \\ a_2 D_\gamma + b_2 D_n &= D^2. \end{aligned}\right\} \tag{4}$$

This system of equations allows us to determine the tissue dose for fast neutrons and γ-radiation separately.

In uniform chambers the energy absorbed by one gram of wall material can be determined from the relation

$$E = \frac{IW}{\varrho_{gas} V}, \tag{5}$$

where I is the number of ion pairs formed in the chamber; ρ_{gas} is the density of the gas which fills the chamber at the temperature and pressure appropriate to the experimental conditions; W is the energy for forming an ion pair in the gas and V is the volume of the chamber.

In order to ensure reliable results and in order to estimate the accuracy of the differential method we have used three chambers rather than two; the first chamber was made from polyethylene and filled with ethylene, the second chamber was made from graphite and filled with CO_2, while the third was made from a special conducting plastic called aerion, which has been described in [12]. The chamber made from aerion was filled with a mixture of ethylene and CO_2 in the ratio 1 : 1.25. The hydrogen content in this gas mixture was the same as the hydrogen content of the aerion, but the ratio of oxygen to carbon in the aerion was different from that in the gas mixture. However, this difference does not cause any appreciable effect, because of the small contribution of the recoil nuclei in the absorbed dose and the fact that the cross-sections for elastic scattering of neutrons are approximately the same in oxygen and carbon.

The conducting layer in the polyethylene chamber consisted of a semi-transparent layer of aluminum, which was deposited by vacuum evaporation. The layer thickness was less than 0.01 mg/cm^2.

The volumes of the chambers made from polyethylene aerion and graphite were respectively 2.12, 2.26, and 2.59 cm^3.

The experiments were carried out at one of the horizontal channels of the IRT reactor [13]. In order to reduce the thermal neutron flux and the γ-flux, we used a system of filters made from boron carbide and bismuth (150 mm thick). The thermal neutron flux was inconsequential and was of no importance in the ionization effect. The ionization chamber was moved along the channel by means of a special drive mechanism. The ionization currents were measured by means of an integrating dosimeter. The electrical sensitivity of the device was determined by calibration and the stability of operation was checked periodically by means of a radioactive control system.

In Eq. (5), W must be the mean value between the energy of formation for ion pairs by electrons W_e, recoil protons W_r and heavy recoil nuclei W_n. Since there are no experimental data available for W_r and W_n, in our calculations we have taken $W_r = W_n = W_\alpha$, where W_α is the energy of formation for ion pairs by α-particles. The values of W_e and W_α are taken from [14]. The values taken for W are as follows. For ethylene 27 ev; for carbon dioxide gas, 33.5 ev, and for the gas mixture, the mean value between these two quantities, 30.2 ev.

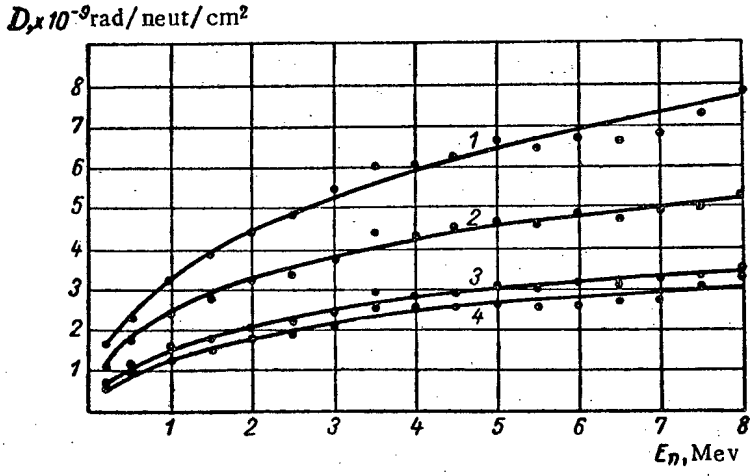

Fig. 1. The first-collision dose as a function of neutron energy: 1) polyethylene; 2) muscle tissue; 3) bone tissue; 4) aerion.

In calculating the coefficients b_i and a_i, we have used the data on the chemical composition of biological tissue and the values of the bulk coefficients for the true absorption in accordance with the recommendations of the International Commission on Radiological Units and Measurements (ICRU). In Table 1 we give the chemical composition of muscle tissue, bone tissue, polyethylene and aerion.

In Table II we give the values of the true bulk coefficients for γ-ray absorption μ/ρ for muscle and bone, polyethylene, aerion and graphite. Using these data we have computed the values of a_i for polyethylene, a_1, aerion, a_2, and graphite, a_3, for muscle tissue and bone tissue a_i^m and a_i^b, respectively. These data indicate that the values of the coefficients a are weakly dependent on the energy-radiation except for a_i^b; in the latter case, for γ-rays of energies of 150 kev this quantity is smaller. However, this difference is not of great importance because of the small soft component in the actual γ-ray spectrum in the reactor channel.

If we consider only elastic neutron scattering, the energy absorbed in one gram of tissue (for 1 neut/cm²) is given by the formula

$$D_n = E \sum_i N_i \sigma_i(E) f_i, \qquad (6)$$

where N_i is the number of nuclei of type i in 1 g of tissue; σ_i is the effective cross section for elastic scattering of a neutron of energy E on a nucleus of type i; $f_i = \frac{2M}{(M+1)^2}$ is the mean fraction of the energy transferred by the neutron to the nucleus of type i; M is the ratio of the mass of a nucleus of type i to the mass of the neutron.

The absorbed dose computed in this way will be called the first-collision dose. For muscle tissue with the chemical composition indicated in the Table I the appropriate calculation has been carried out in [15]. In Fig. 1 we show curves which give the dependence of the absorbed dose (in rad/neut/cm²) on neutron energy for muscle tissue and bone tissue, polyethylene and aerion. The cross-sections have been taken from [16].

Because of the resonance peaks in scattering on carbon and oxygen, the quantity b is not a constant for neutrons of different energy. In particular, as can be shown by calculation, when the neutron energy varies from 0.2 to 5 Mev, the value of b varies from 1.30 to 1.45 in polyethylene, from 0.52 to 0.59 in aerion and from 0.06 to 0.145 in graphite.

Under actual conditions we do not have a monoenergetic neutron flux, but rather a continuous spectrum; hence it is important to estimate the variation in b as the shape of the spectrum is changed.

The appropriate calculation has been carried out for three spectra: 1) for a fission spectrum given by the well-known function $N_1(E) \sim e^{-E} \mathrm{Sh}\sqrt{2E}$, 2) for a moderated fission spectrum given by the function $N_2(E) \sim e^{-2E} \mathrm{Sh}\sqrt{4E}$, [13], and 3) a moderated fission spectrum, whose initial part (up to 1 Mev) is described by a function of a form $N_2(E) \sim 1/E$, but which coincides with a fission spectrum above 1 Mev. These three spectra

TABLE 3

Values of the Coefficients b_i for Different Neutron Spectra

Shape of spectrum	b_i^m			b_i^b		
	polyethylene	aerion	graphite	polyethylene	aerion	graphite
$N_1(E)$	1,41	0,55	0,115	2,15	0,85	0,18
$N_2(E)$	1,41	0,545	0,105	2,17	0,84	0,16
$N_3(E)$	1,41	0,55	0,115	2,15	0,85	0,18

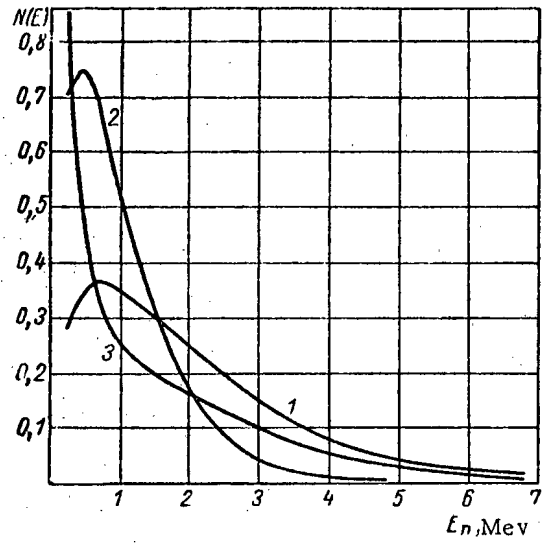

Fig. 2. Neutron energy distributions. 1) $N_1(E) \sim e^{-E} \mathrm{Sh}\sqrt{2E}$; 2) $N_2(E) \sim e^{-2E} \mathrm{Sh}\sqrt{4E}$; 3) $N_3(E) \sim \begin{cases} 1/E \text{ for } E < 1 \text{ Mev.} \\ e^{-E} \mathrm{Sh}\sqrt{2E} \text{ for } E > 1 \text{ Mev.} \end{cases}$

are shown in Fig. 2. As is apparent from Fig. 3, in spite of the great differences in the spectral shapes, the values of b remain essentially the same and are independent of the shape of the spectrum. This is an extremely important consideration since it allows us to determine the tissue dose at different depths of an object without taking account of the change in the spectral composition of the neutron flux at different depths.

The change in b for graphite is found to be unimportant in the calculations of the absorbed dose since the efficiency of the graphite chamber is small for neutrons.

Thus, to determine the absorbed dose of neutrons and γ-rays in muscle tissue and bone tissue for the three-chamber system we have the equation:

$$\left.\begin{aligned} 1{,}04D_\gamma^m + 1{,}41D_n^m &= D_1, \\ 1{,}07D_\gamma^b + 2{,}15D_n^b &= D_1; \end{aligned}\right\} \text{ polyethylene} \quad (7)$$

$$\left.\begin{aligned} 0{,}96D_\gamma^m + 0{,}55D_n^m &= D_2, \\ 0{,}98D_\gamma^b + 0{,}85D_n^b &= D_2; \end{aligned}\right\} \text{ (aerion)} \quad (7)$$

$$\left.\begin{aligned} 0{,}915D_\gamma^m + 0{,}105D_n^m &= D_3, \\ 0{,}94D_\gamma^b + 0{,}18D_n^b &= D_3. \end{aligned}\right\} \text{ (graphite)} \quad (7)$$

Here D_γ^m, D_γ^b, D_n^m, and D_n^b are the tissue doses for γ-rays and neutrons in muscle tissue and bone tissue; D_1, D_2, and D_3 are the absorbed doses in the wall materials.

In order to check the efficiency of the differential method of determining the neutron tissue dose and the γ-ray tissue dose, the measurements were carried out in different points of the channel, where the ratio between D_n and D_γ was considerably different. At each point the system of equations in (7) was used.

The solution of two pairs of equations (polyethylene-graphite and polyethylene-aerion) coincided with an accuracy of 5-6% both at the output of the channel, where D_γ is 20% of D_n, and at points close to the core, where $D_\gamma \approx D_n$.

The system in (7) is incompatible because of the inaccuracy in the determination of D_1, D_2, and D_3.

In order to find the most probable values of D_γ and D_n from (7), we must solve a system of linear normal equations [17].

$$\left.\begin{aligned} D_\gamma \sum_i a_i^2 + D_n \sum_i a_i b_i &= \sum_i a_i D_i; \\ D_\gamma \sum_i a_i b_i + D_n \sum_i b_i^2 &= \sum_i b_i D_i. \end{aligned}\right\} \quad (8)$$

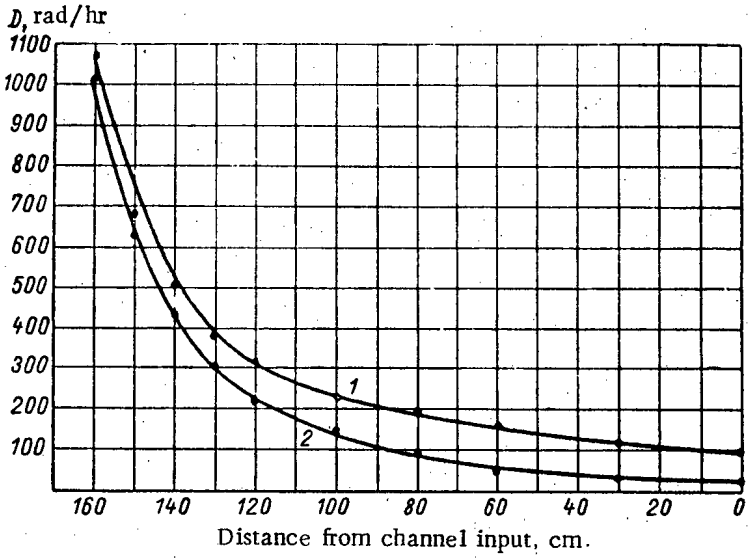

Fig. 3. Distribution of tissue dose strength from neutrons and γ-rays along the reactor channel (for muscle tissue). 1) Tissue dose strength for neutrons; 2) tissue dose strength for γ-rays.

The distribution of tissue-dose strength from neutrons and γ-rays in the reactor channel obtained by this method for muscle tissue is shown in Fig. 3.

It is extremely important to estimate the accuracy in the determination of the tissue doses D_γ and D_n. The basic sources of error are the errors in the determination of the absorbed doses D_i in the walls of the ionization chambers. These errors arise as a consequence of inaccuracies in the determination of the volume of the chamber, instrumental errors in the measurements of the ionization current and the inaccurate value of the energy for formation of ion pairs W for a mixed flux of neutrons and γ-rays. The volume of the chamber is known with an accuracy of 1%, the instrumental errors can be reduced to 1-2% and the error in the determination of W is 3%.

Analysis of the system of two equations

$$\left.\begin{aligned} a_1 D_\gamma + b_1 D_n = D_1 \\ a_2 D_\gamma + b_2 D_n = D_2 \end{aligned}\right\} \quad (9)$$

and

gives the following relation between the errors in the determination of D_n and D_γ, and the error in the determination of D_i:

$$\frac{\Delta D_n}{D_n} = \frac{1+\alpha}{1-\alpha}\frac{\Delta D}{D} \qquad \left(\alpha = \frac{a_1 D_2}{a_2 D_1}\right); \quad (10)$$

$$\frac{\Delta D_\gamma}{D_\gamma} = \frac{1+\beta}{1-\beta}\frac{\Delta D}{D} \qquad \left(\beta = \frac{b_1 D_2}{b_2 D_1}\right). \quad (11)$$

We assume that $\frac{\Delta D_1}{D_1} = \frac{\Delta D_2}{D_2} = \frac{\Delta D_3}{D_3}$. A calculation shows that the coefficients $\frac{1+\alpha}{1-\alpha}$ and $\frac{1+\beta}{1-\beta}$ are weak functions of the ratio between D_n and D_γ, varying from 1.5 to 2.5 for the polyethylene-graphite system.

Thus, when $\frac{\Delta D}{D} = 6\%$, the error in the determination of the tissue dose for neutrons and γ-rays is 9-15% when the measurements are made with two chambers.

It should be emphasized that the error in the determination of the total tissue dose is due to the error in the determination of D_i and is less than 6%. The errors in D_n and D_γ are to be associated with the division into components of the tissue dose, which arises in solving the system of equations in (7).

The determination of absorbed energy with the indicated accuracy satisfies the requirements of most relative radiobiological experiments, which arise in investigations of relative biological efficiency; the requirements of most radiochemical investigations are also satisfied.

In conclusion the authors wish to express their gratitude to Yu. F. Chernilin for help in this experiment and T. B. Radzievskii for discussion of the results.

LITERATURE CITED

1. M. I. Shal'nov, Neutron Tissue Doses [in Russian] (Atomizdat, Moscow, 1960).
2. J. Tait, Brit. J. Radiol. 23, 269 (1950).
3. W. Snyder and J. Neufeld, Brit. J. Radiol. 28, 331, 342 (1955).
4. A. M. Kogan, et al., Atomnaya Énerg. 7, 351 (1959).*
5. H. Rossi and G. Failla, Nucleonics 14, 2, 32 (1956).
6. F. Shonka, I. Rose, and G. Failla, Report USA, Presented by the Second International Conference on the Peaceful Uses of Atomic Energy (Geneva, 1958) Report 753.
7. R. Rhody, Radiation Res. 5, 495 (1956).
8. H. Rossi, Radiology 61, 93 (1953).
9. H. Curtis, et al., Nucleonics 14, 26 (1956),
10. V. I. Veksler, L. V. Groshev, and B. M. Isaev, Ionization Methods in Radiation Investigations [in Russian] (Gostekhteorizdat, Moscow, 1950).
11. C. Neary, R. Munson, and R. Mole, Chronic Radiation Hazards (Pergamon Press, 1957).
12. K. Zimmer, Phys. Z. 42, 360 (1941).
13. V. V. Goncharov, et al., Second International Conference on the Peaceful Uses of Atomic Energy, Geneva, 1958. Report of Soviet Scientists. Nuclear Reactors and Nuclear Power (Atomizdat, Moscow, 1959) Vol. 2, p. 243.
14. G. Kane and H. Brownell, Radiation Dosimetry [Russian translation] (IL, Moscow, 1958).
15. G. Hurst, et al., Radiation Res. 4, 49 (1956).
16. D. Hughes and R. Schwartz, Neutron Cross-Sections (New York, 1957).
17. I. N. Bronshtein and K. A. Semendyaev, Mathematics Handbook [in Russian] (Gostekhteorizdat, Moscow, 1953).

*Original Russian pagination. See C. B. translation.

LETTERS TO THE EDITOR

"IRRADIATION" REACTOR

Yu. S. Ryabukhin and A. Kh. Breger

Translated from Atomnaya Énergiya, Vol. 9, No. 8, pp. 132-133, August, 1960
Original article submitted April 22, 1959

As is well known, one use of atomic energy is to generate electrical power. However, the cost of electrical power produced by atomic energy stations is still high. This cost could be reduced considerably if in addition to obtain electrical power, it were possible to obtain by-products. The high activity of fission products can be exploited for this purpose. Use can also be made of the fact that in certain reactors it is possible to use loops in which the active material is in constant circulation [1-3]. It is even more advantageous to use special reactors for the production of chemical products in addition to electrical power. For example, the literature contains proposals for reactors which produce nitric acid through the use of the kinetic energy of fragments [4], reactors which produce heat and CO^{60} [5], reactors for the gasification of carbon [6], processing of supply materials [7] and so on.

We may also consider a reactor in which the loop for the coolant or nuclear fuel also serves as an irradiation loop; basically this would make use of the γ-radiation from the material circulating in the loop. In what follows we will call a reactor of this kind an "irradiation" reactor. A disadvantage of reactors with circulating nuclear fuel is the presence of retarded neutrons and the relatively low specific activity [1]; a disadvantage of reactors which use sodium coolants is the small specific activity [1] and the danger associated with the high chemical activity of sodium.

Apparently, a reactor with uranium (enriched 10-25%) and a graphite (or beryllium) moderator would be free from the disadvantages listed above. In a reactor of this kind, the coolant and the γ-radiation carrier can be an indium-gallium liquid alloy. As has been shown in [1], the main radiation power in this alloy is due to the indium; the gallium serves to reduce the melting temperature of the alloy. Such an alloy, containing 16.5 at. percent indium (with the remainder gallium) has a melting point of 16°C [8]. The specific radiation power of this alloy in a flux of 10^{13} neut/cm^2 · sec is 1200 w/liter, which is two orders of magnitude higher than the specific power of circulation loops of conventional reactors (with the same neutron flux in the core). The specific radiation power of a reactor with a circulation loop as compared with the specific radiation power of a reactor with a conventional radiation loop [1, 2] with the same activated material, with activation going on beyond the reflector, will also be one-two orders of magnitudes higher.

Preliminary estimates of the heat balance and neutron balance of the reactor and the radiation power in the loop are encouraging. In particular, a heterogeneous uranium-graphite reactor with a fuel with 20% enrichment [thermal power, 20 Mw] can be cooled by 40 liters of the alloy indicated above at 50-300°C.

The radiation power of a theoretically optimum (providing maximum economy of the expensive indium alloy) loop [1] is approximately 40 kw (that is to say, the equivalent of $4 \cdot 10^6$ gram-equivalents of Ra). If the γ-radiation of this loop is used, for example, in the polymerization of ethylene [9], taking G = 1000 mol/100 ev = = 12 kg/kw · hr, we find that the capacity of a reactor (if we make complete use of the energy absorbed in the ethylene) is 4400 tons of ethylene per year. The cost of this output is 200 million rubles.

The considerations given above indicate the usefulness of a detailed investigation of the possibilities of an irradiation reactor of this kind. It should be noted that the energy of the γ-radiation generated in the system is a

maximum of 1.5% of the fission energy, and in the optimum case [1] (0.75%). It would appear that the irradiation reactor is economically feasible. It is apparent that it might be possible to improve the economy of thermal-neutron reactors if one were to make use of a large percentage of the fission energy in irradiation loops.

The authors wish to express their gratitude to Academician A. P. Aleksandrov, V. L. Karpov, S. M. Feinberg, Yu. F. Chernilin, and E. P. Kunegin for valuable discussions of this work.

LITERATURE CITED

1. Yu. S. Ryabukin and A. Kh. Breger, Atomnaya Énerg. 5, 553 (1958); 6, 129 (1959).*
2. A. Kh. Breger, Yu. S. Ryabukhin, S. G. Tul'kes, and E. N. Volkov, Indium-Gallium Radiation Loop for the IRT Nuclear Reactor. Report No. 80 to the International Conference on the Use of Intense Radiation Sources in Industry (Warsaw, Sept., 1959).
3. R. Gordon, "Design of irradiation loops." Report to the Second Conference on Nuclear Science and Technology (Chicago, March, 1958).
4. G. Lellouche and M. Steinberg, Characteristics of chemonuclear reactors and systems," Report to the Third Conference on Industrial Nuclear Technology (Chicago, September, 1959).
5. Canad. Chem. Process. 41, 4, 50 (1957).
6. B. Gamson, Chem. Eng. Progr. 54, 2, 74 (1958).
7. D. Bray and C. Leyse, Nucleonics 15, 7, 76 (1957).
8. W. Svirbely and S. Selis, J. Phys. Chem. 58, 33 (1954).
9. S. S. Medvedev, Proceedings of the All-Union Scientific Technical Conference on the Application of Radioactive and Stable Isotopes and Radiation in the National Economy and Science (April 4-12, 1957). Isotopes and Radiation in Chemistry [in Russian] (Izd. AN SSSR, Moscow, 1958).

*Original Russian pagination. See C. B. translation.

APPROXIMATE DETERMINATION OF THE OPTIMUM THERMODYNAMIC CYCLE FOR A NUCLEAR POWER STATION

Yu. D. Arsen'ev and E. K. Averin

Translated from Atomnaya Énergiya, Vol. 9, No. 8, pp. 133-134, August, 1960
Original article submitted March 24, 1960

The basic difficulty in calculations of the optimum thermodynamic cycle for a nuclear power station, corresponding to the minimum cost of electrical power, consists in the determination of the cost of the individual units of the system which depend on the thermodynamic parameters. As a rule, a more complex cycle implies a higher efficiency and a reduction in the fuel cost c_f, , but an increase in the capitalization cost c_c. Because exact calculations are very complicated, it is of great practical interest to use approximations which allow us to analyze the effect on the fuel cost and the components of the capitalization cost caused by varying the parameters in the thermodynamic cycle. In recent years this problem has received much attention [1-4]. Although a great deal of originality has been shown in this work, and a number of interesting methods have been used, we must note certain errors in some of the original assumptions which tend to reduce the value of the final results which have been obtained.

In [1], from the condition of minimum cost of electrical power $c_e = c_f + c_c$, the author has obtained the basic dependence of the mean temperature of the working material

$$T_{1cy}^{\text{mean opt}} = \sqrt{\frac{\overline{T_p^{\max} T_{2cy}}}{1-z}}, \tag{1}$$

where $T_r^{\max}$ is the maximum wall temperature (T_w) TVEL; T_{2cy} is the temperature in the condenser (T_c); $z = \eta_t \cdot c_f$ the product of the efficiency and the fuel cost.

Correspondingly, from Eq. (1), for a low-cost fuel ($c_f = 0$; $z = 0$) we have

$$T_{1\,cy}^{\text{mean opt}} = \sqrt{T_p^{\max} T_c} \tag{2}$$

We shall now consider some of the main points in [1-4].

1. As the basis for Eq. (1), the author, for the quantity $T_r^{\max}$, assumes either the wall temperature T_w or the temperature at the center of the fuel element T_{cen}. In the problem being considered the temperature at the center of the fuel element does not determine the thermodynamic cycle. Actually, if we consider a plane or cylindrical fuel element with an aperture at the center, there is the possibility of a wide variation in the temperature inside the fuel element; under these conditions the station does not actually experience variations and the thermodynamic parameters remain unchanged.

In order to show that in Eqs. (1) and (2) we cannot take the temperature at the center $T_{cen} = T_r^{\max}$, we must recall the assumptions which lie at the basis of the method being considered. In the derivation of Eq. (2) it is sufficient to take the temperature of the walls T_w, the condenser temperature T_c, the coolant flow G and the heat transfer surface in the reactor F_r and the steam generator F_{sg} as constants. In this case the thermal power of

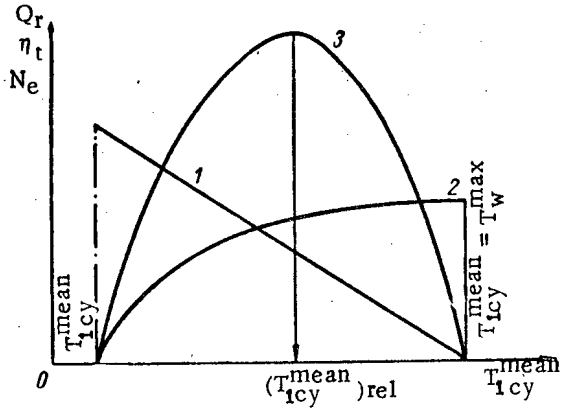

Nature of the variation of the thermal power of a reactor Q_r (1), the thermal efficiency η_t (2) and the electrical power of the installation $N_e = a_2 Q_r \eta_t$ (3).

the reactor can be expressed in terms of $Q_r = a_1 (T_w - T_{1cy}^{mean})$, where all the a's are constant. For a given value of T_w, an increase in T_{1cy}^{mean} reduces Q_r, but increases the efficiency. Since $\eta_t = 1 - T_c / T_{1cy}^{mean}$, then $N_e = a_2 Q_r \eta_t$ has a maximum value (cf. see figure); this maximum can easily be found from the equation $\partial N_e / \partial T_{1cy}^{mean} = 0$, which gives Eq. (2) upon transformation. For a low fuel cost ($c_f = 0$) the maximum N_e corresponds to the minimum cost of electrical power c_e, that is to say, Eq. (2) determines the optimum parameters of the cycle T_{1cy}^{mean}.

Expressing Q_r in terms of any temperature in the core T_i, so as to observe the condition $Q_r = a_i (T_i - T_{1cy}^{mean})$, we can obtain a large number of mathematically correct equations of the form $T_{1cy}^{mean} = \sqrt{T_i T_c}$; however these equations are not always applicable for the mean temperature of the cycle.

Assuming that the diameter of the fuel element d_f is fixed, the author of [1-4] has obtained the expression $Q_r = a_3 (T_{cen} - T_{1cy}^{mean})$ and the corresponding equation $T_{1cy}^{mean} = \sqrt{T_{cen} T_c}$. However, we cannot write $d_f = \text{const}$ even for the given maximum achievable T_w and T_{cen} for a fixed F_r, because the quantity Q_r, which the author used earlier in the derivation of Eq. (1), is limited by this, whereas Eq. (2) is not (cf. figure).

By assuming a definite value for T_w we can impose concrete physical limitations on the thermodynamic cycle(as a consequence of the fact that T_{1cy}^{mean} is always smaller than T_w);this also puts limits on the pressure of the coolant in water-water and organic reactors. Having determined the optimum thermal power of the reactor by this method, using T_w and the maximum allowable T_{cen}, it is easy to find the maximum possible diameter of the fuel element. It should be emphasized that the minimum cost of the core will correspond (for the maximum allowable T_w and T_{cen}) to the largest diameter of the fuel element because in this case the number of the fuel elements is a minimum. In this connection, all properly designed power stations have the maximum allowed temperature both at the wall and at the center and hence, without changing the diameter of the fuel element, it is impossible to increase Q_r.

Consequently, in making a rough determination of the optimum cycle in a station under design we cannot introduce the condition that the diameter of the fuel element remains constant ($d_f = \text{const}$) and substitute $T_r^{max} = T_{cen}$ in Eqs. (1) and (2).

2. In [1, 2] Eqs. (1) and (2) were used not only for cycles with nonregenerative water heating, but also for regenerative cycles. In this case, it is recommended that the quantity T_{2cy} be determined by Eq. (28) from [2], which gives $T'_{2cy} > T_c$. Thus, using Eq. (2) we have

$$\eta_{tp} = 1 - \frac{T'_{2cy}}{T_{1cy}^{mean}} = 1 - \sqrt{\frac{T'_{2cy}}{T_r^{max}}}$$

However, in a nonregenerative cycle, in which case $T_{2cy} = T_c$, or $T_r^{max} = \text{const}$, the efficiency is higher

$$\eta_t = 1 - \frac{T_c}{T_{1cy}} = 1 - \sqrt{\frac{T_c}{T_r^{max}}}$$

It is well known that regenerative heating of the water increases the thermal efficiency of a station. Consequently, Eqs. (1-2) cannot be used for a regenerative cycle, as recommended by the author of [1, 2].

3. In [3], Eqs. (1-2) were used without any justification for an installation with a boiling-water reactor. Among other things it is known that the thermal cycles of such installations have a number of specific features due to the negative steam reactivity of this kind of reactor. Hence, for these installations it is desirable, for example, to use cycles with two pressures with a flash tank or a heat-exchanger. It is obvious that the results of [1-4] cannot be applied for a boiling-water reactor installation since no account is taken of the specific features of this type of reactor.

4. As we have indicated above, the basic complexity in the technical-economic calculations lies in the determination of the cost of the individual units of an installation as a function of thermodynamic parameters. However, in [1-4] no account has been taken of the changes in the cost of an installation due to changes in the electrical power or changes in the steam parameters of the steam applied to the turbine.

Among other things, the capitalization costs of a nuclear power station (S_c) are made up of the capitalization costs of the reactor and generator installations, i.e., $S_c = S_r + S_g$. At the present time, the fraction of the capitalization in the generator installation $b_g = S_g/S_c = 20\%$, while for forced power in the reactor b_g can be increased to 40-45%. The cost of the generator installation can be expressed in terms of $S_g = q_g \cdot N_e$, where q_g is the specific capitalization, which in turn, depends on T_{icy}^{mean}. Thus, even very rough calculations, in which it is assumed that q_g = const, must take account of the change in the capitalization costs at the installation, i.e., $S_c = S_r + q_g N_e$. It must also be noted that in choosing the optimum regeneration temperature, the author of [4] has neglected the cost of the regeneration system.

In conclusion, we may note that since the capitalization costs for the installation were assumed constant in [1-4] and independent of N_e, and since the variation in the cost of the installation due to changes in thermodynamic parameters was not taken into account, the final equations derived in [1-4] are of very limited value.

LITERATURE CITED

1. D. D. Kalafati, Collection: Physics and Thermal Engineering of Reactors [in Russian] (Atomizdat, Moscow, 1958) p. 164.
2. D. D. Kalafati, Tr. Mos. Énerg. Inst. 30, 186 (1958).
3. D. D. Kalafati, Atomnaya Énerg. 8, 5 (1960).*
4. D. D. Kalafati, Teploénergetika 3, 74 (1960).

*Original Russian pagination. See C. B. translation.

APPROXIMATE CALCULATION OF THE MEAN ENERGY OF ELECTRONS PRODUCED BY γ-RAYS IN AN IONIZATION CHAMBER

A. K. Wal'ter, M. L. Gol'din, and V. I. Slavin

Translated from Atomnaya Énergiya, Vol. 9, No. 8, pp. 135-136, August, 1960
Original article submitted February 26, 1960

In the solution of a number of technical problems, in particular, measurements of the density and thickness of materials, it is found that an ionization chamber is a more stable detector than a fluorescent screen [1, 2]. However, the efficiency of ionization chambers is small for γ-rays [3], so that measures are taken to increase this efficiency. The most useful measures appear to be covering the inner surface with lead and the use of multilayer high-voltage collection electrodes [4].

An exact calculation of the ionization current is extremely difficult. This quantity can be found approximately if one knows the mean energy of the electrons produced by γ-rays in the chamber. This method of approximating the mean energy of the electrons has been developed from the data of a number of theoretical and experimental investigations which appear in the literature.

At the present time, the nuclides Co^{60} and Cs^{137} are most widely used in instrument design and construction. Hence, we shall consider the determination of the energy of electrons produced in lead by γ-photons from the nuclides indicated above.

We shall assume that a flux of γ-photons with energy $h\nu_0$ is incident on a plane-parallel plate (cf. figure) normal to the surface. The electrons produced by the γ-photons are due to the photoeffect and the Compton effect.

The flux of γ-photons (J_k), scattered on one electron at a distance r from the scattering center is determined by the Klein-Nishina-Tamma formula [5].

$$J_k = J\frac{r_0^2}{r^2}\frac{1+\cos^2\psi}{2}\left\{\frac{1}{[1+\omega_0(1-\cos\psi)]^2}+\frac{\omega_0(1-\cos\psi)^2}{(1+\cos^2\psi)[1+\omega_0(1-\cos\psi)]^3}\right\}. \quad (1)$$

Here J is the flux of primary γ-photons; r_0 is the classical radius of the electron:

$$\omega_0 = \frac{h\nu_0}{m_0c^2} \quad (2)$$

is the ratio of the energy of the incident γ-photon to the rest energy of the electron; ψ is the scattering angle of the γ-photon, which is related to the angle of emission of the electrons by the expression [6]

$$\operatorname{tg}\theta = \frac{m_0c^2}{m_0c^2+h\nu_0}\operatorname{ctg}\frac{\psi}{2}. \quad (3)$$

The number of electrons which appear in an area dS from an element dV, taking account of the exponential attenuation, is given by the formula [7]

$$dN_1 = J_k n\, dV\, dS\cos\theta e^{-\mu r}, \quad (4)$$

where n is the density of Compton electrons in lead; cos θ is a factor which takes account of the inclination of the area dS with respect to the direction of motion of the electron; μ is the linear attenuation coefficient for electrons in lead; r is a distance between dV and dS.

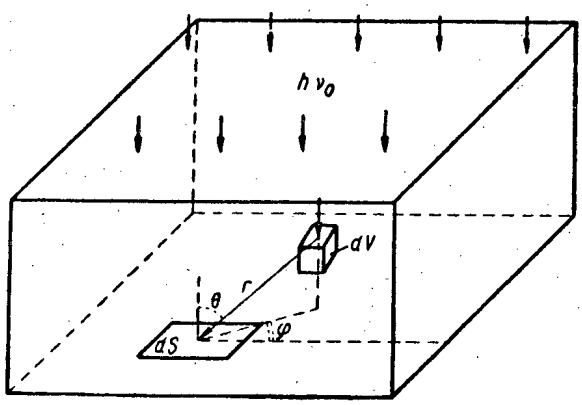

Diagrams showing the production of photoelectrons and Compton electrons in the wall of the ionization chamber.

We compute the energy of these electrons. At emission the energy is

$$E_k = \frac{h\nu_0\omega_0(1-\cos\psi)}{1+\omega_0(1-\cos\psi)}. \tag{5}$$

It is known [6] that the maximum range of electrons (in g/cm^2) as a function of energy is given by the following formulas (for aluminum).

$$R = 0{,}407E_k^{1{,}38}, \qquad 0{,}15 < E_k < 0{,}8\ \text{Mev}. \tag{6}$$

$$R = 0{,}542E_k - 0{,}133, \qquad 0{,}8 < E_k < 3\ \text{Mev}. \tag{7}$$

We can find the energy E' which an electron has after traversing a path r_{Al} ($r \leq R$). Using Eqs. (6) and (7) we write

$$E' = \left(E_k^{1{,}38} - \frac{r_{Al}\varrho_{Al}}{0{,}407}\right)^{-1{,}38}; \tag{8'}$$

$$E' = E_k - \frac{r_{Al}\varrho_{Al}}{0{,}542}. \tag{9'}$$

It should be noted that in the further calculations each of the last relations has been applied not only in the appropriate energy region, but also for lower energy. This procedure is valid because the basic contribution to the intensities and total electron energy comes from the energy region in which Eqs. (6) and (7) are valid, because μ increases as the energy decreases [cf. Eqs. (18)-(20)].

Using the relation $r_{Al}\rho_{Al} \doteq r\rho_{Pb}$, which applies for our energy range, we can obtain the energy of electrons which have traversed a path r in lead. We have

$$E' = \left(E_k^{1{,}38} - \frac{r\varrho_{Pb}}{0{,}407}\right)^{-1{,}38}; \tag{8}$$

$$E' = E_k - \frac{r\varrho_{Pb}}{0{,}542}. \tag{9}$$

The total energy of electrons which originate in the volume dV and enter the area dS is

$$dE' = E'\,dN_1 \tag{10}$$

In order to determine the energy of electrons which enter the working volume of the chamber through a unit surface, we must relate dE' to dS and carry out an integration (in spherical coordinates) over the volume of lead in which the electrons are produced:

$$E_1 = \int_0^{2\pi} d\varphi \int_0^{\pi/2} \sin\theta\, d\theta \int_0^{R(\theta)} \frac{dN_1}{dS} E' r^2\, dr. \tag{11}$$

The number of such electrons is determined as follows:

$$N_1 = \int_0^{2\pi} d\varphi \int_0^{\pi/2} \sin\theta\, d\theta \int_0^{R(\theta)} \frac{dN_1}{dS} r^2\, dr. \tag{12}$$

The mean energy of the Compton electrons is computed from the relation

$$E_{\text{mean k}} = \frac{E_1}{N_1}. \tag{13}$$

Similar formulas can be obtained for the photo-electrons, but now the electron energy is given by

$$E_{ph} = h\nu_0 - E_c, \tag{14}$$

where E_c is the binding energy of the electrons (in what follows we will consider only electrons in the K-shell) while the angular distribution is known [5]. Then

$$E_{\text{mean ph}} = \frac{E_2}{N_2}. \tag{15}$$

Substituting the appropriate values and collecting the common factors, for Cs^{137} we have

$$E_{\text{mean ph}} = \frac{\int_0^R e^{-\mu r}\left(E_{ph}^{1,38} - \frac{r\varrho_{Pb}}{0,407}\right)^{-1,38} dr}{\frac{1}{\mu}(1 - e^{-\mu R})} \tag{16}$$

while for Co^{60}

$$E_{\text{mean ph}} = \frac{\int_0^R e^{-\mu r}\left(E_{ph} - \frac{r\varrho_{Pb}}{0,542}\right) dr}{\frac{1}{\mu}(1 - e^{-\mu R})}. \tag{17}$$

Depending on the energy, the quantity μ can be approximated as follows [8]:

for $E \leqslant 0,15$ Mev

$$\mu = \frac{53,5}{E^2}; \tag{18}$$

for $0,15 < E < 0,6$ Mev

$$\mu = \frac{167}{E - 0,085}; \tag{19}$$

for $0,6 < E < 1,25$ Mev

$$\mu = \frac{104}{E - 0,267}. \tag{20}$$

The mean energy of electrons which enter the effective volume of the chamber can be determined from the weighted mean of the values of E_{mean} and $E_{\text{mean ph}}$.

$$E_{\text{mean}} = \frac{P_{ph} E_{\text{mean ph}} P_k E_{\text{mean k}}}{P_{ph} + P_k} \tag{21}$$

Experimental and Calculated Values of the Mean Energy (E_{mean}, Mev) of Electrons in the Ionization Chamber

Nuclide	Experimental values	Calculated values	Difference in percent
Cs^{137}	0.418	0.349	16.5
Co^{60}	0.702	0.798	13.7

The values of P_{ph} and P_k for Cs^{137} and Co^{60} are taken as proportional to the linear attenuation coefficient for γ-photons in lead [9].

Using numerical integration, by means of Simpson's rule we have carried out the appropriate calculations and obtained the values for a comparison with the experimental results [3] (cf. Table). In this case the mean

energy is computed from the formula

$$E_{mean} = \frac{\Sigma n_i E_i}{\Sigma n_i}, \qquad (22)$$

where n_i is taken in relative units.

A comparison of the results given in the table indicates that this method of calculating the mean electron energy can be used to estimate the ionization current in the chamber.

LITERATURE CITED

1. I. N. Plaksin, A. K. Val'ter, and M. L. Gol'din, Tsvetnye Metalli 5, 16 (1959).
2. A. Dixon, Nucleonics 15, 9, 194 (1957).
3. K K. Aglintsev, V. V. Mitrofanov, and V. V. Smirnov, Atomnaya Énerg. 4, 566 (1958).*
4. M. L. Gol'din, Tsvetnye Metalli 6, 52 (1958).*
5. G. V. Gorshkov, Gamma Radiation of Radioactive Materials [in Russian] (Izd. LGU, 1956).
6. E. Segre, Experimental Nuclear Physics [Russian translation] (IL, Moscow, 1955) Vol. 1.
7. N. G. Gusev, Handbook on Radioactive Radiation and Shielding [in Russian] (Medgiz, Moscow, 1956).
8. N. G. Gusev, Collection: Papers on the Application of Radioactive Isotopes in Medicine [in Russian] (Medgiz, Moscow, 1955) p. 19.
9. Heitler, Quantum Theory of Radiation [Russian translation] (Gostekhizdat, Moscow, 1940).

*Original Russian pagination. See C. B. translation.

INVESTIGATION OF THE BEHAVIOR OF MINERALS ACCOMPANYING URANIUM IN THE ACID LEACHING OF ORES

G. M. Nesmeyanova and N. K. Chernushevich

Translated from Atomnaya Énergiya, Vol. 9, No. 8, pp. 137-138, August, 1960
Original article submitted March 15, 1960

The behavior of nonuranium minerals in the leaching of uranium from ores has substantial significance in that it determines the selectivity of the carbonate or acid leaching. The basic minerals accompanying uranium are oxides and carbonates of iron and, also, sulfides of the heavy metals. Their behavior in hydrometallurgical processes has been studied by a number of investigators [1-5], but not one of these investigations was conducted under uranium-ore leaching conditions.

In the present work we were concerned with the behavior of magnetite, hematite, limonite, siderite, pyrite, and covellite during their leaching with sulfuric acid, nitric acid, and sulfuric acid plus manganese dioxide. The concentration of the solvent was varied from 1 to 400 g/liter, which corresponds to the varying conditions obtained in the leaching of uranium ores [6, 7]. The results of the chemical analysis of the minerals under study are presented in the table. The coarseness of the mineral grains was −0.15 mm. All the experiments were conducted at a temperature of 90°C.

Study of the behavior of limonite in sulfuric acid solutions showed that iron passes easily into solution at sulfuric acid concentrations of 50 g/liter and higher. The extraction of iron is related to the duration of the process and this relationship is more pronounced at low acid concentration. Iron passes into solution to a lesser degree in nitric acid than in sulfuric acid solutions of the same concentration.

In the treatment of magnetite with sulfuric acid solutions the extraction of iron depends on the valence—divalent iron is more completely dissolved. Extractions at concentrations from 100-400 g/liter of nitric acid are better than those from sulfuric acid of the same concentration.

Use of manganese dioxide as an oxidizer substantially reduces the extraction of iron from magnetite in sulfuric acid solution (by a factor of six), but only for a short interval of time (15 min); on further leaching the overall reduction is a factor of two (in comparison with extraction under the same conditions, but without an oxidizer).

Leaching of hematite using solutions of sulfuric and nitric acids having a concentration of 100-400 g/liter showed that the effect of the initial concentration of sulfuric acid is only manifest after prolonged leaching. Just as in the case of magnetite, the iron in hematite more easily dissolves in sulfuric acid solution than in nitric. From siderite (in the absence of magnetite and hematite) iron passes more easily into a solution of nitric acid of a concentration of 1-5 g/liter than into sulfuric acid of the same concentration. However, at concentrations from 50-400 g/liter the quantity of iron that dissolves in nitric acid falls, while the solubility of iron in sulfuric acid increases. The effect of the duration of leaching on the extraction of iron is characterized by the curves presented in Fig. 1b.

Addition of pyrolusite as oxidant to sulfuric acid solutions of concentration 1-400 g/liter lowers the extraction of iron. In this case, exactly as in the experiments with nitric acid, the extraction of iron initially falls and then, on prolongation of the leaching, rises. Only at a nitric acid concentration of 1 g/liter does the extraction of iron increase with time and it reaches 95% after 3 hr of treatment.

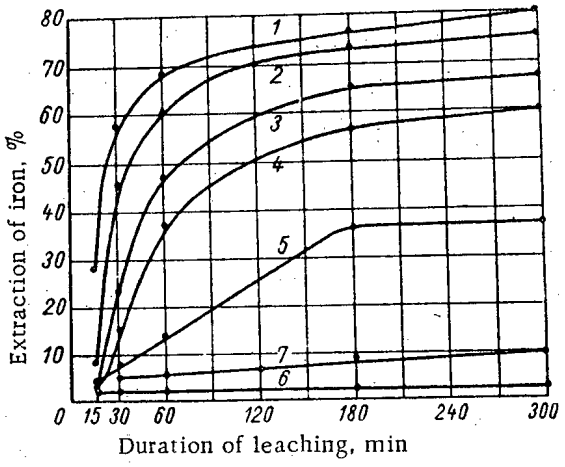

a

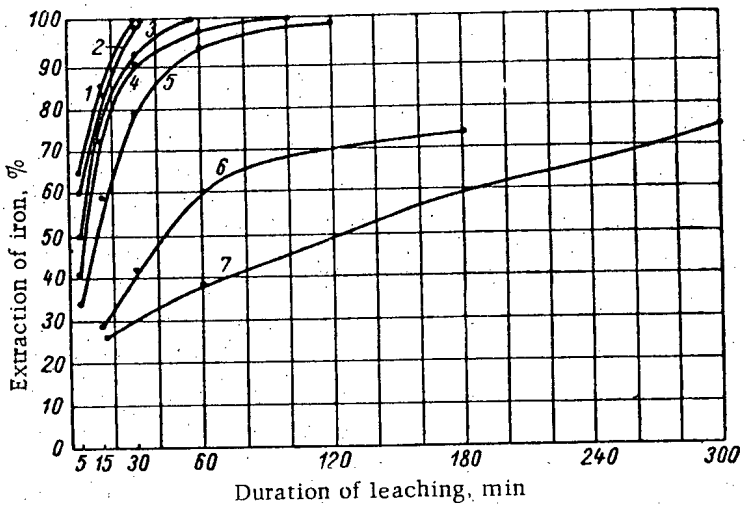

b

Fig. 1. Dependence of the extraction of iron on the duration of leaching of limonite (a) and siderite (b) with various concentrations of sulfuric acid (g /liter). 1) 400; 2) 250; 3) 150; 4) 100; 5) 50; 6) 5; 7) 1.

Results of Chemical Analysis of Minerals

mineral	content %											
	Fe^{2+}	Fe^{3+}	Fe_{tot}	Cu	SiO_2	CO_2	S	As	Al	Mn	MgO	CaO
magnetite	19,23	50,55	69,81	0,01	2,11	—	—	—	0,57	—	—	1,0
hematite	0,08	69,3	69,3	0,01	trace	—	—	—	0,1	—	—	0,1
limonite	0,05	58,6	58,9	0,01	8,02	—	0,093	—	1,0	0,1	0,1	1,0
siderite	22,2	15,4	37,7	0,01	3,2	16,9	—	—	1,0	1,0	4,69	1,35
pyrite	—	—	44,72	0,004	—	—	51,84	0,052	—	—	—	—
covellite	—	—	20,3	38,77	—	—	37,25	—	—	—	—	—

The behavior of sulfides in sulfuric acid solutions sharply differs from the behavior of oxides and siderites. Iron and copper from pyrite and covellite are poorly extracted by sulfuric acid having a concentration from 5 to 400 g/liter. However, nitric acid solutions easily extract iron from pyrite.

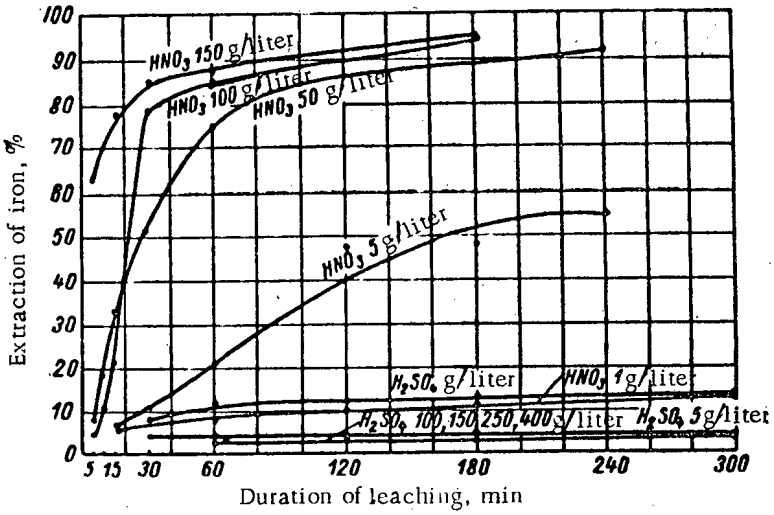

Fig. 2. Dependence of the extraction of iron on the duration of leaching of pyrite with various concentrations of sulfuric and nitric acid.

Although introduction of pyrolusite into the sulfuric acid leaching process increases the extraction of iron from pyrite, the content of iron in solution in this case is 40-50% lower than that in nitric acid medium. The addition of manganese dioxide to sulfuric acid solutions acting on covellite has a more pronounced effect.

Extraction of copper and iron by mixtures of nitric and sulfuric acids (concentration 10-100 g/liter) is greater than extraction by sulfuric acid of the same concentration in the presence of manganese dioxide. Extraction of copper and iron by sulfuric acid of low concentration (1-5 g/liter) is 14 times greater than extraction with mixtures of nitric and sulfuric acid.

Comparison of the results of the extraction of iron from various minerals shows that sulfuric acid solutions dissolve best siderite, limonite, magnetite, hematite and covellite; sulfuric acid with added pyrolusite dissolves siderite, pyrite, and hematite, and nitric acid dissolves best siderite and pyrite.

In choosing the conditions for selective leaching of uranium, one should be cognizant of the fact that regardless of the oxidant used and the concentration of divalent iron in solution, for successful leaching of uranium, it is necessary to have in solution no less than 2 g/liter of trivalent iron [8].

LITERATURE CITED

1. F. M. Loskutov, The Metallurgy of Zinc [in Russian] (Moscow, Metallurgizdat, 1945).
2. V. I. Smirnov, The Hydrometallurgy of Copper [in Russian] (Moscow, Metallurgizdat, 1947).
3. J. Warren, Austral. J. Appl. Sci. 9, 1, 36 (1958).
4. M. L. Chepelevetskii and E. B. Brutskus, Zhur. Neorg. Khim. 1, 7, 1512 (1956).
5. K. Downes and R. Ruce, Canad. Mining and Metallurg. Bull. 48, 515 (1955).
6. I. Ross, Canad. Mining and Metallurg. Bull. 49, 570 (1956).
7. Mining Mag. 94, 1, 26 (1956).
8. J. Arthur and R. Wheele, J. S. Afric. Instn. Mining and Metallurg. 57, 11, 631 (1957).

ATTENUATION OF γ-RADIATION FROM VOLUME SOURCES IN IRON AND LEAD

G. V. Gorshkov and V. M. Kodyukov

Translated from Atomnaya Énergiya, Vol. 9, No. 8, p. 139, August, 1960
Original article submitted February 10, 1960

The present paper represents an experimental study of the laws of attenuation obeyed by γ-radiation from volume sources in iron and lead. The volume source was a metal container in the form of a sawed-off cone filled with aqueous solutions of colloidal gold Au^{198}, E = 0.411 Mev) and NaCl salt (Na^{24}, E_1 = 1.38 Mev and E_2 = = 2.76 Mev). The power of the dose was measured with an ionization chamber with air-equivalent walls. The

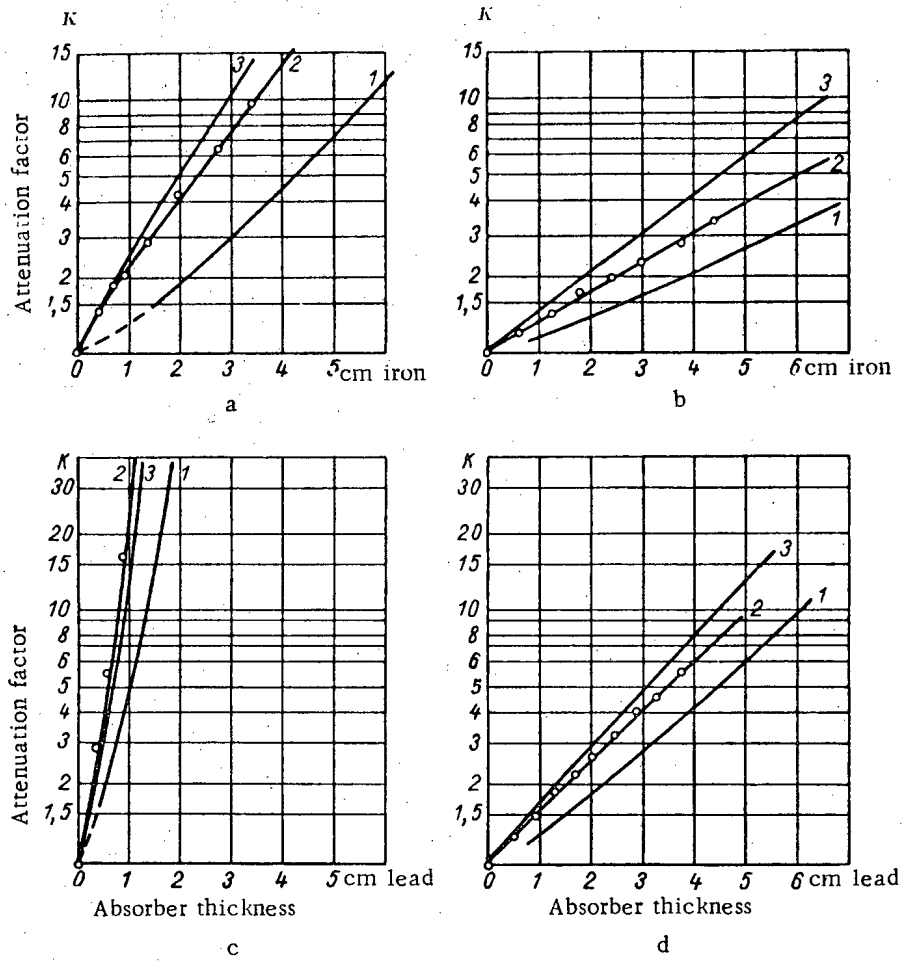

Attenuation factor of γ-radiation dose power. Sources: a,c) Au^{198} (E = 0.411 Mev); b,d) Na^{24} (E_1 = 1.38 Mev and E_2 = 2.76 Mev). Absorbers: a,b) iron, c,d) lead. γ-Radiation attenuation curves: 1) point source, assuming multiple scattering according to Fano's theory; 2) volume source with 100 cm active layer (experimental); 3) volume source, ignoring multiple scattering.

experimental conditions were the same as in [1]. The results of the tests are shown in the figure as the dependence of the attenuation factor K on the number of free paths traversed μl. The factor K was defined as $K = P_0/P_x$, where P_x and P_0 are the powers of the dose in measurements with and without absorber, respectively. From the curves shown in the figure, considering the results of [1] and the theoretical attenuation law for the given geometry [2], the following conclusions can be made:

1. The attenuation of γ-radiation for a volume source is similar in its main features to the attenuation law for a point source, provided one accounts for the rise factor ($B = K_{th}/K_{ex}$);

2. the increase factor for a volume source is less than for a point source; its value depends on the shape of the source (taking into account multiple scattering in the source itself), the spectral composition of the γ-radiation, and the absorber;

3. the increase factor becomes larger with decreasing energy of the γ-radiation and decrease with increasing atomic number of the absorber;

4. in absorbers with high atomic numbers (lead) the increase factor for a volume source is near unity (with $\mu l < 3$);

5. in shielding against γ-radiation from volume sources it is desirable to use materials with a high atomic number or to use combined shielding, placing the material with lower atomic number nearer the source.

LITERATURE CITED

1. G. V. Gorshkov and V. M. Kodyukov, Atomnaya Énerg. 5, 1, 71 (1958).*
2. G. V. Gorshkov, Gamma-Radiation of Radioactive Bodies [in Russian] (Izd. LGU, Leningrad, 1956).

*Original Russian pagination. See C. B. translation.

ATTENUATION OF γ RADIATION FROM POINT SOURCES IN VARIOUS MEDIA

V. M. Kodyukov

Translated from Atomnaya Énergiya, Vol. 9, No. 8, p. 140, August, 1960
Original article submitted February 10, 1960

In practice, protective shields of finite dimensions enjoy wide application, but in spite of this the experimental papers deal primarily with infinite media [1], since the theory of attenuation of γ radiation [2, 3], the analytic results of which are in good agreement with the experimental, is based on such media. In [4] coefficients are given for transition from the increase factor for an absorber of semiinfinite thickness ($B_{t\,\infty}$) to the increase factor for an absorber of finite thickness (B_{tt}). Practically speaking, for medium and large values of the number of free paths traversed the increase factor for an absorber of infinite thickness ($B_{\infty\,\infty}$) coincides with $B_{t\,\infty}$, which permits a transition from $B_{\infty\,\infty}$, calculated by analytic methods, to B_{tt}. In the present paper the attenuation law obeyed by γ radiation from point sources in various media is studied experimentally. The sources are Au^{198} (E = 0.411 Mev), Zn^{65} (E = 1.12 Mev), and Na^{24} (E_1 = 1.38 Mev and E_2 = 2.76 Mev) with an activity of up to 1 C; the size of the sources permitted self-absorption to be neglected. The dose power was measured with an ionization chamber with air-equivalent walls. Absorption in water, iron, and lead was studied. The distance between the detector and source remained constant, while the thickness of the absorber was varied.

Correction Factor $K = B_{tt}/B_{\infty\,\infty}$

Absorber	Source		
	Au^{198} (E = 0.411 Mev)	Zn^{65} (E = 1.12 Mev)	Na^{24} (E_1 = 1.38 Mev, E_2 = 2.76 Mev)
Water	0.6	0.7	0.7
Iron	0.715	0.8	0.825
Lead	0.78	0.88	1.0

In the figure curves are shown for the attenuation factor of the dose power of γ radiation from Au^{198} and Zn^{65} as a function of absorber thickness x ($K = P_0/P_x$). The experimental results were compared with data obtained for attenuation of γ radiation from a point source in an infinite medium [2].

Analysis of the results shown leads to the following conclusions: The value of the increase factor ($B = K_{th}/K_{ex}$) depends on the boundary conditions; with an increase in atomic number of the absorber and energy of the γ radiator the effect of the boundedness of the medium diminishes.

In the table experimentally obtained and averaged corrections are shown for the transition from the increase factor according to Fano's theory (infinite medium) to barrier geometry (with $\mu l > 3$).

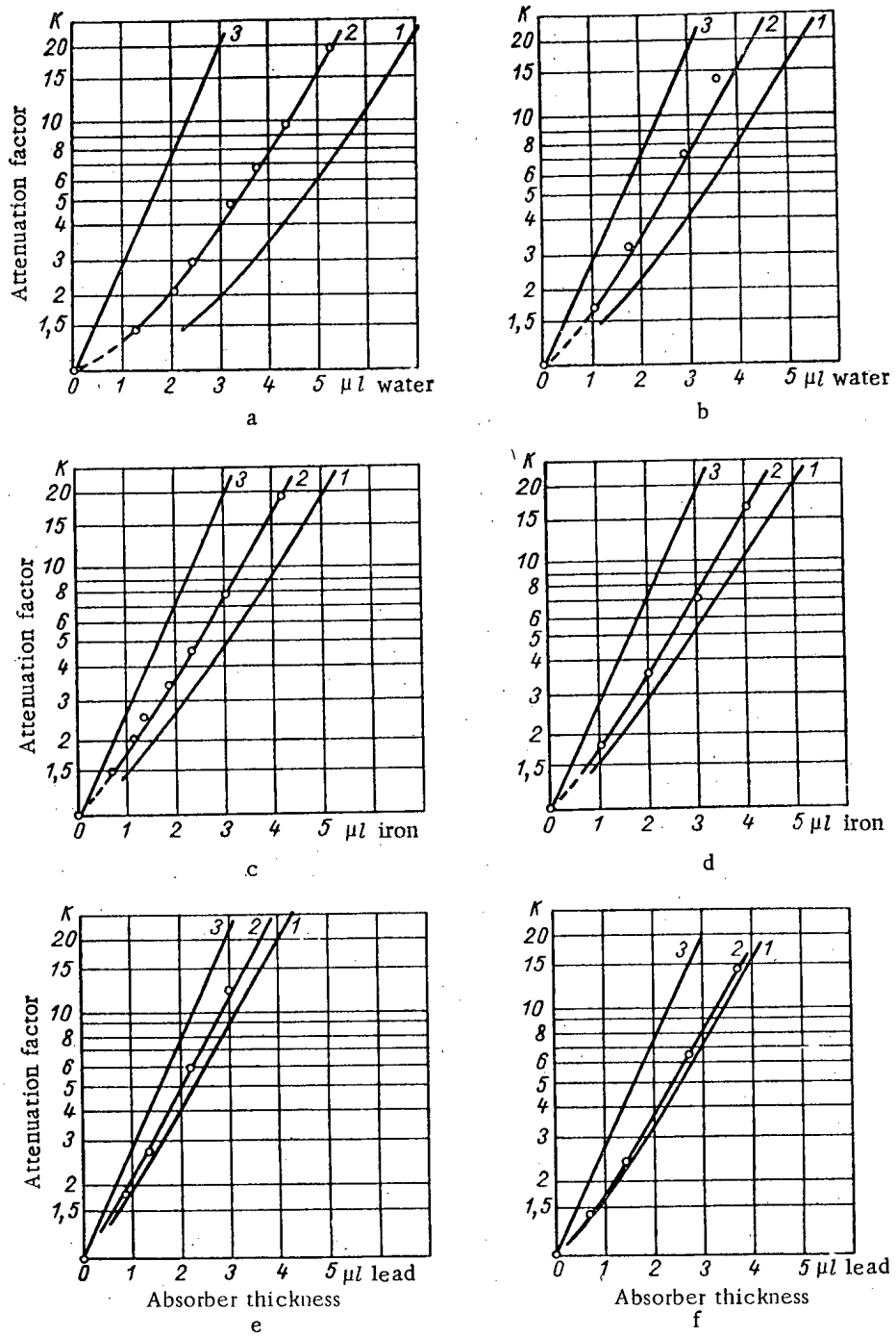

Attenuation factor of γ radiation dose power. Sources: a, c, e) Au^{198} (E ≈ 0.411 Mev); b, d, f) Zn^{65} (E = 1.12 Mev). Absorbers: a, b) water; c, d) iron; e, f) lead. Attenuation curves for γ radiation from a point source: 1) assuming multiple scattering according to Fano's theory; 2) experimental; 3) exponential.

LITERATURE CITED

1. S. G. Tsypin, V. I. Kukhtevich, and Yu. A. Kazanskii, Atomnaya Énerg. 2, 71 (1956).*
2. U. Fano, Nucleonics 11, No. 9, 55 (1953).
3. G. V. Gorshkov and V. M. Kodyukov, Atomnaya Énerg. 5, 1, 71 (1958).*
4. M. Berger and J. Dogget, J. Res. Nat. Bur. Standards 56, 89 (1956).

*Original Russian pagination. See C. B. translation.

ABSORPTION CORRECTIONS IN THE BACKING OF THE 4π-COUNTER

R. M. Polevoi

Translated from Atomnaya Énergiya, Vol. 9, No. 8, pp. 140-142, August, 1960
Original article submitted January 14, 1960

The correction for β-particle absorption in the backing of the source is a fundamental correction which determines the accuracy of measurements of the activity of weightless samples on the 4π-counter[1].

Expressions are obtained for the corrections, valid not only for the simple β-spectrum, as in [2], but also for complex β spectra taking into account conversion electrons and Auger-electrons.

We shall use $\bar{n}$ to denote the number of electrons emitted in a single decay event, including conversion- and Auger-electrons; p_1 is the spectral and solid-angle mean absorption coefficient for electrons in the source backing; p_2 is the spectral and solid-angle mean reflection coefficient for electrons from the backing; N_0 is the number of β-decays in the source per unit time; N_H is the number of pulses per unit time in that half of the counter separated from the source by the backing (usually the lower half); N_B is the number of pulses per unit time in the second half of the counter; N_P is the counting rate with both halves of the counter connected in parallel.

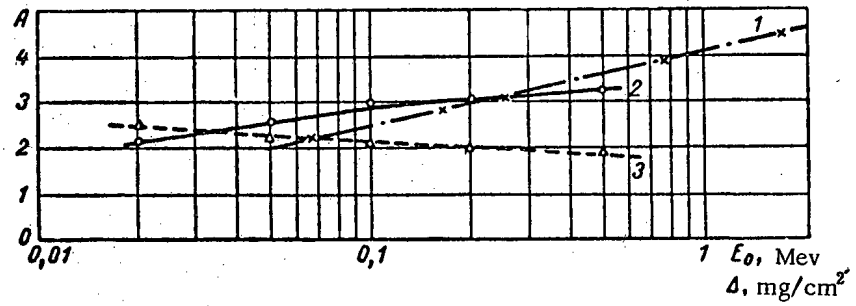

Dependence of the quantity A on the limiting energy of the β-spectrum and thickness of the backing: 1) Dependence of A on E_0 with $\Delta = 100$ μg per cm²; 2) dependence of A on Δ with $E_0 = 254$ kev; 3) dependence of A on Δ with $E_0 = 67$ kev.

Then,

$$N_P = N_0\left[1-\left(\frac{p_1}{2}\right)^n\right]; \tag{1}$$

$$N_B = N_0\left[1-\frac{1}{2^n}+\frac{1-(1-p_2)^n}{2^n}\right]; \tag{2}$$

$$N_H = N_0\left[1-\frac{1}{2^n}-\frac{p}{2}\frac{\left(1-\frac{p^n}{2^n}\right)}{\left(1-\frac{p}{2}\right)}\right], \tag{3}$$

where

$$p = p_1 + p_2.$$

In the first approximation with respect to p_1 and p_2

$$N_B = N_0(1-\alpha+n\alpha p_2); \tag{4}$$

$$N_H = N_0\left(1-\alpha-\frac{p_1+p_2}{2}\right), \tag{5}$$

where

$$\alpha = \left(\frac{1}{2}\right)^n.$$

For $n \neq 1$ Eqs. (1), (4), (5) form a system from which it is possible in principle to determine N_0, by proceeding from the experimental values for N_P, N_B, and N_H. However, in actual practice it is more convenient to determine p_1, making use of the results of [2].

From Eqs. (4) and (5) it follows that

$$p_1 = \frac{2B(1-\alpha)}{(A-1)(2Bn\alpha-2n\alpha-1)-1},$$

where

$$B = \frac{N_B-N_H}{N_B}; \quad A = \frac{p_1+p_2}{p_1}.$$

Since A depends only slightly on the limiting energy of the β-spectrum E_0 and thickness of the backing Δ (see figure), the accuracy of determining p_1 will be good even with a very approximate determination of Δ.

We note in conclusion that the correction equations for simple β spectra (without taking into account Auger-electrons and conversion-electrons) constitute a special case of Eqs. (1, 2, and 3) for n = 1.

LITERATURE CITED

1. H. Seliger and L. Cavallo, J. Res. Nat. Bur. Standards 47, No. 1 (1951).
2. B. Pate and L. Yaffe, Canad. J. Chem. 33, 1656 (1955).

PARTICULARITIES IN THE VARIATION OF THE CAPACITANCE OF IRRADIATED AIR-GAP CAPACITORS

V. P. Sokolov

Translated from Atomnaya Énergiya, Vol. 9, No. 8, pp. 142-143, August, 1960
Original article submitted February 6, 1960

In connection with investigations concerning the effect of nuclear radiation on the operation of electronic equipment it is of interest to consider the problem of changes in the capacitance of air-gap capacitors which are being irradiated. For the sake of simplicity, we shall consider only air-gap capacitors with infinite plates. The capacitance of such capacitors can change only due to the inductive influence exerted on the plates by ions formed in the gap, which is equivalent to variations of the medium dielectric permeability.

It is obvious that the capacitance C of an irradiated capacitor is related to the capacitance C_0 of the same capacitor before irradiation started by the following simple expression:

$$C = C_0 \left[1 + \frac{E(0) + E(d)}{2E_0}\right]$$

where E (0) and E (d) represent the changes in the electrical field strength near the plates of the capacitor which is being irradiated, and $E_0 = -\frac{\varphi_0}{d}$ is the electrical field strength in its gap before irradiation. Consequently, in order to determine C, it is necessary to find E (0) and E (d).

If a constant potential difference φ_0 is applied to the capacitor plates, and if the ionization can be considered as isotropic, the solution of the problem of potential distribution in the air gap can be used for determining E (0) and E (d) [1 and 2].

For $j \simeq eNd$ and for a relative change in capacitance equal to $\Delta C = \frac{C-C_0}{C_0}$, we obtain the following expression: *

$$\Delta C = \frac{(\sqrt{B}+\sqrt{\beta+B})\,d}{2\varphi_0} - 1. \qquad (1)$$

Here, B is a constant, which is the solution of the following transcendental equation:

$$\varphi_0 = \frac{d}{2(K_+ + K_-)}\left[K_-\sqrt{\beta+B} + K_+\sqrt{B} + \frac{K_+}{\gamma}(B-\gamma^2)\ln\left|\frac{\frac{K_-}{K_+}\gamma+\sqrt{\beta+B}}{\sqrt{B}-\gamma}\right|\right],$$

while

$$\beta = \frac{4\pi eN(K_- - K_+)\,d^2}{K_+K_-}; \quad \gamma = 2d\sqrt{\frac{\pi eNK_+}{K_-(K_+ + K_-)}},$$

where N is the ionization intensity, K_+ and K_- are the ionic mobilities, and e is the electron charge.

* It is taken that positive ions move in the direction of the x axis.

If we neglect the effect of the proper electrical field of ions on their motion, we obtain for a simpler expression ΔC:

$$\Delta C = \frac{\pi e N (K_+ + K_-) d^4}{3 K_+ K_- \varphi_0^2}. \tag{2}$$

which is, however, less accurate.

If $j \ll eNd$, the change in capacitance is found by solving the three-layer potential problem for conditions where the potentials and the electric field strengths at the layer boundaries are continuous and for boundary conditions where the potentials at the plates are equal to zero. Then

$$\Delta C_{\max} = \frac{1}{2} (\sqrt{1+\xi_1} + \sqrt{1+\xi_2}) - 1, \tag{3}$$

where

$$\xi_1 = \frac{4\pi e (K_+ + K_-) K_-}{\alpha K_+}; \quad \xi_2 = \frac{4\pi e (K_+ + K_-) K_+}{\alpha K_-};$$

α is the ion recombination coefficient.

It follows from the above expressions that, in irradiation, the capacitance of air-gap capacitors for the static case smoothly increases with an increase in ionization intensity; all other conditions being equal. The capacitance increases from the value C_0 to a certain value C_{max}, which essentially depends not only on S, d, and φ_0, but also (due to the ionic mobility) on air temperature and pressure and, in the general case, on the gas composition and the nature of nuclear radiation. For air pressure equal to $\lesssim 100$ mm Hg and rather small air gaps, Eqs. (1)-(3) lose their validity, since the description of ion motion by means of the mobility concept (see [2], p. 41) ceases to be applicable. It is also assumed that the voltages applied are far below the break down values.

If a variable potential difference is applied to the capacitor plates, the capacitance will depend on time, the applied voltage frequency, and its shape. In order to determine the qualitative particularities of capacitance variation for frequencies that are not too large, it is sufficient (by analogy with papers [1 and 2]) to solve a series of problems connected with the potential distribution in the air gap for the necessary number of charge configurations and for a rectangular alternating voltage while neglecting diffusion and the effect of the ion proper fields on their motion. The calculation results can be reduced to the following. For sufficiently strong fields and

$\left(\omega < \frac{\pi K_+ E_0}{d}\right)$ frequencies, the steady-state change in capacitance, i.e., the capacitance variation averaged with respect to the voltage half-period, is

$$\overline{\Delta C}^{T/2} = \frac{\pi e N (K_+ + K_-) d^4}{3 K_+ K_- \varphi_0^2} + \frac{eN (K_-^2 - K_+^2) d^6}{3 K_-^4 \varphi_0^2} \omega. \tag{4}$$

For $\frac{\pi K_+ E_0}{d} < \omega < \frac{\pi K_- E_0}{d}$ the instantaneous relative change in the capacitance is determined by the expression:

$$\Delta C(t) = \frac{2\pi e n_0 l}{d E_0} (2 K_+ E_0 t + l - d), \tag{5}$$

where l is a constant, and $\overline{n}$ is a certain average value of the volume density of the equilibrium charge, which constantly circulates in the air gap. (Obviously, in this case $\overline{\Delta C}^{T/2} \equiv 0$).

Independently of the field strength, and beginning with certain frequencies

$$\omega_{\text{crit}} \left(\frac{\pi K_- E_0}{d} < \omega_{\text{crit}} < \pi \sqrt{\alpha N}\right)$$

the steady-state capacitance increment in irradiation will gradually decrease with an increase in frequency from values corresponding to the equivalent static increment to zero. Some idea of the character of capacitance variation in dependence on frequency for $\omega \ll \omega_{\text{crit}}$ can be obtained by considering different charge configurations in the gap for "jump-like" ion motion. For instance, for two "jumps" per one half-period, the steady-state change

in capacitance (averaged with respect to one period) is

$$\overline{\Delta C}^T = \frac{2\pi^3 e K N}{3\omega^2}\left(1+\frac{\pi K E_0}{d\omega}\right),$$

if we assume that $K_+ = K_- = K$.

The considered dependence of the capacitance on voltage frequency is connected with volume fluctuations of charges in the air gap and has nothing in common with ion inertia.

For d values which are much smaller than the magnitudes of Compton electron runs in air and for sufficiently thick plates, the degree of ionization in capacitor gaps can be considerably greater than the ionization created in air by primary γ radiation (approximate quantitative determinations indicate that, in cases of practical importance, secondary ionization can be 10 to 100 times as large as primary ionization). The change in the capacitance of air-gap capacitors which are being irradiated can also depend on the plate material. In the case of directed beams of γ rays, geometric anisotropy is possible, i.e., ΔC values can differ in dependence on whether the direction of the incident beam is parallel or perpendicular to the capacitor plates.

The above results are in qualitative agreement with experiments known to the author. Attempts to perform more accurate quantitative calculations of capacitance changes led to expressions unsuitable for practical purposes or were frustrated by basic mathematical difficulties.

The author extends his thanks to B. M. Sorokin, who suggested the subject and helped in the work, and to A. A. Markov, who offered valuable remarks and read the manuscript.

LITERATURE CITED

1. J. Thomson, Conduction of Electricity through Gases, (Cambridge, University Press, 1928) Ed. 3, Vol. 1, p. 193.
2. L. Leb. Basic Processes in Electrical Gas Discharges [in Russian] (Gostekhizdat, Moscow–Leningrad, 1950).

APPLICATION OF NEUTRON PULSE SOURCES FOR INVESTIGATIONS IN OIL WELLS

B. G. Erozolimskii, A. S. Shkol'nikov, and A. I. Isakov

Translated from Atomnaya Énergiya, Vol. 9, No. 8, pp. 144-145, August, 1960
Original article submitted July 15, 1959

At the present time, the neutron pulse method is widely used for determining the parameters of different media [1]. This method also seems to be very promising for the investigation of the parameters of rocks surrounding the drill hole. In the USSR as well as abroad, efforts are now being made to develop a small-size accelerating tube which could be used as a neutron pulse source in sounding devices for the radioactive probing of drill holes [2-7].

The most promising method for investigating rocks is that which is based on measuring the dependence of the thermal neutron density in the rock on the time t, which has elapsed from the moment when the neutron pulse from the source ended, i.e., the method based on measuring the lifetime of thermal neutrons in the rock.

The lifetime of thermal neutrons in rocks depends on the degree of mineralization of the water below petroleum layers by the presence of NaCl. Since oil-bearing strata hardly contain any salt, the measurement of the lifetime τ makes it possible to determine whether petroleum or water is contained in a certain layer. Thus, calculations show that, for instance, in sandstone containing 20% water which is saturated with salt (200 g/liter), $\tau_w = 250$ μsec, while, in the same sandstone containing 20% petroleum, $\tau_o = 570$ μsec. This fact is actually applied in the presently used neutron methods for determining the position of the water–petroleum interface in the hole by means of steady neutron sources. However, in this, the directly measurable quantities are the parameters of the neutron steady-state field around the source, which are related to the τ value of the medium by a proportional dependence (for instance, the density of thermal neutrons or γ-quanta, generated by the capture of neutrons by the rock nuclei, is measured). In using the pulse method, the time dependence n(t), related to the τ parameter by the exponential factor $e^{t/\tau}$, is measured. In this, the dependence of measurement results on the parameter τ is much stronger than in measurements in a steady-state field. Calculations show that, for the above τ parameter values, which differ by 50%, the results obtained in measuring the thermal neutron density in water-saturated and oil-bearing layer portions approximately 1000 μsec after the neutron source pulse ended must show a tenfold difference. In order to verify these estimates, we performed experiments on models of rock layers, which confirmed the above assumptions. The measurement method is described in [1 and 8].

Figure 1 shows the results obtained in measuring the dependence of the thermal neutron density on time t in models filled with a mixture of sand and paraffin or sand and paraffin with salt. The axial opening simulating the hole was surrounded by the drive pipe and a cement ring, to which salt was applied in experiments where paraffin with salt was used (water-carrying layer). A proportional BF_3 counter was used as the thermal neutron indicator. The pulses from the counter were fed to a 100-channel time analyzer. An accelerating deuteron tube with a tritium target served as the source of neutrons with an energy of 14 Mev. By means of this tube, it was possible to obtain neutron pulses with a duration of 5 μsec and a repetition frequency of approximately 300 cps.

The model with unsalted paraffin corresponded to sandstone saturated with oil and having a 20% porosity; the model with salted paraffin corresponded to sandstone of the same porosity, but saturated with water containing 200 g/liter of salt. The model dimensions and the position of the counter and the source are shown in Fig. 2. The measurement results prove that the indicator readings in the oil-bearing and water-saturated layer models show a

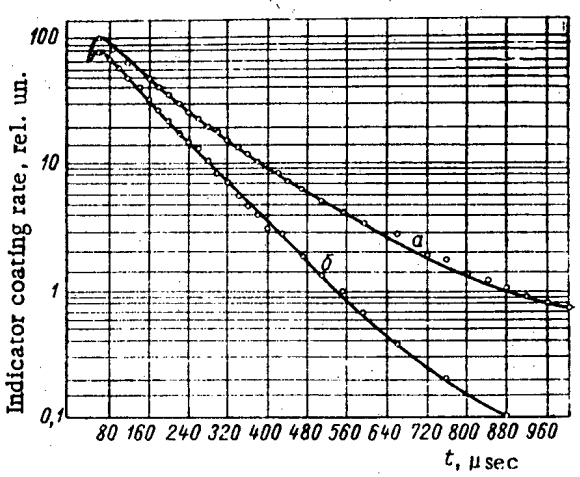

Fig. 1. Diagrams of the thermal neutron density dependence on time t. a) Oil-bearing sandstone model; b) water-bearing sandstone model.

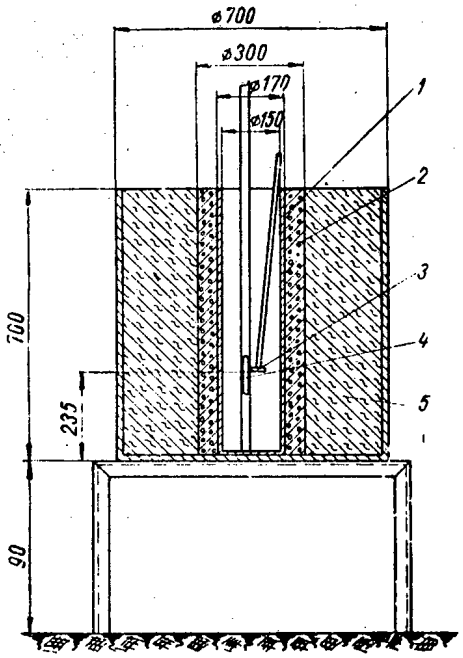

Fig. 2. Diagram of the experimental mock-up. 1) Drive pipe; 2) cement rings; 3) target; 4) counter; 5) mixture of sand and paraffin (and salt).

tenfold difference for t = 800 μsec. For the sake of comparison, it should be noted that the differences in indicator readings obtained by the usual methods of neutron core sampling (with steady sources) did not exceed 40 to 50% for the same models. The method of induced activity with respect to sodium is an exception (two- to threefold differences are obtained); however, this method requires prolonged measurements at one point (lasting approximately 15-20 hr).

The absolute τ_o and τ_w values obtained in these experiments (of the order of 250 and 150 μsec, respectively) differ to a certain extent from the actual lifetimes of thermal neutrons in oil-bearing and water-bearing sandstones due to the finiteness of dimensions of the models used and the consequent neutron leakage as well as due to the influence of the steel column and the cement ring. This applies much less to the observed differences between the experimental τ values, and the obtained data of the n_o/n_w ratio are entirely suitable for estimating the relative effects under actual conditions.

The indicator counting rate in the sandstone model without salt was equal to ~ 10 counts/min in a single channel with a width of 20 μsec for t = 800 μsec and an average flux intensity of the fast neutrons emitted by the accelerating tube equal to ~ 10^6 neutron/sec. This is entirely sufficient for obtaining reliable results after a few minutes.

It should be borne in mind that the pulse method will be much less sensitive to the "adjacent medium" parameters in comparison with methods where a steady neutron source is used [6]. Therefore, one can expect that the obtained information on the rock characteristics will be hardly distorted by the influence of the hole (the drill opening, the steel drive tube, and the cement ring).

On the basis of the above considerations, it can be expected that the pulse method will be used for a positive determination of the water–petroleum interface and apparently even for a quantitative determination of the petroleum content.

In conclusion, we extend our thanks to G. N. Flerov, on whose initiative the experiment was organized, for his valuable remarks in discussing the experimental results, and to I. M. Frank and F. L. Shapiro, who helped in the work.

LITERATURE CITED

1. A. V. Antonov, et al., Materials of the International Conference on the Peaceful Uses of Atomic Energy, Geneva, 1955 [in Russian] (Izd. AN SSSR, Moscow, 1957) Vol. 5, p. 11.

2. G. N. Flerov, F. A. Alekseev, and B. G. Erozolimskii, Materials of the All-Union Conference on the Peaceful Uses of Radioactive Radiations and Isotopes in the National Economy [in Russian] (Gostoptekhizdat, Moscow, 1958) p. 17.
3. Nucleonics, 15, No. 9, 192 (1957).
4. Petrol. Engr. 28, No. 3, B-86 (1956).
5. Scient. Amer. 190, No. 23 (1954).
6. B. G. Erozolimskii, et al., Neftyanoe Khozyaistvo, 11, 21 (1958).
7. B. G. Erozolimskii, et al., Nuclear Geophysics. Collection of articles on the Application of Radioactive Isotopes and Radiations in Petroleum Geology, Ed. by F. A. Alekseev [in Russian] (Gostoptekhizdat, Moscow, 1959) p. 351.
8. A. A. Bergman, et al., Materials of the International Conference on the Peaceful Uses of Atomic Energy, Geneva, 1955 [in Russian] (AN SSSR, Moscow, 1957) Vol. 4, p. 166.

NEWS OF SCIENCE AND TECHNOLOGY

VIII SESSION OF THE LEARNED COUNCIL OF THE JOINT INSTITUTE FOR NUCLEAR RESEARCH

V. Biryukov

Translated from Atomnaya Énergiya, Vol. 9, No. 8, pp. 146-147, August, 1960

The Learned Council of the Joint Institute for Nuclear Research held its VIII session on May 24-28, 1960. Leading scientists of the member nations supporting the Institute were on hand to participate in the deliberations of the Learned Council at Dubna. The Director of the Institute, D. I. Blokhintsev, acquainted those present at the session with the draft of the five-year development plan of the Joint Institute, covering the years 1961-1965. This plan, following careful preparation and discussion, was presented for approval to the Committee of Authorized Representatives in late 1960. The development plan draft provides for retention of the fundamental trend in the activities of the Joint Institute, i.e., fundamental research in the field of the physics of elementary particles and physics of the atomic nucleus. Further improvements and development work on the principal physical facilities are envisaged, as well as an expansion of the capacities of the computing center at the Joint Institute. Particular attention is reserved for work contributing to the development of low-energy physics in the member nations of the Institute.

Wang Kang-ch'ang, Vice-Director of the Joint Institute for Nuclear Research, took the floor with a report on collaboration between the Joint Institute and the scientific research centers of the member nations. He took note of the principal directions being traced out by these collaborative efforts. The research organizations of Bulgaria, Hungary, the German Democratic Republic, the Chinese Peoples Republic, Poland, Rumania, Czechoslovakia, and also some institutes of the Soviet Union are taking part in research work conducted with the aid of nuclear emulsions, which are being bombarded systematically in the proton synchrotron of the Joint Institute. In these efforts, which are to some extent of the character of independent research, and in other cases integrated into joint research efforts by several different teams, processes involving elastic scattering of protons of 6 Bev energy by protons and nuclei, interactions between π-mesons and nucleons and nuclei of an emulsion at 7 Bev energy, the formation of hyperfragments of protons at 9 Bev by collision with heavy nuclei, etc., are under study. The Joint Institute has sent its own equipment to China and Bulgaria to outfit nuclear-emulsion laboratories in those countries.

Collaboration is being promoted in research involving the use of bubble chambers. Some thousands of photographs taken from a bubble chamber have been routed to Warsaw and Budapest, where the responsible scientific groups are studying elastic scattering of π-mesons of 6.8 Bev energy by protons. Such photographs, made with the aid of other bubble chambers, will soon be on their way to laboratories in East Germany, Rumania, and Czechoslovakia.

Wang Kang-chang, noted the fruitful collaboration underway between the Joint Institute and the nationalized Karl Zeiss concern (Jena, East Germany) in the manufacture of instruments for automatic monitoring of nuclear emulsions.

An excellent instance of such collaborative efforts is the joint work going on between the Joint Institute for Nuclear Research and the Warsaw Nuclear Research Institute, where preparations of neutron-deficient isotopes of the rare-earth elements, irradiated in a synchrocyclotron, are being processed. These preparations are also being sent to the Institute of Physics of the Czechoslovak Academy of Sciences.

The collaboration promoted by the Joint Institute is also being developed with other countries, and in other avenues of work. Workshop conferences where the results of collaborative efforts may be surveyed and plans may be drawn up for further collaboration, are being organized systematically by the Joint Institute. During the recent

semester periods alone, conferences have been held here on express techniques in the physical and chemical analysis of new transuranium elements, on the use of semiconductor nuclear radiation detectors, on the development of the theory of dispersion relations, on research carried out with the aid of nuclear emulsions.

The Learned Council of the Institute approved the program of collaboration on many fronts as proposed by the Commission with the participation of representatives of the State Committee of the Council of Ministers of the USSR on Uses of Atomic Energy, having laid stress on the importance of trips by co-workers of the Institute and specialists from scientific research institutes of the Soviet Union to participate in conferences, and also to give lectures and exchange experience with their counterparts in the various member nations of the Institute.

During the VIII Session, panel sessions of the Low-Energy Section, organized at the end of last year, were held. These were attended by prominent scientists of the member nations of the Institute: G. Richter (Germany), Lin (China), Kim Hung Bong (Korea), G. Newodniczanski (Poland), S. Titeica (Rumania), and others. The Soviet Union was represented by N. A. Vlasov, G. N. Flerov, V. V. Goncharov, L V. Groshev, and others. I. M. Frank was unanimously nominated as Chairman of the Session. After detailed discussion, the work plan of the Section was adopted, its gist being to coordinate research in the field of low-energy physics in the socialist countries.

A significant place in the deliberations of the Learned Council was given over to a discussion of the most outstanding scientific research efforts being tackled currently at the Joint Institute for Nuclear Research.

The members of the Learned Council heard a report on the work of the team at the High-Energy Laboratory, headed by Wang Kang-ch'ang and V. I. Veksler, which, working with a propane bubble chamber placed in a constant magnetic field in a beam of negative π-mesons with momentum 8.3 Bev/c, generated by the proton synchrotron, were the first to detect an event of birth and decay of a $\tilde{\Sigma}^-$-hyperon, which was reported in the press. This same team has done a lot of work on investigating the processes involved in the generation and decay of Σ^--hyperons. Several tens of thousands of photographs obtained in the bubble chamber, bombarded by negative π-mesons with momenta of 6.8 and 8.3 Bev/c, were provided for this purpose.

A report on the commissioning of a model of an accelerator of a new type, an annular synchrocyclotron (ring phasotron), which was developed by a team of Soviet and Czechoslovak scientists led by V. A. Petukhov, was heard with great interest. Realization of the proposal advanced as far back as 1953 by Soviet physicists constitutes a new step in accelerator engineering on the way to stepping up the intensity of accelerated charged-particle beams. A time-invariant magnetic field favorably distinguishes this type of accelerator from synchrotrons and proton synchrotrons, including strong-focusing accelerators, since conditions governing engineering of the magnet and the magnet power supplies are greatly relaxed and the number of acceleration cycles per unit time can be substantially increased. In addition, this magnetic field variant removed the requirements for precision in obeying the law of variation of the high-frequency acceleration voltage. The advantages referred to are arrived at by a special form of annular magnetic field growing along the radius and changing in sign in adjacent sectors. The magnetic circuit in a field of this type simultaneously contains a set of equilibrium orbits ranging from the lowest energies to maximum energy.

V. I. Veksler gave an account of new work on the study of elementary particles and the structure of the nucleon, as performed on the proton synchrotron. He told of attempts to detect D-mesons. The problem of the existence of such mesons is of fundamental significance for the theory of elementary particles. The experimental material now available to physicists is, as the reporter pointed out, sufficient only to provide grounds for hypothesizing, but not for drawing a definite inference as to the existence of the D-meson. In view of the importance of the question, work in this direction is being continued. Among the other research projects is the investigation of the decay of long-lived K^0_2-mesons; an interesting event of decay of a K^0_2-meson into π^+-, π^--, and π^0-mesons has been detected.

Experiments dealing with nucleon interactions with nucleons and π-mesons and the discernment of regularities in the generation of strange particles in the high-energy region have been carried out for the purpose of studying nucleon structure. Data obtained on the angular and energy distributions of secondary particles support the view that interaction of the central regions of nucleons is much weaker than expected for processes with a high multiplicity of meson generation. D. I. Blokhintsev discussed a possible theoretical interpretation of the new effects found.

*Atomnaya Energ. 9, No. 6 (1960) [see C. B. translation].

New research work carried out with the synchrocyclotron at the Nuclear Problems Laboratory excited considerable interest. A team headed by V. M. Sidorov studied the process of interaction between π-mesons and μ-mesons through nuclear photoemulsion records. It is of general knowledge that the interaction of π-mesons does not lend itself to direct methods of investigation and that indirect techniques must be brought into play. Experimental researchers comprising this team used the data which they compiled for the $\pi^- + p \rightarrow \pi^+ + \pi^- + n$ reaction occurring in a photographic emulsion at 290 Mev energy. On the basis of the energy distribution of secondary particles in the reaction studied, the cross section of the charge exchange process $\pi^+ + \pi^- \rightarrow \pi^0 + \pi^0$ was determined. To date, efforts have been limited to the attempt to estimate the order of magnitude of the cross section for this interaction.

Yu. D. Prokoshkin presented a review of work carried out at the Nuclear Problems Laboratory in which various aspects of the problem of isotopic spin conservation were probed. In one of the projects, carried out by the team under L. M. Soroko, an investigation was made of the reaction $d + d \rightarrow \pi^0 + \alpha$, which may take place only when isotopic spin is not conserved. Despite the fact that the physicists in this team were also able to measure very minute cross-sections ($\sim 2 \cdot 10^{-32}$ cm^2), they were unsuccessful in detecting this reaction, which argues for a high degree of rigor in the conservation of isotopic spin in the case in point.

A group of experimental physicists led by V. P. Dzhelepov obtained new and intriguing information on the scarcely studied reactions involving the formation of π-mesons: $n + p \rightarrow \pi + n + n$ and $p \rightarrow \pi^- + p + p$. A study of these reactions (taking into account the available data on the reaction $p + p \rightarrow \pi^0 + p + p$) presents the most convenient method for determining the extent of the production cross section of π-mesons by nucleons in an energy state of zero isotopic spin. Experiments conducted on a beam of neutrons at 590 Mev energy yielded cross sections for those processes. The measured angular distributions of the π-mesons yielded the possibility of being able to determine for the first time the character of the angular distribution of π-mesons formed in a state of zero isotopic spin.

In conclusion, Yu. D. Prokosh reported on the results of the experiments conducted by his team in which the ratio of the probabilities of two absorption processes of a π-meson brought to rest by protons was measured: the reaction $\pi^- + p \rightarrow \pi^0 + n \rightarrow \gamma'' + \gamma' + n$ and the reaction $\pi^- + p \rightarrow \gamma + n$ (Panovsky ratio). In this work, in contrast to earlier work, the energy spectrum of gamma photons was not studied, and the value of the ratio was determined directly by comparison of the number of coincidences of two gamma photons formed as a result of the decay of a π-meson to the number of gamma photons issuing from the second reaction. The value obtained for the ratio $P = 1.40 \pm 0.08$, is the most accurate value to date.

A. E. Ignatenko gave an account of research into the nature of the paramagnetism of various μ-mesonic atoms. A group of physicists under his direction performed measurements of the asymmetry of decay electrons from polarized μ-mesons in mesonic atoms, which made it possible to study a series of phenomena caused by the interaction between the magnetic moment of the μ-meson and the magnetic moment of the electron shell of the atoms having zero nuclear spins. Experiments showed that paramagnetism of mesonic atoms in dielectrics is due to the magnetic moment of the μ-meson, while paramagnetism in paramagnetic metals is due to the magnetic moments of the electron shell and of the μ-meson.

In the resolution adopted by the Learned Council, a high estimate is given of the new investigations carried out.

The Learned Council also considered a project for bestowing of annual awards for the most outstanding research carried out at the Joint Institute for Nuclear Research.

ATOMIC ENERGY AT THE CZECHOSLOVAK EXHIBIT IN MOSCOW

Yu. Koryakin and V. Parkhit'ko

Translated from Atomnaya Énergiya, Vol. 9, No. 8, p. 148, August, 1960

The Czechoslovak Exhibit was opened to visitors during May and June 1960 in the "Sokol'niki" (Falcons) Cultural and Recreational Park Grounds in Moscow.

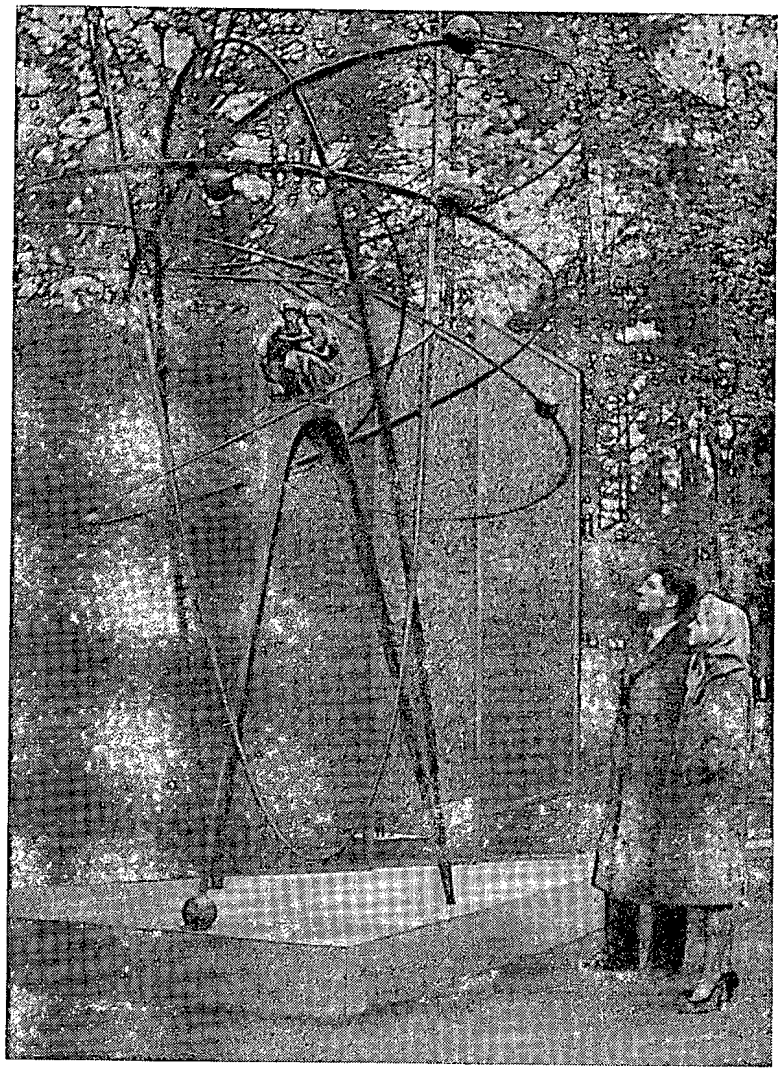

Two spectators viewing the model of the "Atom" at the entrance to the Czechoslovak Exhibit. (photo by the authors)

In the "Science" section of the exhibit, stands and displays told of applications for nuclear energy in Czechoslovakia. One of the stands had on display a map of Czechoslovakia with observatories and research stations taking part in the IGY program duly indicated. Such stations as Lomnicky Sit and Praha-Karkuv are engaged in cosmic ray studies. The Hradec Kralove and Chopok stations in Slovakia, Lomnicky Sit in Hahrach and the Milesovka station in Bohemia are working on nuclear radiations.

Applications of radioactive isotopes in various branches of the national economy and in scientific research were illustrated by several photographs.

The visitors showed great interest in an electron microscope with a magnification of 30,000 ×. Such microscopes are being fabricated on a mass production basis in Czechoslovakia at present. One of the best customers for these microscopes is the Soviet Union.

The guides at the Exhibit informed the visitors about the 150 Mw nuclear electric power station now being built in Czechoslovakia for the Institute of Atomic Energy.

JAPAN'S FIRST NUCLEAR POWER STATION

Not translated

See Nuclear Power, 5, No. 47 (1960)

USA NUCLEAR POWER DEVELOPMENT PLANS FOR 1960-1970

Not translated

USAEC FINANCIAL REPORT FOR 1959

Not translated

680 Mev SYNCHROTRON

V. A. Petukhov

Translated from Atomnaya Energiya, Vol. 9, No. 8, pp. 154-55, August, 1960

An electron accelerator accelerating to a maximum energy of 680 Mev has been commissioned, during 1959, at the Accelerator Laboratory of the P. N. Lebedev Institute of Physics of the Academy of Sciences of the USSR. The accelerator is based on the 10 Bev proton synchrotron as a prototype. The electromagnet, an injector (Van de Graaff generator, 800 kv voltage), the major portion of the supplies system, and the vacuum system are borrowed from the precursor. For most of the acceleration cycle, the machine functions as a synchrotron (with a constant frequency of particle revolution), and the frequency is varied by 8% as in the proton synchroton only for the initial interval. The intensity attained in the accelefator is $(5-6) \cdot 10^8$ electrons/pulse at the end of a cycle. The Van de Graaff generator will soon be replaced by a pulse transformer with the same injection voltage, making it possible to raise the number of accelerated electrons to 10^{10}. Preparatory work has been completed for performing a number of experiments on the accelerator, dealing with the study of photomeson processes, and verifying the range of applicability of quantum electrodynamics. Some of these experiments have already been started.

The "racetrack" type magnet of the synchrotron has four circular sectors spanning 86° each with rectilinear intervals 67 cm in length. The mean radius of the circular sectors of the magnet is 200 cm. The pole width measures 36 cm. The mid-radius pole-gap height is 12 cm. The aperture of the vacuum chamber is 9 × 30 cm. Maximum field strength in the pole gap is 11,600 oersteds (at 960 amp current flowing through the coils). The

magnetic field at injection (for injection energy of 800 kev) is 20 oersteds. The magnetic field index $\underline{n}$ (radial decrease of magnetic field) is 0.55-0.57 (in the region of 22 cm width along the radius for average field and 13 cm at the end of a cycle). The acceleration period is 0.6 sec. The repetition frequency of operating cycles is one cycle per 5 sec. The rate at which the magnetic field builds up with time is constant for a large fraction of the cycle (20,000 oersteds/sec); at the end of an acceleration cycle, it drops by 20%. The frequency of the accelerating high-frequency field is 19 Mc at the initiation of the acceleration cycle, and 20.6 in the synchrotron mode. The amplitude of the high-frequency accelerating voltage during the first acceleration stage is 250 v, and reaches 20 kv during the second stage. The average electron energy increment during a revolution is 60 v. The operating chamber vacuum is $(3\text{-}5) \cdot 10^{-6}$ mm Hg. The vacuum chamber is made of porcelain and is detachable.

While the accelerator was being put into its final paces prior to operational service, considerable difficulties were encountered in correcting the magnetic characteristics in the initial portion of the acceleration cycle, (at fields of 20-60 oersteds), and were found to be a consequence primarily of the effect of the residual field and the eddy-current field present in the electromagnet iron. The following appurtenances were introduced into the power supply system to remove field distortions and stabilize the magnetic characteristics:

1) a demagnetizer with current amplitude 180 amp, whose function was to reduce the strength of the residual field from 50 to 2 oersteds;

2) a device designed to superimpose a negative bias of 35 oersteds at the beginning of the operational cycle;

3) a stabilizer (working to within a precision of $\sim 0.5\%$) of the initial voltage across the electromagnet coils;

4) compensating coils making possible a correction and operational adjustment of the basic magnetic field parameters at low field strengths (azimuthal asymmetry, magnet midplane, value of $\underline{n}$ index).

Radiation losses at ~ 10 kev/revolution at peak energy. This caused the high-frequency system of the accelerator to be separated into two parts. The first, frequency-modulated, carried electron acceleration from the injection energy to 100 Mev energy and provided a total voltage of 250 v across the shortened electrode. The second part accelerates the electrons to peak energy to a constant frequency of 20.6 Mev and a voltage of 20 kev across the toroidal resonator cavity.

A fairly large staff of co-workers of the Laboratory took part in the work on building the machine, and articles by those workers with a fuller and more detailed description of individual components and systems, and of the process of putting the accelerator into service, will appear in the literature in the near future.

A NEW ORE DRESSING PLANT IN FRANCE

Translated from Atomnaya Énergiya, Vol. 9, No. 8, pp. 155-156, August, 1960

A new plant for beneficiation of uranium ores, with a capacity of 1000 tons of raw ore daily, is in operation at the Forese mine [1, 2]. The efficient mechanical upgrading of the comparatively low-grade uranium ore via a combined process is of particular interest (see insert).

First-stage ore dressing consists of sorting on a skip-loader radiometric monitoring station, which yields 30 tons of concentrate containing over 1% uranium, 900 tons of run-of-mill ore (intermediate product) for rerun, and 70 tons of final tailings. The run-of-mill ore is then run through a second sorting stage at the radiometric monitoring point, where it is separated into almost equal lots of average-content ore and low-grade ore to be upgraded via other processes.

The radiometric monitoring station is equipped with a measurements facility including six gas-filled counters (G-M tubes); measuring time for an ore batch is 30-45 sec.

The ore with average uranium content is then subjected to treatment in a heavy slurry, yielding 20 tons of concentrate (0.6-0.8% uranium) and low grade (0.06-0.08% uranium). The low grade is routed to the local hydrometallurgical processing plant for subsequent chemical processing. The weighting compound (specific weight : 2.65) used for the slurry is a mixture of ferrosilicon and magnetite (3 : 1) with soda added to inhibit oxidation of the ferrosilicon.

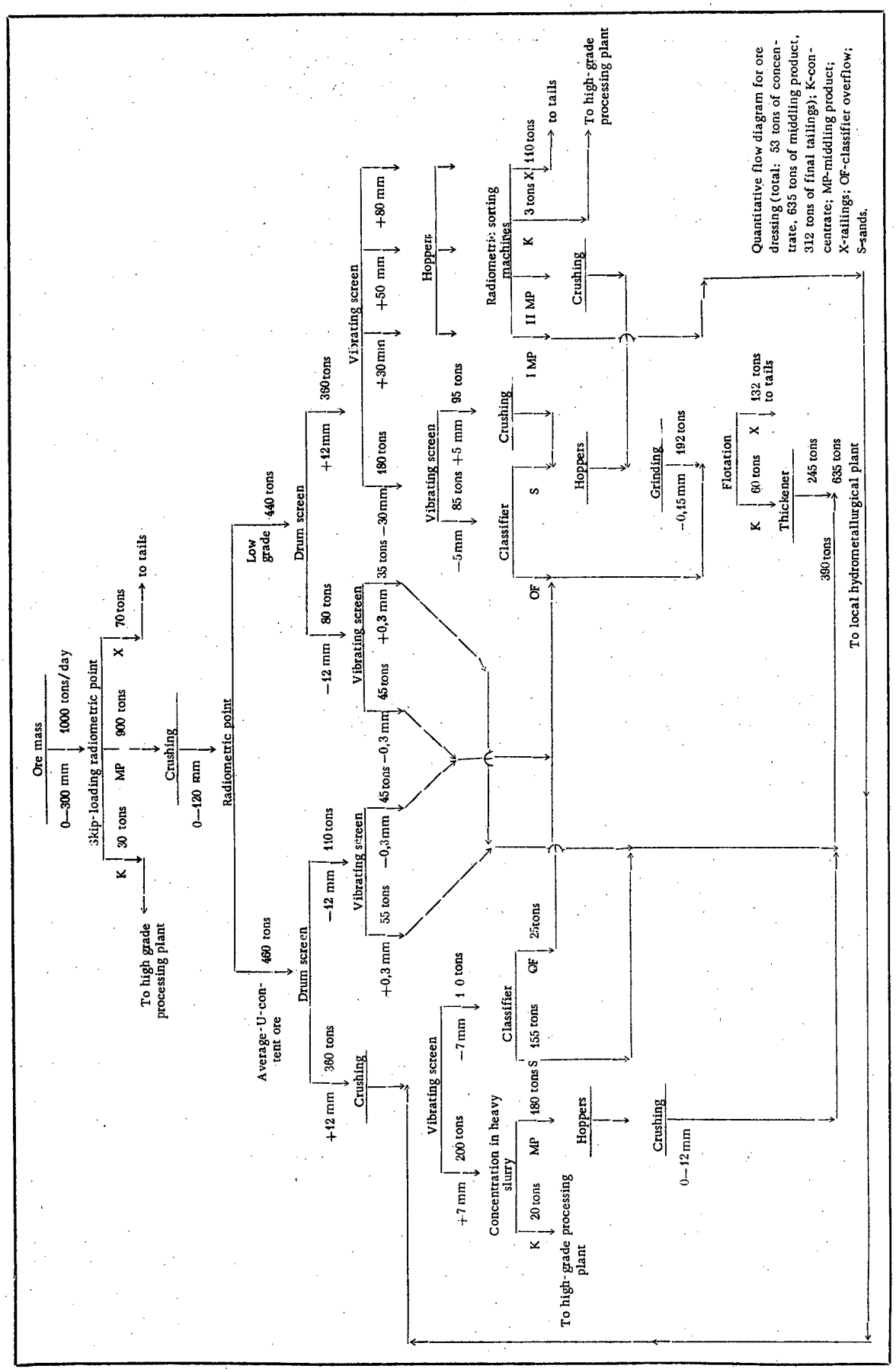

Quantitative flow diagram for ore dressing (total: 53 tons of concentrate, 635 tons of middling product, 312 tons of final tailings); K-concentrate; MP-middling product; X-tailings; OF-classifier overflow; S-sands.

Results of Concentrating Process

Product	Yield, %	Uranium content, %	Uranium recovery, %
Concentrate sorted at radiometric point	3	1.2	23.1
Machine-sorted concentrate	0.3	1.5	2.9
Slurry concentrate	2	0.7	9.0
Concentrate totals	5.3	1.03	35.0
Final middlings	63.5	~ 0.15	61.0
Tailings from radiometric point	7.0	No information available	No information available
Machine-sorted tailings	11.0		
Flotation tailings	13.2		
Total tailings	31.2	~ 0.02	4.0
Raw ore	100	0.156	100

The low-grade ore, after being screened and washed, is run through an additional radiometric beneficiation step on conveyor-belt sizing machines to yield four lots of product: concentrate (3 tons), two middling products (20 tons and 47 tons) and final tailings (110 tons). Machine sizing is used for ore of size −120 + 30 mm, which is screened down to three classes prior to sorting: −120 + 80 mm, −80 + 50 mm, and −50 + 30 mm; these three classes are processed separately. Eight sizing machines are used, with conveyer belt speeds of 1.0 m/sec for the first ore class, 0.8 m/sec for the second class, and 0.5 m/sec for the third. The average throughout of one machine is about 22.5 tons of raw ore daily. Three scintillation counters with thallium-activated sodium iodide crystals are mounted on each machine; the counters are coupled to pneumatic devices which perform the sorting function.

The first middling product, 0.2%– 0.3% uranium content, is directed, together with the average-uranium-content ore sorted out at the radiometric monitoring station, to the heavy slurry concentration point, while the second middling product is directed, together with washed fines, to finish grinding (to −0.15 mm mesh) and then to a flotation step.

An alcoholic emulsion of oleic acid and potassium xanthogenate with liquid glass added as depressant is used in the flotation step. The flotation step also includes cleaning up the tailings.

The over-all results of the concentrating process are tabulated above.

All the concentrates are unloaded for separate processing at the Guignon mill for reprocessing high-grade ore, while the middling products are processed at a local plant in an acid leach scheme with precipitation of the low-grade calcium concentrate, and cleanup by extraction.

Ore concentration by the steps described makes it possible to process 20-25% of the end tailings with small losses. By decreasing the amount of feed to the more expensive hydrometallurgical processing steps, great economies are achieved.

In addition, separate processing of the high-grade and low-grade products assures higher total yield with lower reagent costs, power costs, etc., than direct hydrometallurgical processing of unsized crude ore by one step.

Finally, application of the concentration to a certain degree neutralizes the contents of uranium and chemical composition of the products, which enter into hydrometallurgical processing. This concentration ensures higher economy in hydrometallurgical conversion.

LITERATURE CITED

1. M. Vuchot, Rev. ind. minerale 41, 10, 766 (1959).
2. M. Benlaygne, Rev. ind. minerale 41, 10, 801 (1959).

A FACILITY FOR IRRADIATING PERSONAL FILM HOLDERS

B. M. Dolishnyuk

Translated from Atomnaya Énergiya, Vol. 9, No. 8, pp. 156-157, August, 1960

Photographic-film methods for radiation detection have enjoyed wide popularity in dosimetry, especially in personal film-badge dosimetry applications.

In order to photometrically scan the irradiated films, it is required to plot the calibration curve of film density vs γ-radiation dose absorbed by the photosensitive film layer in developing each of the films [1]. For this purpose, films covered with different screens (to differentiate the spectral response) are γ-irradiated by photons originating in a standard source [2]. An automated facility which has been functioning reliably over a long service period was devised for standard irradiation exposures of the film-packet holders, and is described below.

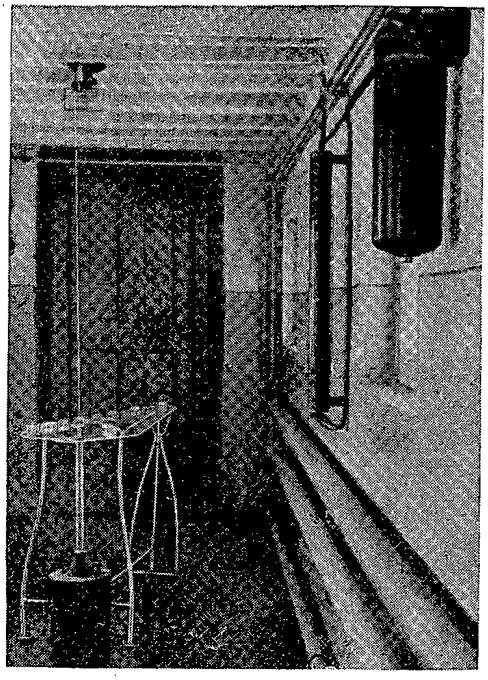

Fig. 1. General view of the irradiation room and exposure table.

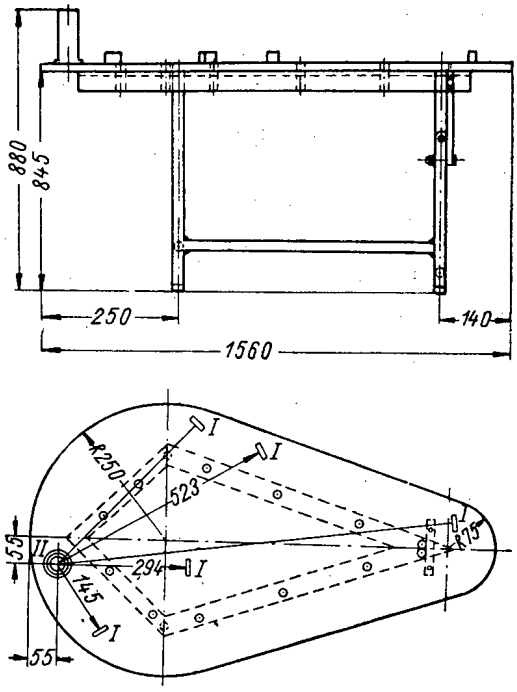

Fig. 2. Diagram of the table built to facilitate stand exposures of film holders (side view and top view).

The exposure table accomodating the film holders is made of 4 mm thick plexiglas and is supported by steel rods 6 mm thick (Fig. 1). The film-pack holders I (Fig. 2), equipped with spring clamps and location pins, are fastened to the plexiglas. A container beneath the table houses the standard source II, held in place by a caprone filament. The caprone filament passes through an array of pulleys and is coupled to the core of a selenoid

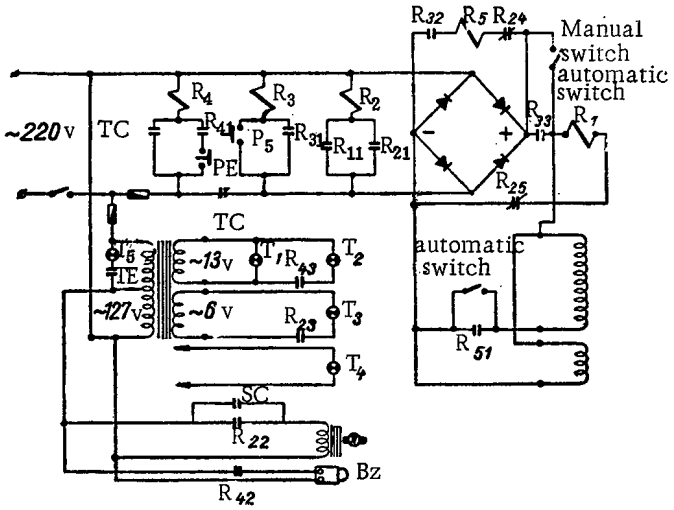

Fig. 3. Circuit diagram of electrical equipment serving the irradiation table. R = relay; PS = pushbutton switch; TC = = timer contacts; T = tube; PE = pushbutton for ending exposure; SC = switch contacts; Bz = buzzer; TE = terminal contacts.

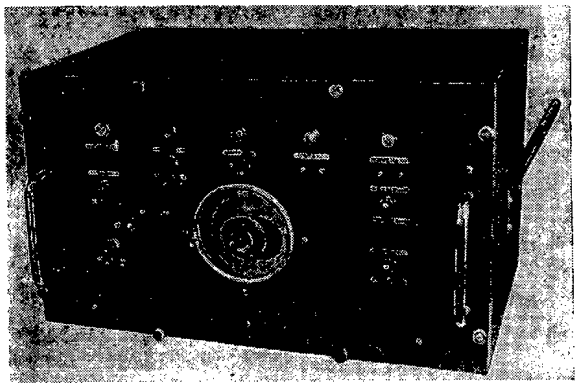

Fig. 4. Exposure table control panel.

attached to the wall of the room (cf. Fig. 1) The selenoid consists of a sectioned coil 820 mm in length with the number of layers of PEL-0.5 wire changing from section to section (viz. 20, 24, 28, 32), and a restraining coil with iron core, which acts as an extension of the solenoid. The solenoid is energized via a special circuit (Fig. 3) incorporating a time delay relay and signal tubes.

The circuit operates as follows: pushbutton PS is pushed to operate relay R_3, which resets automatically (contacts R_{31}) and closes, by means of relays R_5 (R_{51}) and R_1 (R_{33}), the circuits of the plunger solenoid and restraining coil (contacts R_{32} and R_{33}). Relay R_1, acting with a delay of 1.5 sec, closes the circuit of relay R_2 (R_{11}). Relay R_2 resets automatically (R_{21}) and closes the circuit of the timer (R_{22}), the monitoring signal tube T_3 (R_{23}), and opens relays R_5 (R_{24}) and R_1 (R_{25}). To prevent overheating, relay R_5 opens the circuit of the solenoid plunger (R_{51}). The core with the standard is held back during the exposure by the solenoid of the restraining coil. After the exposure time set on the timer has elapsed, the timer contacts (TC) open the circuits of R_2 and R_3 (the standard is dropped into the container), and shortly thereafter close circuit R_4. Relay R_4 resets automatically (R_{41}) and closes the circuit of the buzzer Bz (R_{42}) and tube T_2 (R_{43}) which signal the termination of the exposure. The signal announcing the end of the exposure is shut off by pushbutton PE.

Contacts SC of the terminal switch of the timer disk are closed mechanically one minute after the timer is actuated, so that the timer continues to operate until reset. When the timer circuit is reset, contacts SC are opened and terminal contacts TE, which turn on the T_5 "Ready" tube, are closed mechanically.

The control panel (Fig. 4) and the entire electrical circuitry are housed in the laboratory. The table with containers and solenoid are placed in a room removed from the laboratory (to avoid exposure of personnel and film badges stored in the laboratory). A dosimetric annunciator placed in the same room is on whenever the source is outside the container. Audible and visible dosimetric annunciators are located in the room and in the approaching hallways. A "Danger" signal tube T_4 (cf. Fig. 3) is also connected to the control panel.

The effect of radiation scattered from the container on film darkening has been verified experimentally. Changes in the readings of exposed film with container removed and in place were not noted. The principal advantages in the set-up described here are:

1) personnel exposure is completely eliminated;

2) the laboratory technician is free to attend to any other work while the film-badge holders are being exposed;

3) exposure error is eliminated;

4) highly skilled technicians are not required to operate the arrangement.

LITERATURE CITED

1. K. K. Aglintsev, Dosimetry of Ionizing Radiations [in Russian] (Gostekhizdat, Moscow, 1950).
2. K. K. Aglintsev, Fundamentals of the Dosimetry of Ionizing Radiations [in Russian] (Medgiz, Leningrad, 1955).

BRIEF COMMUNICATIONS

USSR. A seminar on instrumentation for geophysical bore-hole research using radioactive techniques took place May 24-28, 1960, at L'vov. Twenty five papers and reports were heard at the seminar.

In reports presented by the Ukrainian Geophysical Exploration group (Ukrgeofizrazvedka) of Kiev, the All-Union Scientific Research Institute of Exploration Geophysics (Leningrad), the Nuclear Physics Institute of the Academy of Sciences of the Uzbek SSR (Tashkent), and the Moscow branch of the Power Engineering Institute (Orgénergostroi), data were presented on the effectiveness of using radioactive logging techniques for geophysical research, prospecting for minerals, and quality control of structural work in power projects.

Problems related to improving the efficiency, accuracy, and reliability of the functioning of radioactive logging equipment were elucidated in papers presented by the Institute of Machinery and Automation of the Academy of Sciences of the Ukrainian SSR (L'vov), the I. M. Gubkin Institute of the Petrochemical and Gas Industry (Moscow), the All-Union Mineral Raw Materials Institute (Moscow), and the Nuclear Physics Institute of the Academy of Sciences of the Kazakh SSR (Alma-Ata).

Representatives of the I. M. Gubkin Institute of the Petrochemical and Gas Industry (Moscow), the All-Union Scientific Research Institute for Geophysics (Moscow), the Volga-Caspian branch of the All-Union Scientific Research Institute for Geophysics, the Institute of Machinery and Automation of the Academy of Sciences of the Ukrainian SSR (L'vov), and the Geophysics Institute of the Ural branch of the USSR Academy of Sciences (Sverdlovsk) presented reports on the results of new designs of bore-hole and surface-level radiometric equipment for radioactive logging operations.

95 representatives of 35 research and industrial organizations took part in the deliberations of the seminar. The proceedings of this seminar will be published in symposium form.

USSR. The foundations were laid on May 26, 1960, at Salaspils, for Latvia's first research reactor.

Present at the ceremonies were the first secretary of the Central Committee of the Latvian Communist Party, A. J. Pelgis, and the Vice Chairman of the Council of Ministers of the Republic M. J. Pludon, who, in observance of tradition, lowered a steel cartridge containing a memorial inscription and newspapers of May 26 into the foundation site.

The Salaspils nuclear reactor will be used for research work in nuclear isotopes and isotope production.

Germany. Talks between East Germany and Poland on a further expansion of collaboration in the cause of the peaceful uses of atomic energy took place at Berlin. A plan of joint work was signed as a result of the talks.

Poland. A treaty was signed with Hungary dealing with collaborative efforts in the field of the peaceful uses of atomic energy. The treaty calls for joint work on nuclear physics, reactor engineering, uses of radioactive isotopes, design of power installations, and research on radiation effects.

BIBLIOGRAPHY

NEW LITERATURE

REVIEW OF BOOKS AND SYMPOSIA

P. É. Nemirovskii, Contemporary Models of the Atomic Nucleus. Moscow, Atomizdat, 1960. 208 pages. 11 rubles, 15 kopeks.

This book takes up three currently accepted models of the atomic nucleus; the basic concepts of the shell model, collective model, and cloudy crystal ball are presented. The problem of the size and shape of the nucleus is reviewed in the light of data from the most recent theoretical and experimental investigations. A detailed account is given of problems concerning interaction cross-sections for nucleons and nuclei, polarization in scattering of nucleons on nuclei, radiative transitions in nuclei; the stripping reaction, etc.

The book is written for theoretical physicists, as well as graduate students in physics and engineering physics departments.

L. Eisenbud and E. Wigner, Structure of the Nucleus. (Translated from the English.) Moscow, 1959. 178 pages 8 rubles, 35 kopeks.

The Foreign Literature Press (IL) has put out a translation of an interesting and useful book by two prominent American theoretical physicists, L. Eisenbud and E. Wigner.

Despite its modest bulk, the book contains a wealth of material and will meet with an interested reading public of Soviet physicists.

The principal chapter of the book consists of an analysis of the fundamental tenets of the theory of nuclear structure, bringing the most important experimental facts to bear on the topic.

The first three chapters make information available on the fundamental characteristics of nuclei, systematics of nuclei, and the properties of nuclear states.

The fourth chapter offers a survey of nuclear reactions, which are gone into further detail in the ninth and tenth chapters. The fifth chapter deals with two-body systems, predominantly two-nucleon systems.

The following three chapters are devoted to the various models of the nucleus. These chapters came out very successfully. An exemplary analysis of the agreement between the models of the nucleus and empirical data is found in these chapters.

At the end of the book, the reader finds descriptions of beta and gamma emission, which are nevertheless approached solely from the vantage point of the structure of the nucleus. Fairly recent successes achieved in constructing a theory of beta decay related to the discovery of parity nonconservation in weak interactions are not reflected in the book.

The book is written for an audience acquainted with the fundamentals of mechanics and nuclear physics.

I. V. Gordeev, A. A. Malyshev, and D. A. Kardashev, Handbook on Nuclear Physical Constants to Expedite Nuclear Reactor Calculations. Moscow, Atomizdat, 1960. 272 pages. 15 rubles.

The handbook is arranged in four parts. The first and second parts provide information on cross-sections for neutrons in the region of thermal energies and information on resonance level parameters; in the third part

we find empirical data on inelastic scattering cross-sections and transport cross-sections. The fourth part contains data on prompt and delayed fission neutrons, radiative capture cross-sections and fission cross-sections, resonance integrals, fission gammas, and capture gammas.

The appendix informs on methods for the practical utilization of the material included in the handbook.

The handbook was compiled for engineers and physicists working in the field of reactor design and reactor operation.

L. N. Posik, I. V. Koshelev, and V. P. Bovin, Radiometric Express Analysis of Produced Ore. Moscow, Atomizdat, 1960. 80 pages. 3 rubles, 10 kopeks.

The book is devoted to methods and equipment enabling express analysis of ore in stock found in various volumes. Factual material and data accumulated at mining enterprises from 1946 to 1958 were used in the compilation of the book.

The physical fundamentals of the method and sources of error in the measurements are reviewed in brief, and pathways for enhancing the accuracy of radiometric analyses are pointed out. Flowsheets of the technological complexes of typical mining pits using radiometric monitoring facilities are included. The specific features of express analysis of mined ore are described for a broad range of metal concentrations found in various volumes.

The book is written for technicians in the uranium industry.

Methods for Obtaining and Measuring Radioactive Preparations. Symposium consisting of articles, edited by V. V. Bochkarev. Moscow, Atomizdat, 1960. 308 pages. 11 rubles, 70 kopeks.

This symposium is arranged in three sections. The first section, comprising 16 articles, is devoted to problems encountered in the manufacture of radioactive isotopes and inorganic radioactive preparations, some colloidal preparations and other preparations for medicinal purposes, as well as the technology involved in the production of some preparations made with short-lived isotopes.

The second section, embracing 15 articles, describes the methods used to produce several labeled organic compounds, both the pathway of classical synthesis via key compounds, and with the aid of isotope exchange, neutron bombardment of prepared nonradioactive compounds, biosynthesis, etc.

The third section, consisting of 8 articles, deals with absolute and relative measurements of activity, and with radiometric analysis of preparations; some new instruments and devices are described, and practical hints on methods and techniques of measurement are given.

The book is written for a broad readership of persons engaged in the handling of radioactive isotopes.

Yu. I. Ostroushko, et al., Lithium Chemistry and Technology. Moscow, Atomizdat, 1960. 199 pages. 7 rubles, 30 kopeks.

The first chapter of this book is devoted to the geochemistry and mineralogy of lithium; the second and third chapters deal with the chemistry of lithium and its compounds, and the analytical chemistry of lithium; in the fourth and fifth chapters, we find methods for concentrating and processing lithium-bearing ores; the sixth chapter, the last, outlines the problems encountered in lithium metallurgy. A list of literature consulted appears at the end of each chapter, encompassing the period from 1818 to 1958 in its full complexity.

The book is written for scientific research workers, metallurgical engineers and chemists working in the field of the chemistry and technology of exotic and dispersed elements, for engineers and technicians engaged in lithium production, and for students in engineering and technical schools.

G. Seaborg and J. Katz, Chemistry of the Actinide Elements, translated from English and edited by G. N. Yakovlev. Moscow, Atomizdat, 1960. 542 pages. 27 rubles, 80 kopeks.

This book is written by two famous American scientists, Glenn Seaborg and J. Katz. Other American scientists in addition to the authors participated in the preparation of individual sections of the work.

Fourteen actinide elements are known at present. The elements found in nature are actinium, thorium, protactinium, and uranium, which were discovered some time ago. The heavier (transuranium) elements have been obtained by synthetic means. Their discoveries are intimately linked with the achievements in nuclear physics registered during the past two decades, and are of great importance for present-day inorganic chemistry. The study of the chemistry of the actinide elements, in particular thorium, uranium and plutonium, plays a prominent role in the development of atomic industry.

The actinides symposium ("Aktinidy") published in Russian in 1955 is quite outdated by this time. The publication of Chemistry of the Actinide Elements is therefore very timely. The American edition of the book includes material published up to the end of 1956. Footnotes to the present edition of the book provide more recent data on actinide element studies to date, primarily in the USSR, USA, and Great Britain, plus the work presented at the Second Geneva Conference on the peaceful uses of atomic energy.

The book contains a wealth of highly compressed material. Each element, including the transcurium elements, has a separate chapter reserved for it. The order of exposition of the material is uniform for all the chapters: nuclear properties of isotopes, methods of production and isolation, production of elements in the metal state, properties of metals and compounds, behavior of ions in solution.

Chapters II-X are devoted to a description of the chemistry of actinium, uranium, neptunium, plutonium, americium, curium, and the transcurium elements. The geochemistry of thorium and uranium and the technology of thorium and uranium ore processing are described in detail, as are the processes employed in atomic industry to produce synthetic actinides.

Chapter XI is of unusual interest. Here, the authors perform a comparison of the chemical properties of the actinide elements, the crystal structure of the metals and compounds, absorption spectra and fluorescent emission spectra. On the basis of a detailed study of magnetic susceptibility, paramagnetic resonance and spectral data, the up-to-date view of the electronic structure of various oxidation states of the actinides and their positions within the framework of the periodic system are examined. This chapter also surveys the possible pathways leading to the isolation and identification of new elements, including a transactinide series.

The book may prove useful as a textbook manual or reference in the study of the chemistry of actinides. The bulk of the empirical data and the extensive bibliography indicate clearly that the present edition will constitute a valuable reference text for a wide audience of specialists.

International Directory of Radioisotopes. Vol. II. Compounds of Carbon-14, Hydrogen-3, Iodine-131, Phosphorus-32, and Sulfur-35. International Atomic Energy Agency, Vienna 1959. 213 pages [in English].

This second volume of the reference series provides information on chemical compounds containing C^{14}, H^3, and I^{131}, P^{32}, S^{35}. Standard isotope sources are listed. The compounds of each isotope are arranged in alphabetical order according to the most commonly employed terminology. An alphabetical index at the end of the book cross-references synonyms to facilitate the task of the user. Prices of the isotopes and sources used to produce them are listed.

ARTICLES FROM THE PERIODICAL LITERATURE

I. Nuclear Power Physics

Neutron and reactor physics. Physics of hot plasmas and controlled nuclear fusion. Physics of charged-particle acceleration.

Zh. Tekhn. Fiz. 30, 4 (1960).

L. N. Dobretsov, pp. 365-394. Direct-conversion thermionic devices.

Yu. Ya. Lembra, pp. 405-412. On estimating the amplitude variation of vertical betatron oscillations in accelerators when the beam is extracted by a regenerative deflector.

* The list of foreign periodicals scanned in the "Bibliography" section is published in the January 1960 issue of the Journal For information on the contents of Soviet periodicals, the reader may refer to the Letopis'zhurnal'nykh statei (Annals of Soviet Periodicals) published by the All-Union Book House.

V. M. Zakharov, et al., pp. 442-449. On medium-pressure probe measurements. Zhur. Tekhn. Fiz. 30, No. 5 (1960).

Ts. I. Gutsunaev and Ya. P. Terletskii, pp. 491-496. Contribution to the theory of electron motion in a linear betratron.

T. F. Volkov, pp. 497-503. On the stability of a plasma column in a high-frequency magnetic field.

É. D. Andryukhina, et al., pp. 529-538. Some features of induction gas discharges.

Yu. F. Bydin and A. M. Bukhteev, pp. 546-554. Ionization of fast Na, K, Rb, and Cs atoms in collisions with H_2, D_2, N_2, and O_2 molecules.

E. M. Kuchkov, pp. 570-572. The shape of lines in the mass spectrum and the role of a pulsed ion source in a radio-frequency mass spectrometer.

A. A. Kuznetsov, pp. 592-597. Mechanical stresses in a multilayer coil for a uniform current loading and rectangular cross section of coil wire, where stresses are due to a radially imposed electromagnetic force.

Zhur. Éksp. i Teoret. Fiz. 38, No. 4 (1960).

A. M. Fogel', et al., pp. 1053-1060. Ionization of gases by negative ions.

M. S. Rabinovich and L. V. Iogansen, pp. 1183-1187. Coherent radiation of electrons in a synchrotron. III.

G. G. Getmant and V. O. Rapoport, pp. 1205-1211. On the build-up of electromagnetic waves in a plasma moving through a dispersionless dielectric in the presence of a constant magnetic field bias.

Yu. L. Klimontovich, pp. 1212-1221. Relativistic kinetic equation for a plasma. II.

V. G. Skobov, pp. 1304-1310. Contribution to the theory of the conduction of an electron gas in an intense magnetic gas.

Nauka i Zhizn', No. 5 (1960).

M. I. Solov'ev, pp. 8-10. A new particle in the microcosmos.

M. S. Rabinovich, pp. 17-23. Accelerator engineering today and tomorrow.

Priroda, 4 (1960).

V. I. Gol'danskii, pp. 49-55. Discovery of the antiproton.

Trudy Fiz. Inst. Akad. Nauk SSSR 13 (1960).

A. A. Kolomenskii, pp. 3-109. Research on the Theory of the Particle Motion in Modern Cyclic Accelerators.

E. M. Moroz, pp. 130-173. Theoretical Research on Methods for Upgrading the Efficiency of Cyclic Accelerators.

Atomkernenergie 5, No. 4 (1960).

J. Trumper, pp. 121-128. Electronically ignited parallel-electrode spark counter aids in determining particles paths.

W. Kliefoth, pp. 148-151. Starting the CERN proton synchrotron.

Canad. J. Phys. 38, 4 (1960).

G. Michaud and R. Boucher, pp. 555-564. Pu-Be neutron sources.

K. Geiger, pp. 569-572. Canadian neutron standards.

Contemporary Physics 1, No. 3 (1960).

D. Chick, pp. 169-190. Plasma research.

N. Feather, pp. 191-203. The study of neutrons and nuclei, Part I.

Industries Atomiques 4, No. 3-4 (1960).

R. Gabillard, pp. 49-61. Some interesting aspects of the operating and design principles of the 29 Mev proton synchrotron.

R. Levy-Mandel, pp. 69-81. The SATURN proton synchrotron at Saclay.

J. Appl. Phys. 31 No. 3 (1960).

O. Yonts, et al., p. 447-450. High-energy sputtering of fast ions on metal surfaces.

D. Thompson and V. Paré, pp. 528-535. Effect of fast neutron bombardment at various temperatures upon the Young's modulus and internal friction of copper.

C. Fowler, et al., pp. 588-594. Production of very high magnetic fields by implosion.

Nuclear Power 5, No. 48 (1960).

-- pp. 124-126. The trend of development of nuclear and reactor physics instrumentation in France.

--- pp. 136-137. Electrostatic generators and accelerators at Grenoble.

II. Nuclear Power Engineering

Nuclear reactor theory and calculations. Reactor design. Operation of nuclear reactors and nuclear electric power generating stations.

Izvest. Akad. Nauk KazakhSSR, Ser. Énerg. No. 2 (1959)

N. U. Isaev and A. T. Luk'yanov, pp. 122-129. A criticality simulation experiment using static electronic integrators.

Atomkernenergie 5, No. 5 (1960)

J. Clauss, pp. 128-134. Contribution to the calculation of the hot channel factor for a nuclear reactor. Part II.

W. Strewe, pp. 134-141. Numerical method for thermal design of channels for an arbitrary distribution of heat sources throughout a fuel element.

W. Kliefoth, pp. 151-153. Is the development of atomic power showing a tendency to level off?

Industries Atomiques 4, No. 3 4 (1960)

J. Juillard, pp. 105 109. The nuclear powered ship "Savannah."

Jaderná Energie 5, No. 5 (1960)

J. Dvořák, pp. 146-149. Some problems of high-pressure vessel strength for nuclear reactor pressure vessels.

J. Jůza, pp. 150-154. The thermal cycle of nuclear electric power stations based on gas-cooled reactors. Part 2.

A. Dvořák, pp. 155-162. Corrosion problems affecting structural materials in contact with liquid metals.

M. Brit. Nuclear Energy Conf. 5, No. 1 (1960)

W. Lewis, pp. 30-36. Some data on operating experience of heavy water power reactors.

J. Brit. Nuclear Energy Conf. 5, No. 2 (1960)

A. Bowden and J. Drum. pp. 49-63. Design and testing of big-inch gas piping.

N. Wilkins and J. Wanklyn, pp. 89-96. Corrosion of aluminium and its alloys when exposed to superheated steam.

Nuclear Energy 14, No. 144 (1960)

--- pp. 205-209. The American program for developing nuclear reactors to serve medical needs.

--- p. 224. A facility for testing airborne nuclear propulsion engines.

Nuclear Power 5, No. 47 (1960)

P. Lindley and K. Mitchell, pp. 104-107. Japan's first nuclear power station.

R. Hicks, pp. 108-110. Japan's first nuclear power station. II. Earthquake-proofing problems.

R. Bird, pp. 110-113. Japan's first nuclear power station. III. Optimization of parameters.

B. Stonehouse and T. O'Neill, pp. 113-116. Japan's first nuclear power station. IV. Reactor control and health physics.

Y. Otsuki and S. Wearne, pp. 117-118. Japan's first nuclear power station. V. Construction work and organizational structure.

F. Hammit, pp. 125-126. A fast breeder burning gaseous fuel.

G. Bracewell, p. 126-129. Transient behavior of an organic-moderated shipborne nuclear reactor.

--- pp. 130-132. Completion of construction work on the DR-3 heavy water reactor.

Nuclear Power 5, No. 48 (1960)

--- p. 112. Nuclear power development program in France.

J. Andriot, p. 113. French nuclear power economics.

J. Weinstein, pp. 114-115. French legislation in the realm of nuclear power.

A. Mouturat, pp. 115-116. Organization of French atomic industry.

J. Burkett, pp. 116-117. The activities of the Commissariat de l'Energie Atomique.

M. Bienvenu, et al., pp. 118-123. France's second nuclear power station.

G . Derom and A. Ertaud, pp. 127-129. Fuel transfer in plutonium burners.

--- p. 140. The ten-year program of nuclear power development in the USA.

Nuclear Power 5, No. 49 (1960)

A. Fonda, pp. 93-96. Instability problems in gas-cooled reactors.

J. Burkett, pp. 97-100. Low-power reactor survey.

B. Ediss, pp. 101-104. Heat exchanger design for gas-cooled reactors.

--- pp. 105-108. Fuel transfer at the Berkeley power station.

Nuclear Sci. and Eng. 7, No. 3 (1960)

M. Nelkin, pp. 210 216. Intensity decay of a thermalized neutron pulse.

M. Fleishman and H. Soodak, pp. 217-227. Methods and cross-sections data for computing fast effect.

H. Überall, pp. 228-234. Neutron absorption by control rods of varying transparency.

J. Melcher, pp. 235-239. A useful analogy for single-group neutron diffusion theory.

D. Bell, pp. 245-251. Correlation of burnout heat-flux data at 140.6 atmos (4000 psia).

A. Vernon, pp. 252-259. Calculation of the effective resonance integral for U^{238}.

L. Dresner, pp. 260-262. Comparison theorems for determining mean collision probabilities.

J. Hardy, et al., pp. 263-267. Experimental check of a Monte Carlo-calculated distribution of resonance neutron capture in a gold rod.

J. Lewins, pp. 268-274. Time-dependent importance of neutrons and precursors.

J. Thie, pp. 275-276. A method for interpolation in moderator to fuel ratio-dependent bucklings.

S. Kaplan and S. Margolis, pp. 276-277. Delayed neutron effects during flux tilt transients.

L. Seren and D. Tsakarissianos, pp. 277-280. Analysis of neutron flux data needed to accurately determine relaxation length.

Nucleonics 18, No. 4 (1960)

--- pp. 71-82. AEC long-range power reactor program.

Nucleonics 18, No. 5 (1960)

--- pp. 108-109. Outlook for nuclear power development.

Nukleonik 2, No. 2 (1960)

H. Teutsch, et al., pp. 41-43. Thermal-neutron spectrum of the WWR-S reactor at Budapest.

H. Smets, pp. 44-45. The general property of criticality in stable and unstable operation of nuclear reactors.

L. Dresner, pp. 45-47. The effect of the geometric symmetry of a heterogeneous reactor on thermal neutron flux distribution.

F. Cap and H. Reimann, pp. 47-54. Closed solution of a stationary multigroup diffusion equation for a reflected reactor, and replacement of a cylindrical reactor by a spherical geometry.

A. Müller, pp. 54-67. Contribution to the theory of resonance neutron absorption in heterogeneous reactors. I.

A. Müller, pp. 67-73. Contribution to the theory of resonance neutron absorption in heterogeneous reactors. II.

W. Hage, pp. 73-79. Spatial integration of neutron fields by means of movable neutron detectors.

III. Nuclear Fuels and Materials

Nuclear geology and primary ore technology. Nuclear metallurgy and secondary technology. Chemistry of nuclear materials.

Azerbaidzh. Khim. Zh. No. 6 (1959).

G. Kh. Efendiev, and A. N. Nuriev, pp. 105-108. Distribution of radium and uranium between phases (oil-water phases).

Vestnik Moskv. Univ., Ser. Mat.,Mekh.,Astron.,Fiz.,Khim. No. 4 (1959)

T. A. Belyavskaya and Mu Ping-wen, pp. 207-214. Contribution to the problem of the state of zirconium in mineral acid solutions.

Geol. Budn. Mestorozhdenii, No. 1 (1960)

V. I. Rekharskii, pp. 92-97. On the behavior of pitchblende affected by fluorine-containing hydrothermal solutions.

R. P. Rafal'skii and Yu. M. Kandykin, pp. 98-106. Some empirical data on crystallization of uranium dioxide under hydrothermal conditions.

Zhur. Anal. Khim. 15, No. 1 (1960) *

V. P. Shvedov, et al., pp. 16-19. Separation of several isotopes by the focusing ion exchange method.

E. A. Vernyi and V. N. Egorov, pp. 24-26. Spectroscopic determination of aluminum in uranium.

V. G. Sochevanov, et al., pp. 77-83. Effect of some ions on precipitation of uranyl ferrocyanide in aqueous solution.

V. F. Eskevich and L. A. Komarova, pp. 84-87. Uranium assay by amperometric titration.

D. I. Ryabchikov, et al., p. 88-95. Separation of uranium from metal impurities in association with it, by ion exchange chromatography.

Zhur. Neorg. Khim. 5, No. 4 (1960)

R. G. Denotkina, et al., pp. 805-810. Solubility product of the disubstituted phosphate of plutonium (IV) and its solubility in various acids.

*Original Russian pagination. See C. B. translation.

A. I. Stabrovskii, pp. 811-820. Polarization of uranium compounds in carbonate and bicarbonate solutions.

V. M. Vdovenko, et al., pp. 935-940. On HCl extraction of uranium with tri-n-butyl phosphate.

Zavodskaya Lab. 26, No. 3 (1960)

V. I. Kuznetsov and I. V. Nikol'skaya, pp. 266-269. Photometric determination of uranium with the arsenazo reagent.

Zavodskaya Lab. 26, No. 4 (1960)

M. S. Petrova, pp. 502-504. Glove box for handling radioactive substances in small hot laboratories.

Izvest. Akad. Nauk KirgizSSR, Ser. Estestv. i Tekh. Nauk 2, No. 5 (1960)

N. T. Voskresenskaya, pp. 49-64. 1. Solvent extraction of uranium from coal with various solvents. 2. Study of reaction of humic acids with uranyl salts.

Radiokhimiya 2, No. 2 (1960)

V. I. Grebenshchikova and R. V. Bryzgalova, pp. 152-158. Study of coprecipitation of Am and Eu with lanthanum oxalates.

V. I. Grebenshchikova and R. V. Bryzgalova, pp. 159-163. Study of coprecipitation of $V^{(III)}$ with lanthanum oxalates.

D. N. Bykhovskii and A. A. Grinberg, pp. 164-174. Coprecipitation of trivalent cerium with uranium oxalates.

O. Ya. Samoilov and V. I. Tikhomirov, pp. 183-191. Salting-out and exchange of water molecules which are nearest neighbors to ions in aqueous solutions.

M. G. Panova, et al., pp. 197-207. A study of yttrium chelation. I. Oxinates (8-hydroxyquinolates) of yttrium.

M. G. Panova, et al., pp. 208-214. A study of yttrium chelation. II. Sulfate, nitrate, and chloride complexes of yttrium.

M. F. Pushlenkov, et al., pp. 215-221. A study of complex formation of uranyl nitrate with organophosphorus compounds.

I. A. Tserkovnitskaya and A. K. Charykov, pp. 222-230. Tracer study of the possibility of extractive separation of thorium from certain elements. I. Extraction of thorium phenylacetate by diethyl ether.

V. P. Shvedov and Fu Yi-pei, pp. 234-238. Isolation of radioactive isotopes on a mercury cathode. III. Study of deposition of cerium.

B. K. Preobrazhenskii, et al., pp. 239-242. Contribution to the problem of the effect of the size of chelating molecules and temperature on the ion exchange separation of radioactive rare earths.

V. M. Permyakov, pp. 255-258. Comparative evaluation of methods of preparing radium-beryllium sources.

V. P. Shvedov and A. V. Stepanov, pp. 261-262. More accurate values of instability coefficients of complex compounds of some lanthanides with the EDTA anion.

Uspekhi Khim. 29, No. 4 (1960)

A. K. Pikaev, pp. 508-524. Radiation chemistry of aqueous solutions of inorganic compounds of nitrogen.

V. I. Kuznetsov, pp. 525-567. Progress in analytical chemistry of uranium, thorium and plutonium.

Uspekhi Khim. 29, No. 5 (1960)

F. Weigel, pp. 686-707. The chemistry of polonium.

Chem. and Process Eng. 41, No. 4 (1960)

F. Paulsen, pp. 153-157. Fuel element research in France.

Industries Atomiques 4, Nos. 1-2 (1960)

L. Pichat, pp. 47-56. Isotope-tagged organic molecules.

Industries Atomiques 4, Nos. 3-4 (1960)

S. Choumoff, pp. 95-103. Nondestructive testing of uranium fuel elements for gas-tightness, by the helium-leak detection technique.

J. Brit. Nucl. Energy Conf. 5, No. 1 (1960)

S. Gregg and W. Jepson, pp. 1-19, Oxidation of magnesium in dry and moist oxygen at high temperatures.

J. Murray, pp. 20-23. The thorium-aluminium system.

D. Dawe, et al., pp. 24-29, Study of the compatibility of certain creep-resistant steels with liquid bismuth in nonisothermal systems.

H. Finniston, pp. 37-48, Some metallurgical problems affecting nuclear reactors.

J. Brit. Nuclear Energy Conf. No. 2 (1960)

E. Perryman, pp. 97-109. Aluminium alloys for water-cooled power reactors.

L. Graham and G. Wilson, pp. 128-132. Study of rate of dissolution of iron of certain ferritic steels in liquid bismuth.

J. Inorg. and Nuclear Chem. 12, Nos. 3/4 (1960)

K. Wolfsberg, et al., pp. 201-205. Identification of Xe^{142} and measurement of cumulative yield of Xe^{142} upon fission of U^{235} by thermal neutrons.

J. Sattizahn, et al., pp. 206-222. Short-lived bromine and selenium nuclides in fission products.

J. Marinsky and E. Eichler, pp. 223-227. A new fission product: Ga^{74}.

L. Bunney, et al., 228-233. Half-lives of Pm^{149} and Pm^{151}.

F. Brauer, et al., p. 234-235. New neutron-deficient terbium activities.

K. Toth and J. Rasmussen, pp. 236-240. New neutron-deficient terbium activities.

P. Gray, pp. 304-314. Separation of cesium-137 from fission product waste solutions.

R. Zingaro and J. White, pp. 315-326. Solvent extraction of nitric acid and thorium nitrate by tri-n-octylphosphine oxide in cyclohexane.

W. Keder, et al., pp. 327-335. Extraction of actinides from nitrate solutions by tri-n-octylamines.

C. Warren and J. Suttle, pp. 336-342. Solvent extraction of scandium, yttrium, and lanthanum by mono-alkyl orthophosphoric acids.

V. Padmanabhan, et al., pp. 356-359. Thermal decomposition of oxalates of uranium, thorium, lanthanum.

A. Beadle, et al., pp. 359-361. Half-life of Am^{243}.

J. Krtil and V. Kouřím, pp. 367-369. Sorption of cesium on ammonium phosphomolybdate and ammonium phosphotungstate.

D. Cartwright, and E. Robbins, pp. 373-376. Source of error in determining U^{235} by gamma-ray spectroscopy.

A. Kertes, pp. 377-378. Unstable hydrates of hydrochloric acid in tri-n-butyl phosphate.

T. Sato, pp. 382-383. Decomposition of nitric acid co-extracted with uranyl nitrate by tri-n-butyl phosphate.

J. Nuclear Materials 2, No. 1 (1960)

G. Libowitz, pp. 1-22. Nature and properties of hydrides of the transition metals.

B. Blumenthal, pp. 23-30. Phase-transition temperatures of high-purity uranium.

J. Antill and K. Peakall, pp. 31-38. Oxidation of graphite by various gases at low partial pressures and high temperatures.

R. Roof, pp. 39-42. Experimental determination of the characteristic temperature of PuO_2.

U. Gonser, p. 43-50. Growth of α-uranium under irradiation, as a result of correlated collisions.

G. Bannister, et al., pp. 51-61. Ageing and hardness curves in the high-temperature range for several thorium alloys.

A. Sawatzky, pp. 62-68. Diffusion and solubility of hydrogen in the α phase of Zircaloy-2.

J. Laniesse, et al., pp. 69-74. Neutron diffraction study of the texture of uranium lumps.

P. Costa, pp. 75-80. Determination of the thermoelectromotive force of uranium and plutonium.

A. Dwight, pp. 81-87. Equilibrium phase diagram for uranium-molybdenum at temperatures below 900°C.

R. Cahn and H. Tomlinson, pp. 88-89. The nature of the sub-boundaries appearing in the α-β phase transformation of uranium.

J. Bloch, pp. 90-91. Phase transformation and disordering of U_2Mo compounds subjected to irradiation.

J. Williams, pp. 92-93. Sintering of uranium oxides.

Nuclear Energy 14, No. 144 (1960)

F. Paulsen, pp. 221-223. Radiation applications in the chemical processing industry. II.

Nuclear Power 5, No. 48 (1960)

H. Huet, pp. 130-131. Uranium production at Le Boucher.

J. Elston, pp. 131-133. The range of application of beryllia.

J. Bernard, et al., pp. 133 135. Development of new-type fuel elements in France.

--- pp. 137-139. The Marcoule plutonium extraction plant.

--- p. 139. Fuel element fabrication at Annecy.

D. Harries, pp. 142-145. Radiation damage to iron and steel-2.

Nucleonics 18, No. 4 (1960)

F. Lampe, pp. 60-65. Irradiation reactions in hydrocarbon gases.

M. Levoy, pp. 68-70, 118. Uranium isotope separation by nozzles.

Nucleonics 18, No. 5 (1960)

P. Bissonnette and J. Carr. pp. 110-115. Direct current simulates fission heat in fuel-element test loop.

M. Vogel, pp. 116-121. Designing high-pressure in pile test thimbles.

Nukleonik 2, No. 2 (1960)

M. Salesse, pp. 79-83. Metallurgy and atomic energy.

IV. Nuclear Radiation Shielding

Radiobiology and health physics. Theory and practice. Instrumentation.

Biofizika 5, No. 1 (1960)

G. A. Volkov and G. R. Rik, pp. 60-68. Contribution to the problem of alpha dosimetry in boundary zones of heterogeneous media.

V. V. Khvostova and S. A. Valeva, pp. 81-84. Contribution to methods for applying ionizing radiations to plant selection.

Biofizika 5, No. 2 (1960)

Yu. I. Moskalev, pp. 202-207. On the role of the time factor in injury induced by radioisotopes.

G. B. Radzievskii, pp. 208-216. Measurement of absorbed dose in an inhomogeneous radiation field with the aid of a diaphragmed extrapolation chamber.

A. M. Kononenko and V. A. Petrov, pp. 217-224. Some problems in the dosimetry of distributed beta sources.

S. A. Valeva, pp. 244-248. Data on Radiosensitivity of agricultural crops.

Gigiena i Sanitariya, No. 4 (1960).

G. I. Bondarev, pp. 92-96. Foodstuffs irradiated by ionizing radiations, and their suitability for human use.

Gigiena Truda i Prof. Zabolevaniya, No. 3 (1960) Work safety and occupational diseases

L. A. Il'in, pp. 28-32. On the contamination of animal integuments by radioactive substances and the comparative effectiveness of various decontamination techniques.

V. A. Kisilenko and M Ya. Boyarintseva, pp. 49-50. Working conditions in handling radioactive materials in the laying of main pipelines, and proper preventive health measures.

Atomkernenergie 5, No. 4 (1960)

G. Böhler, pp. 144-147. Removal of radioactive wastes (Survey of papers presented at the 1959 Monaco Conference).

Industries Atomiques 4, Nos. 3-4 (1960)

R. Beaugé, p. 65-67. Determination of efficiency of boron shielding and measurement of the amount of boron present in boron shielding.

Jaderná Energie 6, No. 5 (1960)

Z. Spurny, pp. 163-165. Use of optical glasses of Czech manufacture for industrial dosimetry.

J. Brit. Nuclear Energy Conf. 5, No. 2 (1960)

A. Cottrell, pp. 64-77. Effect of nuclear radiations on structural materials.

G. Bacon and R. Dyer, pp. 78-81. Instrumentation for measuring neutron diffraction from a nuclear reactor with high neutron flux.

K. Maddocks, pp. 110-127. Some aspects of nuclear reactor safety practices aboard nuclear-propelled ships.

Nuclear Energy 14, No. 144 (1960)

--- pp. 212-213. Radiation shielding. Measurements techniques.

Nuclear Power 5, No. 48 (1960)

D. Taylor, pp. 147-148. Dosimetric instrumentation. I.

Nuclear Power 5, No. 49 (1960)

D. Taylor, pp. 110-114. Dosimetric instrumentation. II.

A. Clare, p. 117-118. Measurement of neutron dose.

Nuclear Sci. and Eng. 7, No. 3 (1960)

W. Olson, et al., pp. 199-209. Analog computation of air-blast shock wave effects due to simulated reactor core accident.

L. Kothari and P. Khubchandani, pp. 240-241. Neutron slowing-down in graphite at energies close to thermal equilibrium.

Nucleonics 18, No. 4 (1960)

M. Wilhelmsen, et al., pp. 84-88. Automatic film-badge reader.

R. Ginther and H. Schulman, pp. 92-95. New glass dosimeter is less energy-dependent.

E. Fowler, et al., pp. 102-105. Bacterial "infection" of the Omega-West reactor.

--- p. 106. Telemetering broadens gauging and monitoring.

L. Kempe, pp. 108-113. Complementary effects of heat and radiation on food microorganisms.

Nucleonics 18, No. 5 (1960)

D. Kalkwarf, pp. 76-81, 130-131. Chemical protection from radiation effects.

---pp. 85-100. Symposium feature on scintillators and semiconductors. Scintillation theory. New scintillators; photomultiplier development; recording of particle tracks with luminescent chamber; semiconductor detectors.

E. Bylander, pp. 102-104. Ion-chamber response in high-level radiation field.

V. Radioactive and Stable Isotopes

Labeled-atom techniques. Use of radioactive radiations. Direct conversion of nuclear energy to electrical energy.

Avtomobil. Prom. No. 3 (1960)

A. Kh. Éliava, pp. 34-37. Planning and outfitting of laboratories for hot-isotope testing of automobile engines.

Vestnik Sel'sko-khoz. Nauki, No. 4 (1960) (Agricult. Sci. bull)

Yu. N. Artem'ev, pp. 64-73. Tracer study of tractor engine performance.

Zapiski Voronezh. Sel'sko-khoz. Inst. 28, No. 2 (1959)

P. N. Zhitkov, pp. 355-359. Determination of the weight by volume of particle board by the labeled-atom technique.

Izvest. Akad. Nauk SSSR, Otdel. Tekh. Nauk. Metallurgiya i Toplivo, No. 1 (1960).

V. D. Goroshko and L. P. Nikanorova, pp. 152-157. On the applicability of radioactive radiations to monitoring of ash content of coals.

Kolloid. Zhur. 22, No. 1 (1960)*

D. M. Sandomirskii and M. K. Vdovchenkova, pp. 69-73. Tracer study of gelatinized rubber latex species.

Stal', No. 3 (1960)

T. M. Saar, et al., pp. 208-211. Tracer study of skin formation of steel ingots. Trudy Gidrolog. Inst. No. 77 (1960).

A. M. Dimaksyan, pp. 129-141. On a tracer technique for measuring the concentration of fluvial alluvia.

Khim. Nashinostroenie, No. 2 (1960)

V. N. Fainberg, pp. 41-43. Experience in the use of gamma flaw detection with a scintillation counter (for quality control of products).

Elektr. Stantsii, No. 4 (1960)

V. G. Segalin, et al., pp. 20-23. Radiometric level gauge for continuous measurement of coal-hopper and liquid-tank levels.

*Original Russian pagination. See C. B. translation.

Nucleonics 18, No. 5 (1960)

S. Beacom and B. Riley. pp. 82-84. Radioactive tracer follows leveler in electroplating bath.

J. Duncan, et al., pp. 126-129. Versatile gamma facilities at U. of Florida.

2 outstanding new Soviet journals

KINETICS AND CATALYSIS

The first authoritative journal specifically designed for those interested (directly or indirectly) in kinetics and catalysis. This journal will carry original theoretical and experimental papers on the kinetics of chemical transformations in gases, solutions and solid phases; the study of intermediate active particles (radicals, ions); combustion; the mechanism of homogeneous and heterogeneous catalysis; the scientific grounds of catalyst selection; important practical catalytic processes; the effect of substance – and heat-transfer processes on the kinetics of chemical transformations; methods of calculating and modelling contact apparatus.

Reviews summarizing recent achievements in the highly important fields of catalysis and kinetics of chemical transformations will be printed, as well as reports on the proceedings of congresses, conferences and conventions. In addition to papers originating in the Soviet Union, KINETICS AND CATALYSIS will contain research of leading scientists from abroad.

Contents of the first issue include:

Molecular Structure and Reactivity in Catalysis. A. A. Balandin

The Role of the Electron Factor in Catalysis. S. Z. Roginskii

The Principles of the Electron Theory of Catalysis on Semiconductors. F. F. Vol'kenshtein

The Use of Electron Paramagnetic Resonance in Chemistry. V. V. Voevodskii

The Study of Chain and Molecular Reactions of Intermediate Substances in Oxidation of *n*-Decane. Z. K. Maizus, I. P. Skibida, N. M. Emanuél' and V. N. Yakovleva

The Mechanism of Oxidative Catalysis by Metal Oxides. V. A. Roiter

The Mechanism of Hydrogen-Isotope Exchange on Platinum Films. G. K. Boreskov and A. A. Vasilevich

Nature of the Change of Heat and Activation Energy of Adsorption with Increasing Filling Up of the Surface. N. P. Keier

Catalytic Function of Metal Ions in a Homogeneous Medium. L. A. Nikolaev

Determination of Adsorption Coefficient by Kinetic Method. I. Adsorption Coefficient of Water, Ether and Ethylene on Alumina. K. V. Topchieva and B. V. Romanovskii

The Chemical Activity of Intermediate Products in Form of Hydrocarbon Surface Radicals in Heterogeneous Catalysis with Carbon Monoxide and Olefins. Ya. T. Eidus

Contact Catalytic Oxidation of Organic Compounds in the Liquid Phase on Noble Metals. I. Oxidation of the Monophenyl Ether of Ethyleneglycol to Phenoxyacetic Acid. I. I. Ioffe, Yu. T. Nikolaev and M. S. Brodskii

Annual Subscription: $150.00

Six issues per year – approx. 1050 pages per volume

JOURNAL OF STRUCTURAL CHEMISTRY

This significant journal contains papers on all of the most important aspects of theoretical and practical structural chemistry, with an emphasis given to new physical methods and techniques. Review articles on special subjects in the field will cover published work not readily available in English.

The development of new techniques for investigating the structure of matter and the nature of the chemical bond has been no less rapid and spectacular in the USSR than in the West; the Soviet approach to the many problems of structural chemistry cannot fail to stimulate and enrich Western work in this field. Of special value to all chemists, physicists, geochemists, and biologists whose work is intimately linked with problems of the molecular structure of matter.

Contents of the first issue include:

Electron-Diffraction Investigation of the Structure of Nitric Acid and Anhydride Molecules in Vapors. P. A. Akishin, L. V. Vilkov and V. Ya. Rosolovskii

Effects of Ions on the Structure of Water. I. G. Mikhailov and Yu P. Syrnikov

Proton Relaxation in Aqueous Solutions of Diamagnetic Salts. I. Solutions of Nitrates of Group II Elements. V. M. Vdovenko and V. A. Shcherbakov

Oscillation Frequencies of Water Molecules in the First Coordination Layer of Ion in Aqueous Solutions. O. Ya. Samilov

Second Chapter of Silicate Crystallochemistry. N. V. Belov

Structure of Epididymite $NaBeSi_3O_7OH$. A New Form of Infinite Silicon–Oxygen Chain (band) $[Si_6O_{15}]$. E. A. Podedimskaya and N. V. Belov

Phases Formed in the System Chromium–Boron in the Boron-Rich Region. V. A. Epel'baum, N. G. Sevast'yanov, M. A. Gurevich and G. S. Zhdanov

Crystal Structure of the Ternary Phase in the Systems Mo(W)–Fe(CO,Ni)–Si. E. I. Gladyshevskii and Yu. B. Kyz'ma

Complex Compounds with Multiple Bonds in the Inner Sphere. G. B. Bokii

Quantitive Evaluation of the Maxima of Three-Dimensional Paterson Functions. V. V. Ilyukhin and S. V. Borisov

Application of Infrared Spectroscopy to Study of Structure of Silicates. I. Reflection Spectra of Crystalline Sodium Silicates in Region of 7.5-15μ. V. A. Florinskaya and R. S. Pechenkina

Use of Electron Paramagnetic Resonance for Investigating the Molecular Structure of Coals. N. N. Tikhomirova, I. V. Nikolaeva and V. V. Voevodskii

New Magnetic Properties of Macromolecular Compounds with Conjugated Double Bonds. L. A. Blyumenfel'd, A. A. Slinkin and A. E. Kalmanson

Annual Subscription: $80.00

Six issues per year – approx. 750 pages per volume

Publication in the USSR began with the May-June 1960 issues. Therefore, the 1960 volume will contain four issues. The first of these will be available in translation in April 1961.

(c/b) CONSULTANTS BUREAU 227 W. 17 ST., NEW YORK 11, N. Y.